UCRL-18454

cy 2

TRANSVERSE SPACE-CHARGE EFFECTS IN CIRCULAR ACCELERATORS

Frank James Sacherer
(Ph.D. Thesis)

October 30, 1968

LAWRENCE RADIATION LABORATORY
UNIVERSITY of CALIFORNIA BERKELEY

UCRL-18454

UCRL-18454

UNIVERSITY OF CALIFORNIA

Lawrence Radiation Laboratory
Berkeley, California

AEC Contract No. W-7405-eng-48

TRANSVERSE SPACE-CHARGE EFFECTS IN CIRCULAR ACCELERATORS

Frank James Sacherer

(Ph.D. Thesis)

October 30, 1968

TRANSVERSE SPACE CHARGE EFFECTS IN CIRCULAR ACCELERATORS

Contents

TRANSVERSE SPACE-CHARGE EFFECTS IN CIRCULAR ACCELERATORS

Frank James Sacherer

Lawrence Radiation Laboratory
University of California
Berkeley, California

October 30, 1968

ABSTRACT

The particles in an accelerator interact with one another by electromagnetic forces and are held together by external focusing forces. Such a many-body system has a large number of transverse modes of oscillation (plasma oscillations) that can be excited at characteristic frequencies by errors in the external guide field.

In Part I we examine one mode of oscillation in detail, namely the quadrupole mode that is excited in uniformly charged beams by gradient errors. We derive self-consistent equations of motion for the beam envelope and solve these equations for the case in which the space-charge force is much less than the external focusing force, i.e., for strong-focusing synchrotrons. We find that the resonance intensity is shifted from the value predicted by the usual transverse incoherent space-charge limit; moreover, because the space-charge force depends on the shape and size of the beam, the beam growth in always limited. For gradient errors of the magnitude normally present in strong-focusing synchrotrons, the increase in beam size is small provided the beam

parameters are properly chosen; otherwise the growth may be large. Thus gradient errors need not impose a limit on the number of particles that can be accelerated.

In Part II we examine the other modes of collective oscillation that are excited by machine imperfections. For simplicity we consider only one-dimensional beams that are confined by harmonic potentials, and only small-amplitude oscillations. The linearized Vlasov and Poisson equations are used to find the twofold infinity of normal modes and eigenfrequencies for the stationary distribution that has uniform charge density in real space. In practice, only the low-order modes (the dipole, quadrupole, sextupole, and one or two additional modes) will be serious, and the resonant conditions for these modes are located on a tune diagram. These results, which are valid for all beam intensities, are compared with the known eigenfrequencies for the stationary distribution that has uniform particle density in phase space, and are extrapolated to the Gaussian distribution observed in the Brookhaven AGS.

INTRODUCTION

The beam of particles in an accelerator is a many-body system of charged particles interacting with one another by electromagnetic forces and held together by external focusing forces. Such a many-body system has a large number of modes of collective oscillations that can be excited by machine imperfections at characteristic frequencies. In the limit of low intensities, the interactions are negligible, and the collective modes and eigenfrequencies are easy to find. Consider, for example, a one-dimensional beam in an external harmonic potential; in the absence of space charge, the individual particles obey the equation

$$\frac{d^2x}{d\phi^2} + \nu^2 x = 0 \quad , \tag{1}$$

and any distribution of particles rotates rigidly in the $x - \frac{1}{\nu}\frac{dx}{d\phi}$ phase space with the frequency ν. A distribution with circular symmetry (Fig. 1a) is stationary, while a distribution with circular symmetry, but displaced from the origin (Fig. 1b), oscillates with the

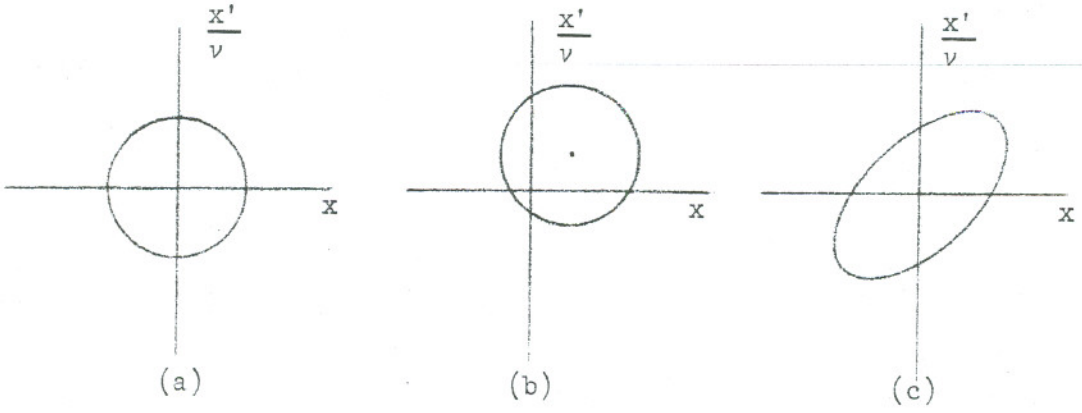

Fig. 1.

frequency ν - in real space, the beam oscillates rigidly back and forth at the frequency ν. In fact, there is an infinite number of modes with the circular form of Fig. 1b, each with a different radial dependence, but each oscillating at frequency ν. Similarly, there is an infinite number of modes with the elliptical symmetry of Fig. 1c; in real space, these modes expand and contract with frequency 2ν. In general, there is an infinite number of modes with a given n-fold symmetry of rotation, and each mode oscillates with the frequency $n\nu$. Therefore, in the absence of space charge, the eigenfrequencies for any distribution are just harmonics of the unperturbed betatron frequency, and each eigenfrequency is infinitely degenerate.

Resonance can occur when an eigenfrequency is an integral multiple of the rotation frequency in the accelerator, i.e., when $n\nu = m$; this condition is of course identical with that obtained from the single-particle approach, which is equivalent to the many-body approach in the limit of zero intensity. Thus if a driving tern of the form $x^n \cos k\phi$ is added to Eq. (1), the various dipole modes (Fig. 1b) will be excited if $\nu = k$ and $n = 0,2,4,\cdots$; the quadrupole modes (Fig. 1c) are excited if $\nu = \frac{k}{2}$ and $n = 1,3,5,\cdots$; the sextupole modes if $\nu = \frac{k}{3}$ and $n = 2,4,6,\cdots$, and so on for the higher-order modes.

Space-charge interactions modify these results. For intensities of interest in synchrotrons, and for small-amplitude oscillations, the eigenfrequencies are shifted by small amounts proportional to the beam intensity, and the degeneracy is removed so that the eigenfrequencies

occur in clusters near the unperturbed, degenerate values $n\nu$. As a result, each of the forbidden lines on a tune diagram that would occur for an integer, half-integer, or subharmonic value of ν in the absence of space charge is split into an infinite number of closely spaced lines. For example, the various dipole modes that are excited for the same frequency $\nu = k$ in the absence of space charge are excited in the presence of space charge at different frequencies that are clustered below the value $\nu = k$: there is one mode for which the beam oscillates rigidly back and forth at the unperturbed frequency ν, but there is also an infinite number of nonrigid modes whose eigenfrequencies are shifted below $\nu = k$ by amounts proportional to the beam intensity.

The above remarks apply only to small-amplitude oscillations. For larger-amplitude oscillations, space charge provides a very effective mechanism for limiting beam growth through the nonlinear dependence of the space-charge forces on the shape and size of the beam. A quantitative study of this important effect is extremely difficult in the general case; however, it was shown by Lloyd Smith[1] and by P. M. Lapostolle[2] that the quadrupole mode excited by gradient errors in uniformly charged beams can be analyzed even in the nonlinear regions.

In Part I of this paper we examine this case in detail. In Section 1, self-consistent equations of motion for the beam boundary are derived for uniformly charged beams with one and two degrees of freedom. The derivation, which is more general than we need, is applicable whenever the self-forces and external forces acting on the individual particles within the beam are linear. In Section 2, the

envelope equation for the one-dimensional (planar) beam is solved, and in Section 3, various two-dimensional (cylindrical) beams are examined. For either case, the nonlinear character of the space-charge force causes the frequency of the quadrupole mode of oscillation to depend on its amplitude. Thus the beam growth caused by gradient errors is always bounded. We also investigate the process of resonance crossing that results from slow variations in external focusing or effective space-charge force and find, for gradient errors of the magnitude normally encountered in AG synchrotrons, that resonances can be crossed in the direction of increasing frequency with only a small increase in beam size. However, if the resonance is crossed in the direction of decreasing frequency, a substantial increase in beam size can occur. For example, if the beam is caused to bunch in the synchrotron, the space-charge force increases, and the beam size can grow quite large near the intensity predicted by the bunched incoherent space-charge limit. However, a prebunched beam whose intensity is considerably larger than the incoherent space-charge limit may be successfully accelerated. In this case, the resonance is crossed in the direction of decreasing space-charge force, and very little beam growth occurs. Thus, the incoherent space-charge limit, as usually defined, need not impose a limit on the beam intensity. Similar results have been derived by F. Sacherer,[3] and by P. M. Lapostolle and L. Thorndahl.[4]

In Part II we investigate the other modes of collective oscillation that are excited by machine imperfections. For simplicity we restrict our attention to one-dimensional, planar beams, and consider

only small-amplitude oscillations. In this case the twofold infinity of normal modes (plasma oscillations) and eigenfrequencies can be found by means of the linearized Vlasov equation and Maxwell's equations. Harker[5] has given a general prescription for reducing these equations to an integral equation of the Fredholm type, but numerical methods are usually required to extract the eigenfunctions and eigenvalues. However, an important result of this paper is a direct method for finding all the normal modes and eigenfrequencies for the stationary distribution corresponding to a uniform charge distribution in real space.

In Section 1 of Part II, we find the eigenfunctions and eigenvalues for this case, and determine which modes are excited by a given external driving force. Then, since the complete eigenvalue spectrum is known, the resonant frequencies for the various dipole, quadrupole, and higher-order modes can be located on a tune diagram. Besides being useful in themselves, these results provide considerable insight into the more difficult normal mode problem for nonuniform beams.

In Section 2, this mode structure is compared with that obtained by Ehrman[6] for the stationary distribution that has a uniform particle distribution in phase space. In this case the charge density in real space is approximately uniform, and we find that the eigenvalue spectra for the two distributions are very similar. We also extend these results to a distribution with Gaussian charge density similar to that measured for the Brookhaven AGS.

PART I. UNIFORMLY CHARGED BEAMS IN THE PRESENCE OF GRADIENT ERRORS

1. Envelope Equations

In this section we find self-consistent envelope equations for the case in which both external forces and self-forces acting on the particles in a beam are linear. The requirement of linear forces restricts us to uniformly charged beams and to linear machine imperfections, namely gradient errors, but allows us to study the effects of space charge on large-amplitude oscillations of the beam.

We first consider the simple case of a beam with only one degree of freedom, then extend the derivation to two degrees of freedom, and finally show that the derivation can not be extended to three degrees of freedom.

The One-Dimensional Beam

In the absence of space-charge forces, we take the equation of motion for the individual particles to be

$$\frac{d^2x}{ds^2} + K(s)\, x = 0 \ , \tag{1-1}$$

where $K(s)$ is the external focusing function, s measures distance along the equilibrium orbit, and all the particles are assumed to have the same velocity $\frac{ds}{dt} = v_p$.

The self-forces acting on a particle arise from the internal charges and currents within the beam,[7] as well as from the charges and currents induced in the vacuum chamber walls,[8] and also from

collisions between particles. Fortunately, the effect of collisions is negligible for the times of interest, and for the low particle densities typical in accelerators.[9]

We incorporate the image force into the external focusing term $K(s)\,x$, and neglect its nonlinear components and its weak dependence on the beam size. Then the net effect of the image force is to shift the tune by an amount that depends on intensity and energy but not on the beam size,[8] in contrast to the direct self-force.

We also neglect the magnetic field component that results from the transverse particle velocities because $\frac{dx}{dt}$ is only a hundredth to a thousandth of the longitudinal velocity $\frac{ds}{dt}$. The force from the remaining magnetic field component is just $\frac{v_p^2}{c^2}$ times the electric force, and need not be calculated explicitly. The complete self-force is $1/\gamma^2$ times the electric force.[7]

The electric field calculation is simplified by neglecting the curvature of the equilibrium orbit and by neglecting the variation of the beam cross section with s. Actually the beam is modulated around the orbit circumference, but the modulation length is approximately half the betatron wavelength and is therefore negligible in comparison with the transverse dimensions of the beam.

The beam geometry then has the rectilinear form shown in Fig. 2, and in order that the self-forces be linear, the charge density must be uniform between the boundary planes, $x = \pm X(s)$. We assume for the

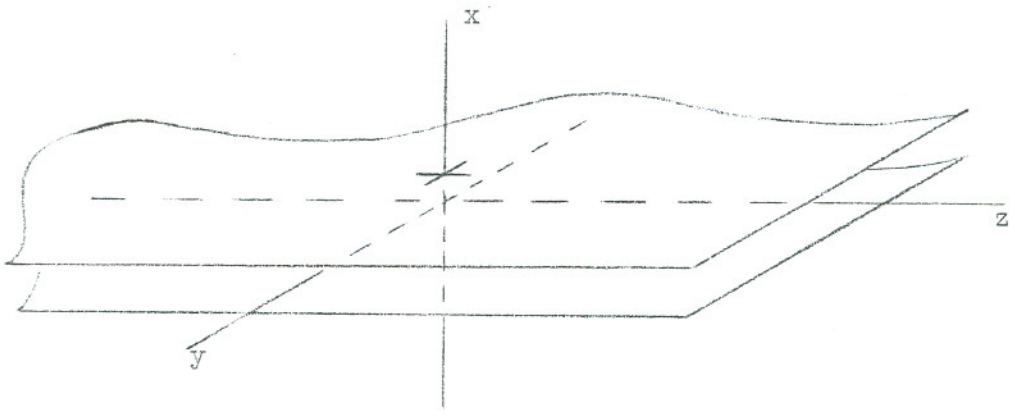

Fig. 2.

moment that the particles can be arranged in the $x - \frac{dx}{ds}$ phase space to produce the required uniform charge density, and that the charge density remains uniform as the system evolves under the action of the assumed linear forces. Then the equation of motion for the individual particles is

$$\frac{d^2x}{ds^2} + K(s)x - \frac{4\pi e^2}{\gamma^3 m v_p^2} \cdot \frac{N_1}{2X(s)} x = 0 \quad , \qquad (1\text{-}2)$$

where $\frac{eN_1}{2X(s)}$ is the charge density and eN_1 is the total charge per unit surface area. It is convenient to write (1-2) in the form of the two first-order equations

$$\frac{dx}{ds} = p \quad ,$$

$$\frac{dp}{ds} = \left[-K(s) + \frac{4\pi e^2}{\gamma^3 m v_p^2} \cdot \frac{N_1}{2X(s)}\right] x \quad , \tag{1-3}$$

and to define $\chi = \begin{pmatrix} x \\ p \end{pmatrix}$ so that Eqs. (1-3) can be written in the compact matrix form

$$\frac{d\chi(s)}{ds} = F(s)\,\chi(s) \quad . \tag{1-4}$$

We also introduce the transfer matrix $T(s, s_0)$

$$\chi(s) = T(s, s_0)\,\chi(s_0) \quad , \tag{1-5}$$

and note that the elements of $T(s, s_0)$ satisfy

$$\frac{dT(s, s_0)}{ds} = F(s)\,T(s, s_0) \quad . \tag{1-6}$$

Since we know the equations of motion for the individual particles, we can determine the evolution of any distribution of particles in phase space. In particular, if the distribution at any position s_0 has the elliptical boundary $\tilde{\chi} M^{-1}(s_0)\chi = 1$, where $M(s_0)$ is an arbitrary symmetric matrix, then the boundary remains elliptical at other values of s and has the form

$$\tilde{\chi} M^{-1}(s)\chi = 1 \quad , \tag{1-7}$$

where $M(s) = T(s, s_0)\, M(s_0)\, \tilde{T}(s, s_0)$. We can use (1-6) to write the equation of motion for $M(s)$ in the differential form

$$\frac{dM(s)}{ds} = F(s)\, M(s) + M(s)\, \tilde{F}(s) \quad , \tag{1-8}$$

which depends only on the known quantities $F(s)$.

The relationship between the components of M and the boundary ellipse is shown in Fig. 3, where the area of the ellipse is $\pi\sqrt{\text{Det } M}$, which we designate by πE. We are primarily interested in the beam half-

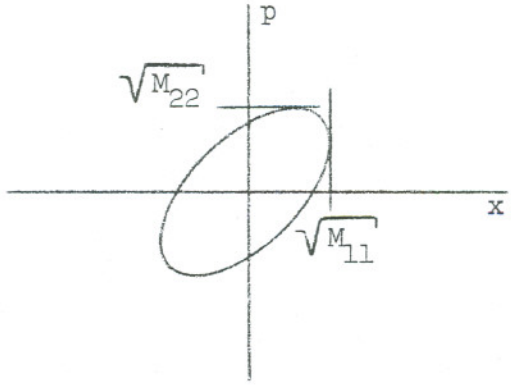

Fig. 3.

width $X(s) = \sqrt{M_{11}(s)}$, and it is convenient to parameterize $M(s)$ in the form

$$M = \begin{bmatrix} X^2 & XP \\ XP & P^2 + \dfrac{E^2}{X^2} \end{bmatrix} \quad , \tag{1-9}$$

where $\sqrt{P^2 + \frac{E^2}{X^2}}$ is the maximum extent of the distribution in the p-direction. Then the equations of motion for the quantities X(s), P(s), and E(s) follow immediately from (1-8):

$$\frac{dX}{ds} = F_{11}X + F_{12}P \quad ,$$

$$\frac{dP}{ds} = F_{21}X + F_{22}P + F_{12}\frac{E^2}{X^3} \quad , \tag{1-10}$$

$$\frac{dE}{ds} = \frac{1}{2}\left(F_{11} + F_{22}\right)E \quad .$$

For a Hamiltonian system, $F_{11} + F_{22} = 0$, and thus E is constant, which is just Liouville's theorem. When the form of F(s) corresponding to Eq. (1-3) is used, Eqs. (1-10) reduce to

$$\frac{d^2X}{ds^2} + K(s)X - \frac{E^2}{X^3} - \frac{2\pi e^2 N_1}{\gamma^3 m v_p^2} = 0 \quad , \tag{1-11}$$

for the beam half-width X(s).

We now demonstrate the Eq. (1-11) is self-consistent, i.e., that the individual particles can be distributed in phase space to produce the assumed uniform charge density within $x = \pm X(s)$. We require that the particle density in x-p space at $s = s_0$ have the form $f(x, p, s_0) = f[\tilde{X}M^{-1}(s_0)X]$, where $f(x, p, s)dxdp$ is the number of particles at s within the ranges $(x, x + dx)$ and $(p, p + dp)$. Then

at arbitrary s the distribution has the form $f(x, p, s) = f[\tilde{X}M^{-1}(s)X]$, and the functional form of f is determined by the requirement

$$\frac{N_1}{2X(s)} = \int_{-\infty}^{\infty} f[\tilde{X}M^{-1}(s)X]dp \quad . \tag{1-12}$$

We solve this equation by introducing the new variables

$v = \begin{pmatrix} v_1 \\ v_2 \end{pmatrix} = D(s)X$, where the matrix $D(s)$ satisfies

$$\tilde{D}(s)\, D(s) = M^{-1}(s) \quad . \tag{1-13}$$

Then the quadratic form $\tilde{X}M^{-1}(s)X$ is transformed into $v_1^2 + v_2^2$, and the elliptical distribution becomes circular, as shown in Fig. 4.

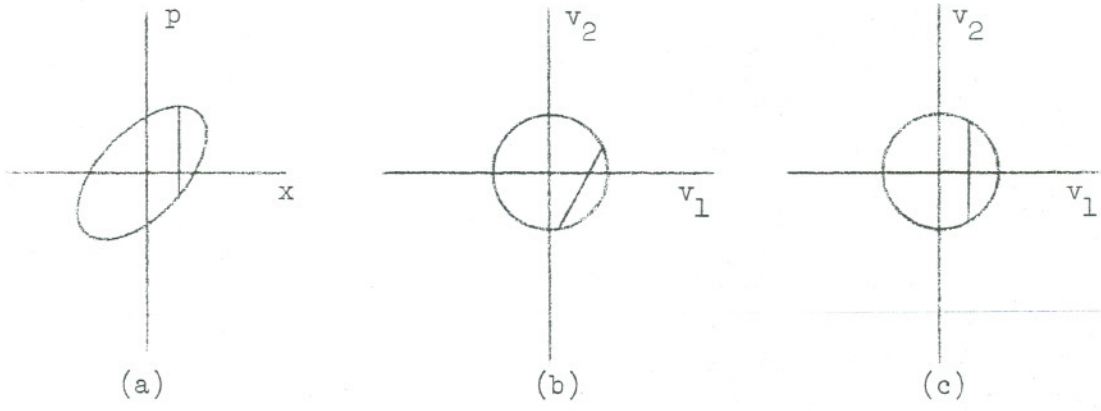

Fig. 4.

Actually, the four components of $D(s)$ are not uniquely specified by (1-13) because $M(s)$ depends on only three parameters; the ellipse is mapped into a circle but the orientation of the circle is not specified.

We fix the form of $D(s)$ by requiring that the vertical lines x = constant be mapped into vertical lines in v (Fig. 4c). Then $D_{12} = 0$, and $D(s)$ is determined by (1-13) to be

$$D = \begin{bmatrix} \frac{1}{X} & 0 \\ \frac{P}{E} & \frac{X}{E} \end{bmatrix} . \tag{1-14}$$

This is a convenient choice for $D(s)$ because it maps the integration over p in Eq. (1-12) into an integration over v_2, with $dv_2 = \frac{X(s)}{E} dp$. The requirement of uniform charge density is then simply

$$\frac{N_1}{2E} = \int f(v_1^2 + v_2^2) dv_2 \quad , \tag{1-15}$$

where the range of integration is restricted to $v_1^2 + v_2^2 \leqslant 1$. Note that (1-15) is independent of s. In terms of the radius $r = \sqrt{v_1^2 + v_2^2}$, Eq. (1-15) becomes

$$\frac{N_1}{2E} = \int_{v_1}^{1} \frac{f(r^2) r dr}{\sqrt{r^2 - v_1^2}} . \tag{1-16}$$

This integral equation can be inverted by Abel's theorem[10] to give

$$f(\tilde{X}_M^{-1} X) = \frac{N_1}{2\pi E \sqrt{1 - \tilde{X}_M^{-1} X}} \equiv \frac{N_1}{2\pi \sqrt{E^2 - (Xx' - X'x)^2 - \left(\frac{Ex}{X}\right)^2}} , \tag{1-17}$$

which is the unique solution of (1-12). This demonstrates that the particle distribution required to produce a uniform charge density does indeed exist. It occupies the interior of the boundary ellipse $\tilde{X}M^{-1}X = 1$, and the particle density approaches infinity at the boundary. Equation (1-11) is then the envelope equation for this distribution.

Actually, this method for finding self-consistent envelope equations is not restricted to uniformly charged beams, but is applicable whenever the external forces and self-forces are linear. For example, it was used by H. G. Hereward and A. Sørenssen to study longitudinal beam effects[11] where, due to the shielding of the vacuum chamber, a parabolic charge density is required to produce linear self-forces. For any case, the envelope equations are just equations (1-10) where $F(s)$ is specified by the equations of motion (1-4) for the individual particles. The distribution $f(\tilde{X}M^{-1}X)$ that produces the required charge density $\rho(x)$,

$$\rho(x) = \int_{-\infty}^{\infty} f(\tilde{X}M^{-1}X)dp \quad , \tag{1-18}$$

can be found by the same procedure that was used for the case of uniform charge density. The condition $\int_{-X}^{X} \rho(x)dx = N_1$ requires that $\rho(x)$ have the form $\frac{N_1}{2X} g\left(\frac{x}{X}\right)$, and Eq. (1-18) can be transformed by $D(s)$ into the circular form

$$\frac{N_1}{2E} g(v_1) = \int f(v_1^2 + v_2^2)dv_2 \quad , \tag{1-19}$$

which can be inverted by Abel's theorem provided $\frac{dg(v_1)}{dv_1}$ is continuous.[10] Thus, the self-consistency of the envelope equations is guaranteed provided $\rho(x)$ has a continuous first derivative.

The Two-Dimensional Beam

In principle this method can also be extended to beams with two and three degrees of freedom. The matrix equations remain formally valid when the vector $\chi(s)$ is increased to four or six component, but now the constants of the motion $\tilde{\chi}M^{-1}(s)\chi$ describe hyperellipsoids in the four- or six-dimensional phase spaces. The required distribution function $f(\tilde{\chi}M^{-1}\chi)$ that produces linear self-forces can be found by transforming the defining equation for f into the circular form analogous to (1-19), but now for four or six dimensions.

Consider first the case of a beam with two degrees of freedom. We again assume that all the particles have the same velocity $v_p = \frac{ds}{dt}$, and for the purpose of calculating the electric field, that the beam is in the form of a cylinder with an infinite extent in the s direction. Then the condition of linear self-forces requires that the beam have an elliptical cross section and a uniform charge density. However, the axes of the elliptical cross section need not be aligned with the coordinate axes, and the external focusing force may include linear coupling between the two transverse directions. The evolution of the distribution is then determined by a four-by-four matrix $F(s)$ (Eq. 1-4), and the constants of the motion $\tilde{\chi}M^{-1}\chi$ describe hyperellipsoids in the x, $\frac{dx}{ds}$, z, $\frac{dz}{ds}$ phase space.

We can immediately write the defining equation for f in the form

$$\text{constant} = \int f(v_1^2 + v_2^2 + v_3^2 + v_4^2)dv_3 dv_4 \quad , \qquad (1\text{-}20)$$

where the integration is restricted to $v_1^2 + v_2^2 + v_3^2 + v_4^2 \leqslant 1$, and where the constant can be determined by the normalization of f.[12] This shortcut avoids the specification of $D(s)$. With a change of variables, Eq. (1-20) becomes

$$\frac{N_2}{\pi^2\sqrt{\text{Det } M}} = \int_0^1 f(q)\, dq \quad , \qquad (1\text{-}21)$$

where N_2 is the number of particles per unit length in the beam. The required distribution function is the solution of (1-21):

$$f(\tilde{\chi}M^{-1}\chi) = \frac{N_2}{\pi^2\sqrt{\text{Det } M}}\, \delta(1 - \tilde{\chi}M^{-1}\chi) \quad , \qquad (1\text{-}22)$$

where $\delta(x)$ is the usual delta function. The particles are distributed with uniform density on the surface of the four-dimensional hyper-ellipsoid $\tilde{\chi}M^{-1}\chi = 1$, whose shape and orientation is specified by the ten independent parameters of the four-by-four matrix $M(s)$.

The self-forces are determined by the projection of this distribution onto the physical x-z plane. This projection is uniform and has the boundary

$$M_{33}x^2 + 2M_{13}xz + M_{11}z^2 = M_{11}M_{33} - M_{13}^2 \quad , \qquad (1\text{-}23)$$

which describes an ellipse of area $\pi\sqrt{M_{11}M_{33} - M_{13}^2}$. In terms of the major and minor axes and angle of rotation as shown in Fig. 5,

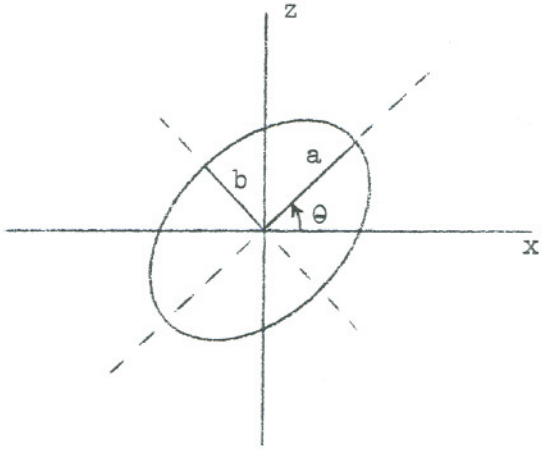

Fig. 5.

these matrix elements are

$$M_{11} = a^2 \cos^2\theta + b^2 \sin^2\theta \quad ,$$

$$M_{33} = a^2 \sin^2\theta + b^2 \cos^2\theta \quad , \qquad (1\text{-}24)$$

$$M_{13} = (b^2 - a^2)\sin\theta \cos\theta \quad ,$$

and the self-forces are easily determined.

The evolution of the distribution is then determined by

$$\frac{dM(s)}{ds} = F(s)\,M(s) + M(s)\,\tilde{F}(s) \quad , \qquad (1\text{-}25)$$

where $F(s)$ contains the known external forces as well as the self-forces, which depend on the matrix elements M_{11}, M_{13}, and M_{33}. In general all ten equations of (1-25) are necessary to describe the evolution of the system. However, if the equations of motion for the individual particles do not involve coupling between the two transverse planes, and if the hyperellipsoid is oriented so that the off-diagonal submatrix with elements M_{13}, M_{14}, M_{23}, M_{24} is zero, then the hyperellipsoid will maintain this orientation and these matrix elements will remain zero. The remaining six equations (three for the x direction and three for the z direction) can be parameterized in the form analogous to (1-9) for the one-dimensional beam. The self-fields for this case are

$\mathcal{E}_x = \frac{4eN_2}{X(X+Z)}\,x$ and $\mathcal{E}_z = \frac{4eN_2}{Z(X+Z)}\,z$, and the envelope equations become

$$\frac{d^2X}{ds^2} + K_x(s)X - \frac{E_x^2}{X^3} - \frac{4e^2N_2}{\gamma^3 m v_p^2}\cdot\frac{1}{X+Z} = 0 \quad ,$$

$$\frac{d^2Z}{ds^2} + K_z(s)Z - \frac{E_z^2}{Z^3} - \frac{4e^2N_2}{\gamma^3 m v_p^2}\cdot\frac{1}{X+Z} = 0 \quad , \qquad (1\text{-}26)$$

where $X(s)$ and $Z(s)$ are the beam half-widths, and E_x and E_z are the beam emittances in the $x - \frac{dx}{ds}$ and $z - \frac{dz}{ds}$ phase spaces. These

self-consistent envelope equations, which describe a cylindrical beam oriented with $\theta = 0$ in Fig. 5, were first obtained by I. M. Kapchinsky and V. V. Vladimirsky.[13]

The Three-Dimensional Beam

Finally consider the case of a beam with three degrees of freedom. The condition of linear self-forces requires that the beam have an ellipsoidal shape in real space and a uniform charge density. Then Eq. (1-8) will specify the beam envelope provided a distribution of the form $f(\tilde{\chi}M^{-1}\chi)$ exists that produces the required uniform charge density. In this case the defining equation for f has the form

$$\text{constant} = \int f(v_1^2 + v_2^2 + v_3^2 + v_4^2 + v_5^2 + v_6^2)dv_4dv_5dv_6 \quad . \tag{1-27}$$

This equation unfortunately has no solution that can be interpreted as a distribution function. The forms of the one- and two-dimensional distributions indeed suggest that the progression from $f \propto (1 - \tilde{\chi}M^{-1}\chi)^{-\frac{1}{2}}$ in one dimension to $f \propto \delta(1 - \tilde{\chi}M^{-1}\chi)$ in two dimensions will have no extension to three or more dimensions. The actual proof, due to Maurice Neuman (private communication), is reproduced in Appendix A.

2. The One-Dimensional Beam

We are now in a position to investigate the motion of the uniform one-dimensional beam in a self-consistent manner. We rewrite the envelope equation (1-11),

$$\frac{d^2X}{ds^2} + K(s)X - \frac{E^2}{X^3} - \frac{2\pi e^2 N_1}{\gamma^3 m v_p^2} = 0 \quad , \tag{2-1}$$

where $X(s)$ is the beam half-width, πE is the beam emittance, N_1 is the number of particles per unit surface area of the beam, and v_p is the particle velocity. The external focusing term $K(s)$ includes both the ideal focusing forces and gradient errors. The nonlinear emittance term arises from the conservation of the beam emittance, and has the same form as the centrifugal force term that results from the conservation of angular momentum in central force problems. It prevents a beam with finite emittance from becoming arbitrarily small, but in the absence of space charge, it does not limit the large-amplitude growth.[14] However, in the presence of space charge, the combination of the last two terms in (2-1) will limit the resonant growth of the beam.

We first eliminate the rapidly varying part of $K(s)$ from the envelope equation by transforming to "smooth" variables. In the absence of space charge, the periodic solution of (2-1), $X_p(s) = X_p(s + C)$, where C is the orbit circumference, can be found by standard methods once $K(s)$ is known. It is conventionally written in the form

$$X_p(s) = \sqrt{E\beta(s)} \quad , \tag{2-2}$$

where $\beta(s)$ is the familiar amplitude function of Courant and Snyder.[15] Then if we transform to the dimensionless variables

$$x = \frac{X(s)}{X_p(s)} , \qquad \phi = \int \frac{ds}{\nu\beta} , \tag{2-3}$$

the unperturbed envelope equation (in the absence of space charge and gradient errors) becomes

$$\frac{d^2x}{d\phi^2} + \nu^2 x - \frac{\nu^2}{x^3} = 0 , \tag{2-4}$$

where ν is the number of betatron oscillations per revolution and ϕ increases by 2π each revolution. The general solution of this equation is

$$x^2 = \sqrt{1 + A^2} + A \sin(2\nu\phi + \alpha) , \tag{2-5}$$

where A and α are arbitrary constants. The matched solution is $A = 0$ and $x = 1$, and any other solution oscillates about this matched solution with the frequency 2ν. Thus the dimensionless variable x measures the beam envelope in units of the unperturbed matched envelope.

In terms of the variables x and ϕ the complete envelope equation becomes

$$\frac{d^2x}{d\phi^2} + (\nu^2 + 2\nu\Delta\nu_s \cos n\phi)x - \frac{\nu^2}{x^3} - 2\nu\Delta\nu_{sc} = 0 , \tag{2-6}$$

where we have assumed an nth-harmonic gradient error with stopband width $\Delta\nu_s$, and where the last term is actually a function of s (or ϕ),

$$2\nu\Delta\nu_{sc} = \frac{\nu^2\beta^{3/2}(s)}{\sqrt{E}} \cdot \frac{2\pi e^2 N_l}{\gamma^3 m v_p^2} \quad . \tag{2-7}$$

In what follows, we replace $\beta(s)$ by its average value $\frac{R}{\nu}$ and neglect the high-frequency small-amplitude ripple components in the already small space-charge term. Then $\Delta\nu_{sc}$ is independent of ϕ and has the form

$$\Delta\nu_{sc} = \frac{1}{2\nu} \frac{4\pi e^2 R^2}{\gamma^3 m v_p^2} \frac{N_l}{2a} \quad , \tag{2-8}$$

where $a = \sqrt{\frac{ER}{\nu}}$ is the average amplitude of the unperturbed envelope. The quantity $\Delta\nu_{sc}$ is the space-charge-induced frequency shift for a beam whose envelope is constrained to the constant value a; it is a convenient measure of the beam intensity and is in fact identical with the expression conventionally used for predicting a space-charge limit.

Before solving the nonlinear envelope equation, it is informative to examine its small-amplitude solutions. In the absence of gradient errors, Eq. (2-6) has the constant solution $x = 1 + \frac{\Delta\nu_{sc}}{2\nu}$, and for oscillations of small amplitude δ about this constant value, the equation becomes

$$\frac{d^2\delta}{d\phi^2} + (4\nu^2 - 6\nu\Delta\nu_{sc})\delta = -2\nu\Delta\nu_s \cos n\phi \quad . \tag{2-9}$$

Thus the envelope oscillates with the natural frequency $2(\nu - \frac{3}{4}\Delta\nu_{sc})$, and resonance occurs for $2(\nu - \frac{3}{4}\Delta\nu_{sc}) = n$. If ν is larger than a half-integer by the amount $\Delta\nu$, i.e., $\nu = \frac{n}{2} + \Delta\nu$, then resonance occurs at a beam intensity corresponding to the value

$$\Delta\nu_{sc} = \frac{4}{3}\Delta\nu \quad , \tag{2-10}$$

which is one third larger than the value usually assumed. The fallacy in the usual procedure for predicting space-charge limits lies in the assumption of a constant beam size: if the envelope modulation is neglected, resonance occurs when the individual particle frequency $\nu - \Delta\nu_{sc}$ falls within the stopband at $\frac{n}{2}$; in other words, for the intensity $\Delta\nu_{sc} = \Delta\nu$. However, the modulation of the envelope causes the self-fields to exactly cancel the effect of the gradient error at this intensity,[16] and the resonance is shifted to $\Delta\nu_{sc} = \frac{4}{3}\Delta\nu$. This shift in resonant intensity is not restricted to uniform beams; it occurs for any mode of collective oscillation and is discussed in detail in Part II.

The amplitude of the periodic solutions of the linearized equation (2-9) are shown in the form of a response diagram for fixed $\frac{\Delta\nu_s}{\Delta\nu}$ in Fig. 6. The $\frac{\Delta\nu_s}{\Delta\nu} = 0$ asymptote represents the free envelope oscillations, which are periodic for the intensity $\Delta\nu_{sc} = \frac{4}{3}\Delta\nu$. The remainder of this section is concerned with the distortion of these curves in the large-amplitude region by the nonlinear terms in (2-6).

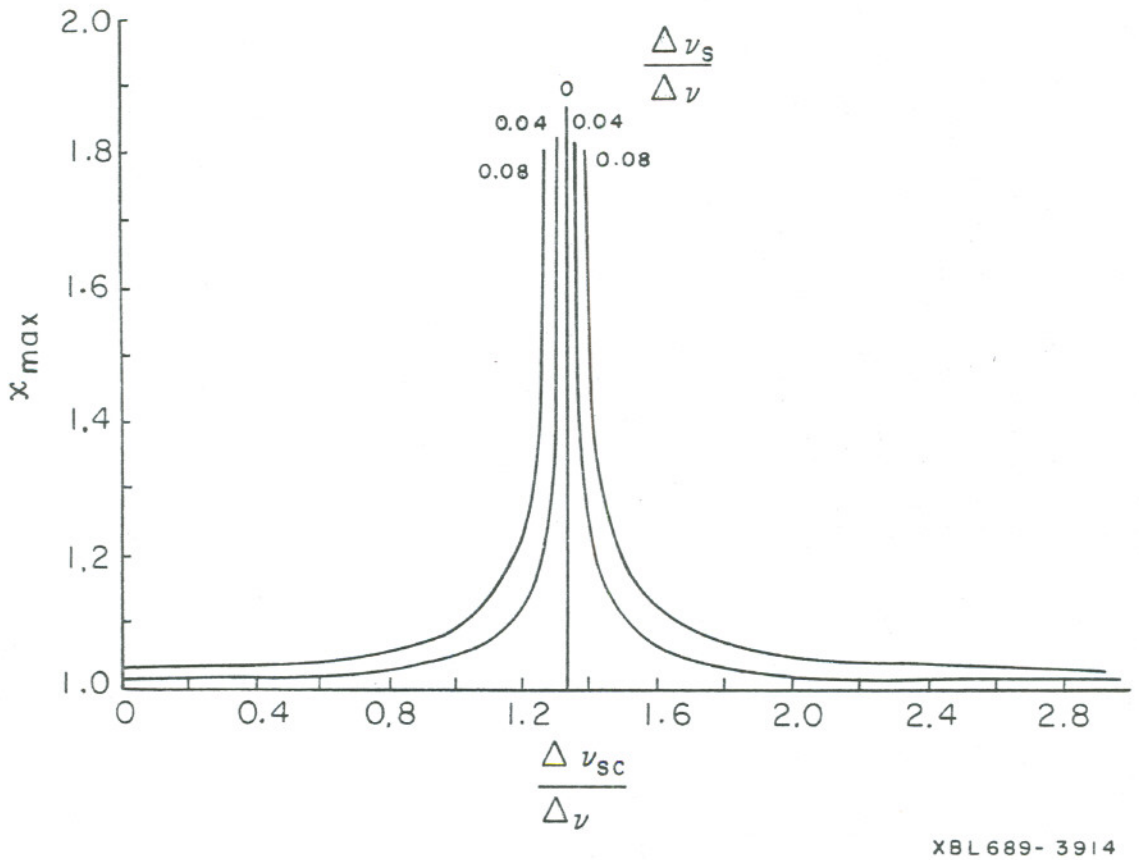

Fig. 6. Response diagram for the linearized envelope equation:

$x_{max} = 1 + \frac{\Delta \nu_s}{|3\Delta \nu_{sc} - \Delta \nu|}$, where the quantity $\frac{\Delta \nu_{sc}}{2\nu}$ in the constant solution $x = 1 + \frac{\Delta \nu_{sc}}{2\nu}$ has been neglected.

General Solution of the Envelope Equation

Both the space-charge term and the gradient-error term are small for alternating-gradient synchrotrons--they are of order $\frac{\Delta\nu_{sc}}{\nu}$ and $\frac{\Delta\nu_s}{\nu}$ compared with the remaining terms. Consequently we treat these terms as perturbations and use in place of x and $\frac{dx}{d\phi}$ the variables A and α defined by

$$x^2 = \sqrt{1 + A^2} + A \sin(2\nu\phi + \alpha) \quad ,$$
$$x \frac{dx}{d\phi} = \nu A \cos(2\nu\phi + \alpha) \quad . \tag{2-11}$$

In the absence of perturbations, both A and α are constant, while for small perturbations they change slowly in time, with small high-frequency variations superimposed. If Eqs. (2-11) are inserted in the envelope equation (2-6), the following first-order equations for A and α result:

$$\frac{dA}{d\phi} = -\Delta\nu_s \sqrt{1 + A^2} \cos[(2\nu - n)\phi + \alpha] \quad , \tag{2-12}$$

$$A \frac{d\alpha}{d\phi} = \Delta\nu_s \sqrt{1 + A^2} \sin[(2\nu - n)\phi + \alpha] - \frac{\Delta\nu_{sc}}{\pi} \int_0^{2\pi} \frac{A + \sqrt{1 + A^2} \sin u}{\sqrt{\sqrt{1 + A^2} + A \sin u}} du \quad , \tag{2-13}$$

plus additional terms that vary with the frequencies 2ν, 4ν, etc., which are neglected.

Equations (2-12) and (2-13) may be combined and integrated to obtain the constant of the motion,

$$\text{constant} = A \sin Q + \frac{2\Delta\nu}{\Delta\nu_s}\sqrt{1 + A^2} - 8\,\frac{\Delta\nu_{sc}}{\Delta\nu}\cdot\frac{\sqrt{2A}}{k}\,E(k) \quad , \qquad (2\text{-}14)$$

where $Q = (2\nu - n)\phi + \alpha$ and $E(k)$ is the complete elliptic integral of the second kind[17] with modulus $k^2 = \dfrac{2A}{A + \sqrt{1 + A^2}}$. This equation specifies the phase trajectories in the A, Q space, or alternatively by means of (2-11), in the $x - \frac{dx}{d\phi}$ phase space at any point along the orbit, i.e., for any azimuth ϕ. In particular, Figs. (7a) and (7b) show typical trajectories for azimuth $\phi = 0$ and for two values of the beam intensity, while Fig. (7c) shows the same trajectories as Fig. (7b), but for azimuth $\phi = \frac{\pi}{n}$. As expected, the phase trajectories are always bounded and the beam size remains finite.

Of special interest are the fixed points, which have constant values of A and Q. They are determined by Eqs. (2-12) and (2-13) to have $Q = \pm\frac{\pi}{2}$ and

$$A = \mp\frac{1}{2}\,\frac{\Delta\nu_s}{\Delta\nu}\sqrt{1 + A^2} + \frac{\Delta\nu_{sc}}{\Delta\nu}\cdot\frac{1}{2\pi}\int_0^{2\pi}\frac{A + \sqrt{1 + A^2}\,\sin u}{\sqrt{\sqrt{1 + A^2} + A \sin u}}\,du \quad , \qquad (2\text{-}15)$$

which determines A as a function of $\frac{\Delta\nu_s}{\Delta\nu}$ and $\frac{\Delta\nu_{sc}}{\Delta\nu}$. The beam motion corresponding to these fixed points is described by

$$x^2 = \sqrt{1 + A^2} \pm A \cos n\phi \quad , \qquad (2\text{-}16)$$

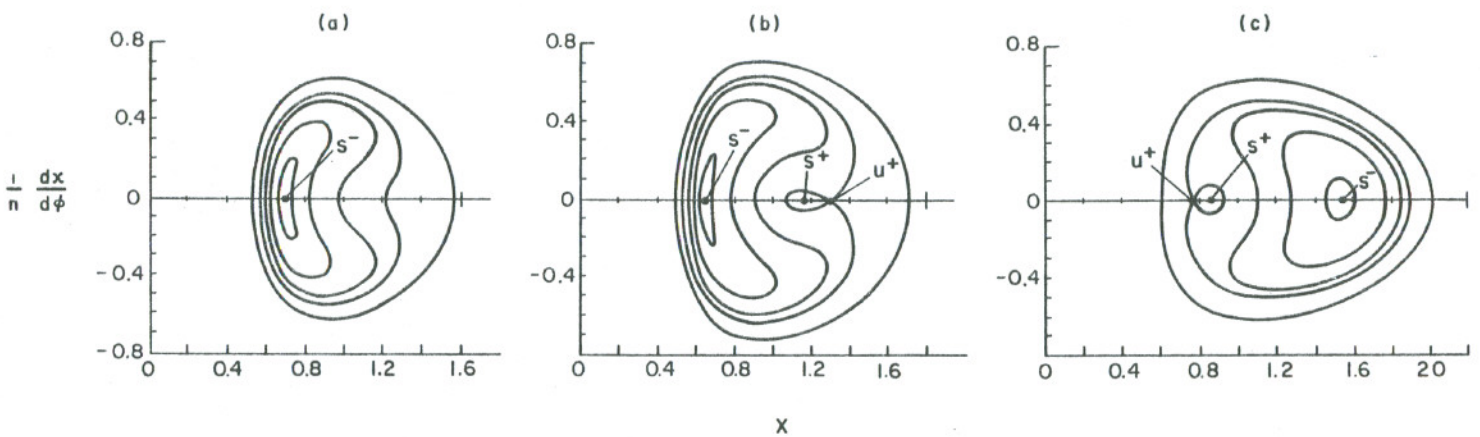

XBL689-3899

Fig. 7. Phase trajectories for $\frac{\Delta\nu_s}{\Delta\nu} = 0.04$. Figure (a) shows the trajectories at azimuth $\phi = 0$ for the intensity $\frac{\Delta\nu_{sc}}{\Delta\nu} = 1.40$; (b) shows the trajectories at the same azimuth but for the larger intensity $\frac{\Delta\nu_{sc}}{\Delta\nu} = 1.45$. The trajectories in (c) are the same as those in (b) but now for $\phi = \frac{\pi}{n}$. The separatrix is the trajectory that passes through U^+.

which represents a beam oscillating with the periodicity of the gradient error. The amplitudes for these periodic oscillations or fixed points are shown in Fig. 8 for several values of the stopband width $\Delta\nu_s$. The response curves are distorted from the linearized diagram Fig. 6 because the nonlinearity causes the frequency of the envelope oscillations to depend on amplitude; the $\frac{\Delta\nu_s}{\Delta\nu} = 0$ curve shows directly the amplitude dependence of the periodic free envelope oscillations. As a result, the resonant amplitudes are always finite. Another consequence of this distortion is the existence of three fixed points for $\frac{\Delta\nu_{sc}}{\Delta\nu}$ greater than the critical value (which depends on $\frac{\Delta\nu_s}{\Delta\nu}$) rather than the usual single fixed point. The two labeled S^+ and S^- are stable whereas U^+ is unstable; it can be seen from Fig. 7 that configuration points near S^+ and S^- oscillate with small amplitude about these points whereas points near U^+ may follow the separatrix and make much larger excursions. As the quantity $\frac{\Delta\nu_{sc}}{\Delta\nu}$ decreases, the phase trajectories of Fig. 7b are transformed smoothly into those of Fig. 7a; the stable region around S^+ shrinks down to a point and then disappears for $\frac{\Delta\nu_{sc}}{\Delta\nu}$ less than its critical value.

In the absence of both space charge and gradient errors, the matched beam corresponds to the solution $x = 1$. In the presence of space charge and gradient errors, the matched condition corresponds to the lowest fixed point of Fig. 8. This solution is periodic, so that the beam envelope remains stationary with respect to the accelerator, but it is modulated n times around the orbit circumference, where n

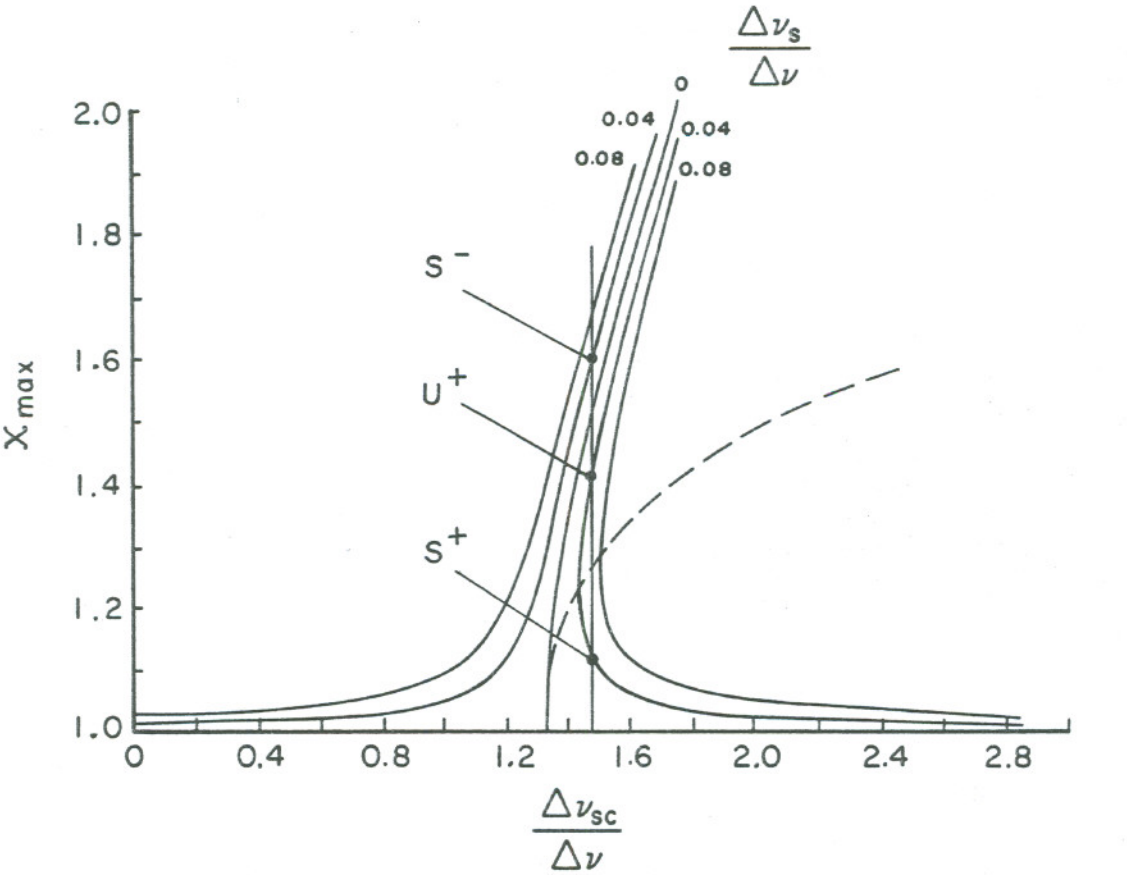

XBL689-3911

Fig. 8. Response diagram: $x_{max} = \left(\sqrt{1 + A^2} + A\right)^{\frac{1}{2}}$. The curves to the left of $\frac{\Delta\nu_s}{\Delta\nu} = 0$ correspond to the upper sign in Eqs. (2-15) and (2-16); those to the right correspond to the lower sign. The points where the slope is vertical (indicated by the dashed curve) are referred to as critical points.

is the periodicity of the gradient error. Any mismatch will lead to slow oscillations in the envelope about this matched value just as in the more familiar low-intensity case. The frequency of these oscillations depends on which phase trajectory of Fig. 7 the beam is on, but near stable fixed points it is approximately $2\Delta\nu$ times per revolution. Note from Fig. 8 that the matched condition for large intensities closely approaches the low-intensity matched value $x = 1$, provided the gradient errors are small and the intensity is not too near the resonant value $\Delta\nu_{sc} = \frac{4}{3}\Delta\nu$.

Resonance Crossing

The foregoing considerations apply only to a coasting beam whose parameters remain fixed. However, the parameters describing an accelerated beam change with time, and the beam may cross the $\Delta\nu_{sc} = \frac{4}{3}\Delta\nu$ resonance. We consider the worst case of a slow, adiabatic crossing.

The envelope equations can be derived from a Hamiltonian with the canonical variables x and $\frac{dx}{d\phi}$, and therefore Liouville's theorem applies to the $x - \frac{dx}{d\phi}$ phase space. Configuration points lying on closed contours continue to lie on closed contours as the parameters are varied adiabatically, and the area enclosed by these contours remains constant. However, the adiabatic assumption breaks down near the stagnation point U^+, so that the area enclosed by the sepatrix changes. For example, the stable phase area around S^+ becomes smaller as $\frac{\Delta\nu_{sc}}{\Delta\nu}$ decreases.

Consider first the case of a resonance crossing in the direction of decreasing $\frac{\Delta\nu_{sc}}{\Delta\nu}$. A beam whose intensity is larger than the resonant value and whose envelope was adjusted before injection to the matched value $x \approx 1$ oscillates with small amplitude about S^+ in Fig. 8, and corresponds to a point on one of the trajectories around S^+ in Figs. 7b and 7c. As the beam is accelerated, $\frac{\Delta\nu_{sc}}{\Delta\nu}$ decreases and the stable area around S^+ shrinks until the configuration point is forced onto the sepatrix. At this point the beam suddenly oscillates with a larger amplitude as its configuration point moves around the separatrix. The maximum beam size can be read directly from Fig. 9, which shows the maximum and minimum beam size for a point on the separatrix at the critical value of $\frac{\Delta\nu_{sc}}{\Delta\nu}$. If the vacuum chamber is large enough to accommodate this increase in beam size, then the resonance has been safely passed and the oscillations become smaller as $\frac{\Delta\nu_{sc}}{\Delta\nu}$ continues to decrease.

On the other hand, it is possible for a beam to cross the resonance in the opposite direction. For example, if the beam is bunched after injection, $\Delta\nu_{sc}$ increases. Also $\Delta\nu = \nu - \frac{n}{2}$ may change during acceleration and cause $\frac{\Delta\nu_{sc}}{\Delta\nu}$ to increase. In this case a nearly matched beam that oscillates around S^- continues to lie on a contour enclosing S^- as $\frac{\Delta\nu_{sc}}{\Delta\nu}$ increases, and therefore the beam size increases indefinitely as $\frac{\Delta\nu_{sc}}{\Delta\nu}$ increases (Fig. 8).

Summary

This completes our analysis of the uniform one-dimensional beam. In the presence of gradient errors, the beam envelope oscillates, and

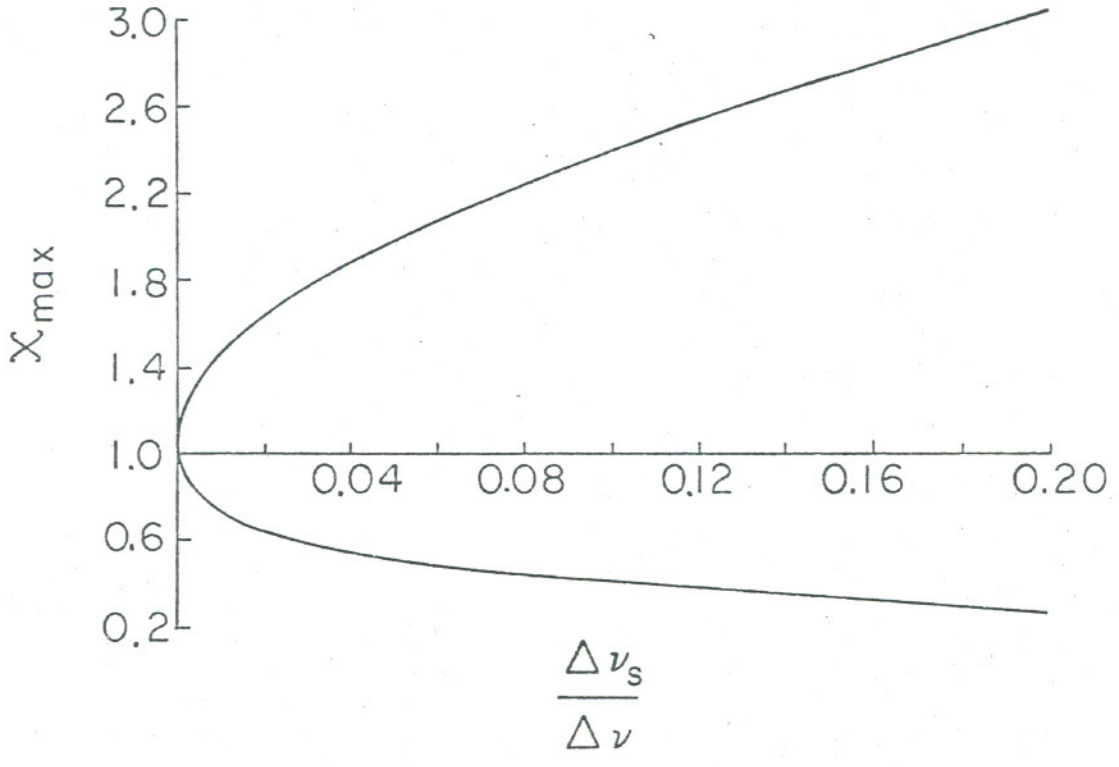

XBL689-3912

Fig. 9. The maximum and minimum beam sizes are shown for a point on the separatrix at the critical value of $\frac{\Delta \nu_{sc}}{\Delta \nu}$, the value for which the stable area around S^+ shrinks to a point.

resonance occurs for the beam intensity corresponding to $\Delta\nu_{sc} = \frac{4}{3}\Delta\nu$; this is one third larger than the usual space-charge limit, which assumes that the beam size is constant. Furthermore, because of the nonlinear dependence of the space-charge force on the beam size, the envelope is always bounded. The amount of beam growth caused by crossing the resonance in the direction of decreasing $\frac{\Delta\nu_{sc}}{\Delta\nu}$ has been calculated for nearly matched beams (Fig. 9), and is less than fifty percent for stopband widths $\Delta\nu_s \leqslant 0.01\,\Delta\nu$. This resonant growth is minimized for small gradient errors and for large values of $\Delta\nu = \nu - \frac{n}{2}$. On the other hand, adiabatic resonance crossing in the direction of increasing $\frac{\Delta\nu_{sc}}{\Delta\nu}$ would produce very large resonant growths, and should be avoided.

3. Two-Dimensional Beams

The envelope equations for the two-dimensional cylindrical beam can be written in terms of the dimensionless variables x and z as

$$\frac{d^2x}{d\phi^2} + [\nu_x^2 + 2\nu_x\Delta\nu_{sx}\cos n\phi] - \frac{\nu_x^2}{x^3} - \frac{b\omega_p^2}{ax + bz} = 0 \quad , \qquad (3\text{-}1)$$

$$\frac{d^2z}{d\phi^2} + [\nu_z^2 + 2\nu_z\Delta\nu_{sz}\cos n\phi] - \frac{\nu_z^2}{z^3} - \frac{a\omega_p^2}{ax + bz} = 0 \quad , \qquad (3\text{-}2)$$

where again the ripple components have been neglected. The quantities ν_x and ν_z are the betatron frequencies in the absence of space charge and gradient errors. As in the last section, x and z are the beam semi-axes measured in units of $a = \sqrt{\frac{E_x R}{\nu_x}}$ and $b = \sqrt{\frac{E_z R}{\nu_z}}$ respectively, where a and b are the semi-axes of the matched beam in the absence of gradient errors and space charge. The quantity $\omega_p^2 = \frac{2N}{\pi B}\frac{r_0 R}{ab}\frac{1}{\beta^2\gamma^3}$, where N is the number of particles in the beam, $r_0 = \frac{e^2}{mc^2}$ the classical electrostatic particle radius, and B is the bunching factor (the fraction of the circumference occupied by particles). The space charge induced frequency shifts for a beam with the constant envelope $x = 1$, $z = 1$ are $\Delta\nu_{scx} = \frac{b}{a+b}\cdot\frac{\omega_p^2}{2\nu_x}$ and $\Delta\nu_{scz} = \frac{a}{a+b}\cdot\frac{\omega_p^2}{2\nu_z}$. An nth-harmonic gradient error has been included with stopband widths $\Delta\nu_{sx}$ and $\Delta\nu_{sz}$.

The overall envelope motion described by (3-1) and (3-2) is very simple: the envelope has two modes of oscillation, corresponding to its two degrees of freedom, and the resonant growth of each mode is limited by the nonlinear space charge terms just as for the one-dimensional beam. However, the mathematical details are more complicated now: whereas the motion of the one-dimensional beam depends on only the two parameters $\frac{\Delta\nu_{sc}}{\Delta\nu}$ and $\frac{\Delta\nu_{s}}{\Delta\nu}$ and can be represented by a configuration point moving on a trajectory in a two-dimensional phase space, the motion of the two-dimensional beam depends on six parameters and requires a four-dimensional phase space.

Physically, the envelope motion can be characterized by the degree of coupling between the x and z directions, which arises from the space-charge terms in (3-1) and (3-2). Very loose coupling occurs when the individual particle frequency $\nu_x - \Delta\nu_{scx}$ is very different from $\nu_z - \Delta\nu_{scz}$. Then the envelope motion is nearly one-dimensional and the solutions are similar to those found in the last section. On the other hand, very tight coupling occurs when $\nu_x - \Delta\nu_{scx}$ is approximately equal to $\nu_z - \Delta\nu_{scz}$; in this case the x and z amplitudes of envelope oscillations are approximately equal and the envelope motion is two-dimensional. In the following we concentrate on a few special cases. In A the solution for the tightly coupled case $\nu_x = \nu_z$ and $E_x = E_z$ is presented in detail; in B several cases leading to the one-dimensional limit are briefly examined.

A. Equal Frequencies and Emittances

In this case the envelope equations without gradient errors are

$$\frac{d^2x}{d\phi^2} + \nu^2 x - \frac{\nu^2}{x^3} - \frac{4\nu\Delta\nu_{sc}}{x+z} = 0 \quad , \tag{3-3}$$

$$\frac{d^2z}{d\phi^2} + \nu^2 z - \frac{\nu^2}{z^3} - \frac{4\nu\Delta\nu_{sc}}{x+z} = 0 \quad , \tag{3-4}$$

where $\nu_x = \nu_z = \nu$ and $\Delta\nu_{scx} = \Delta\nu_{scz} = \Delta\nu_{sc}$, with $\Delta\nu_{sc} = \frac{\omega_p^2}{4\nu}$. If we consider oscillations of small amplitude δ_x, δ_z about the constant solution $x = z = 1 + \frac{\Delta\nu_{sc}}{2\nu}$, we find a symmetric mode with circular cross section $(\delta_x = \delta_z)$ that oscillates with the frequency $2(\nu - \frac{1}{2}\Delta\nu_{sc})$, and an antisymmetric mode with elliptical cross section $(\delta_x = -\delta_z)$ that oscillates with the frequency $2(\nu - \frac{3}{4}\Delta\nu_{sc})$. Therefore, in the presence of gradient errors of frequency n, resonances occur for the beam intensities corresponding to $\Delta\nu_{sc} = 2\Delta\nu$ and to $\Delta\nu_{sc} = \frac{4}{3}\Delta\nu$ where again $\Delta\nu = \nu - \frac{n}{2}$. Note that these resonant intensities differ from the usual space-charge limit $\Delta\nu_{sc} = \Delta\nu$ that is calculated for a static beam. Any collective mode of oscillation produces similar frequency shifts, as will be seen in Part II.

We now examine these two modes in the nonlinear regime. The symmetric mode is driven by the symmetric gradient error $\Delta\nu_{sx} = \Delta\nu_{sz}$, and the antisymmetric mode is driven by the antisymmetric gradient error $\Delta\nu_{sx} = -\Delta\nu_{sz}$. When either gradient error is included in (3-3) and

(3-4), the equations can be solved by the same method that was used for the one-dimensional envelope equation. The results are presented here, while the calculations are outlined in Appendix B.

For the symmetric gradient error, we find symmetric solutions of the form

$$x^2 = z^2 = \sqrt{1 + A^2} + A \cos(n\phi + Q) \quad , \qquad (3\text{-}5)$$

where the slowly varying quantities A and Q satisfy the equation

$$\text{constant} = A \cos Q + \frac{2\Delta\nu}{\Delta\nu_s}\sqrt{1 + A^2} - 2\frac{\Delta\nu_{sc}}{\Delta\nu_s} \ell n\left(1 + \sqrt{1 + A^2}\right) \quad , \qquad (B13)$$

which specifies a trajectory in the two-dimensional A,Q space. The corresponding trajectories in $x - \frac{dx}{d\phi}$ space or $z - \frac{dz}{d\phi}$ space have the same form as those found for the one-dimensional beam (Fig. 7), but now the fixed points occur for $Q = 0,\pi$ and for values of A that satisfy

$$A = \mp \frac{1}{2}\frac{\Delta\nu_s}{\Delta\nu}\sqrt{1 + A^2} + \frac{\Delta\nu_{sc}}{\Delta\nu}\frac{\sqrt{1 + A^2} - 1}{A} \quad . \qquad (B16)$$

These fixed points describe a circular beam that oscillates with the periodicity of the gradient error. They are shown in the form of a response diagram in Fig. 10, which is again distorted from the linearized diagram so that only bounded solutions are possible. Note from (3-5) that the symmetric character of the normal mode solution ($\delta_x = \delta_z$) remains symmetric even in the nonlinear regime, the only effect of the nonlinearity being to limit its resonant amplitude.

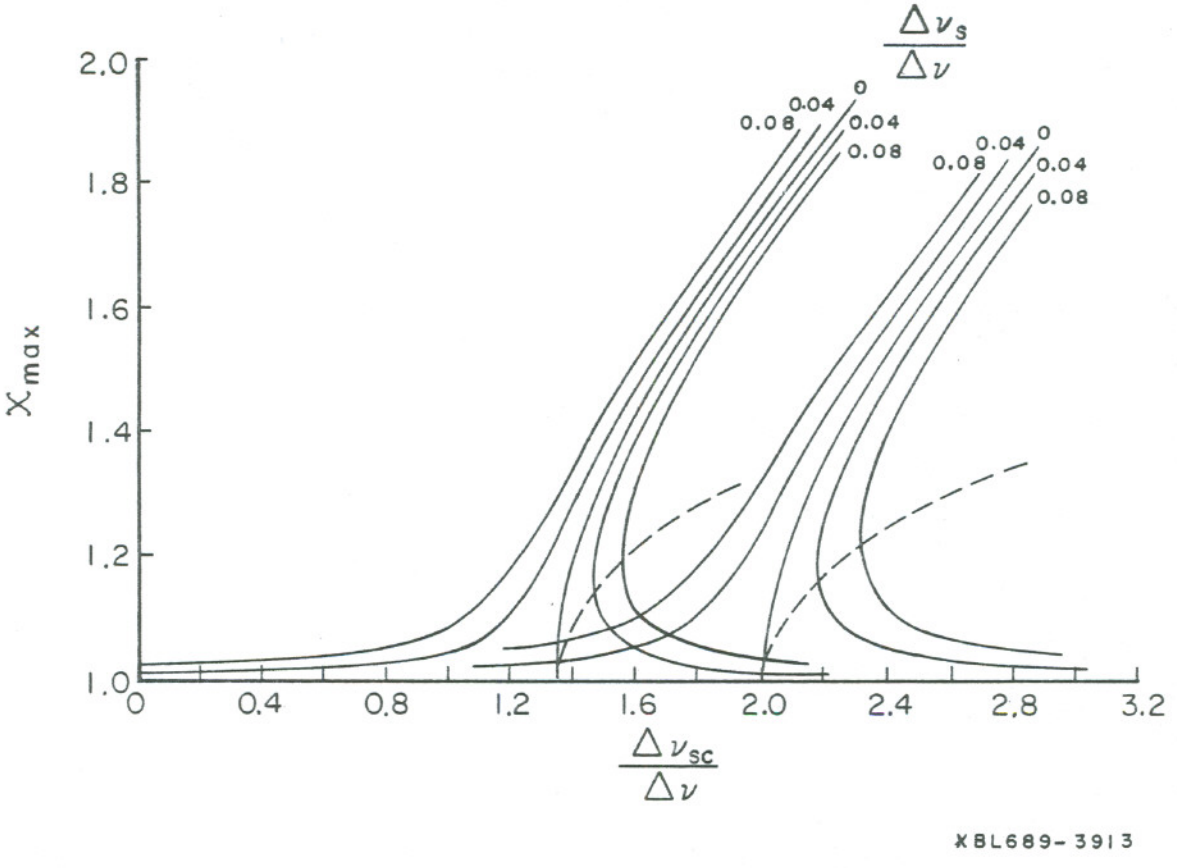

Fig. 10. The response curves for a symmetric gradient error, with resonance near $\Delta\nu_{sc} = 2\Delta\nu$, are superimposed on those for an antisymmetric gradient error, with resonance near $\Delta\nu_{sc} = \frac{4}{3}\Delta\nu$. For either case, $x_{max} = z_{max} = \left(\sqrt{1 + A^2} + A\right)^{\frac{1}{2}}$.

For the case of an antisymmetric gradient error, there are antisymmetric solutions of the form

$$x^2 = \sqrt{1 + A^2} + A \cos(n\phi + Q) \quad ,$$
$$z^2 = \sqrt{1 + A^2} - A \cos(n\phi + Q) \quad , \tag{3-6}$$

which describe an elliptical beam. Now A and Q satisfy

$$\text{constant} = A \cos Q + 2 \frac{\Delta\nu}{\Delta\nu_s} \sqrt{1 + A^2} - 2 \frac{\Delta\nu_{sc}}{\Delta\nu_s} \left[\ell n\, A - \frac{2}{\pi} \int \frac{K(k)}{k}\, dk \right] , \tag{B13}$$

where $K(k)$ is the complete elliptical integral of the first kind.[17] The resulting trajectories in $x - \frac{dx}{d\phi}$ or $z - \frac{dz}{d\phi}$ space again have the same form as those for the one-dimensional envelope, but now the fixed points occur for $Q = 0, \pi$ and for values of A that satisfy

$$A = \mp \frac{1}{2} \frac{\Delta\nu_s}{\Delta\nu} \sqrt{1 + A^2} + \frac{\Delta\nu_{sc}}{\Delta\nu} \frac{1}{k} \left[1 - \frac{2}{\pi} \frac{k^2}{A^2} K(k) \right] \quad , \tag{B16}$$

where $k = \dfrac{A}{\sqrt{1 + A^2}}$. They describe a beam that oscillates antisymmetrically with the periodicity of the gradient error, i.e., x is largest when z is smallest and vice versa, and are also shown in Fig. 10. For either mode of envelope oscillation, the $\Delta\nu_s = 0$ curves represent the free envelope oscillations that are periodic.

Note from (3-6) that the antisymmetric character of the normal-mode solution $(\delta_x = -\delta_z)$ is approximately maintained in the nonlinear

regime. Indeed, this is a general result: the character of the normal-mode solutions determined by the linearized envelope equations (the ratio $\frac{\delta_x}{\delta_z}$) is approximately maintained in the nonlinear regime, the main effect of the nonlinearity being to limit the resonant amplitudes of each mode.

The nonlinearity also produces an additional effect that is not predicted by linear theory, namely, it produces a weak coupling between a gradient error of one symmetry and a mode of envelope oscillation of opposite symmetry. Thus the response curves for the symmetric mode of oscillation in Fig. 10 are modified by the presence of an antisymmetric gradient error, and vice versa. Although this effect is small, it has been a source of confusion, so we briefly describe it here. We write the fixed points in the form

$$\begin{aligned} x^2 &= \sqrt{1 + A^2} + A\cos(n\phi + Q) \quad , \\ z^2 &= \sqrt{1 + A^2} - A\cos(n\phi - Q) \quad , \end{aligned} \tag{B18}$$

where for the symmetric fixed points, $Q = 0,\pi$, while for the antisymmetric fixed points, $Q = \frac{\pi}{2}, \frac{3\pi}{2}$. Figure 11a shows the fixed-point solutions in the absence of gradient errors, in other words the $\frac{\Delta\nu_s}{\Delta\nu} = 0$ curves of Fig. 10. They specify the amplitude dependence of the free envelope oscillations that are periodic. If now an antisymmetric gradient error is present, the antisymmetric fixed points still occur in the $Q = 0,\pi$ planes, but contrary to linear theory, the $\frac{\Delta\nu_s}{\Delta\nu} = 0$ curves for the symmetric fixed points are modified, as indicated in

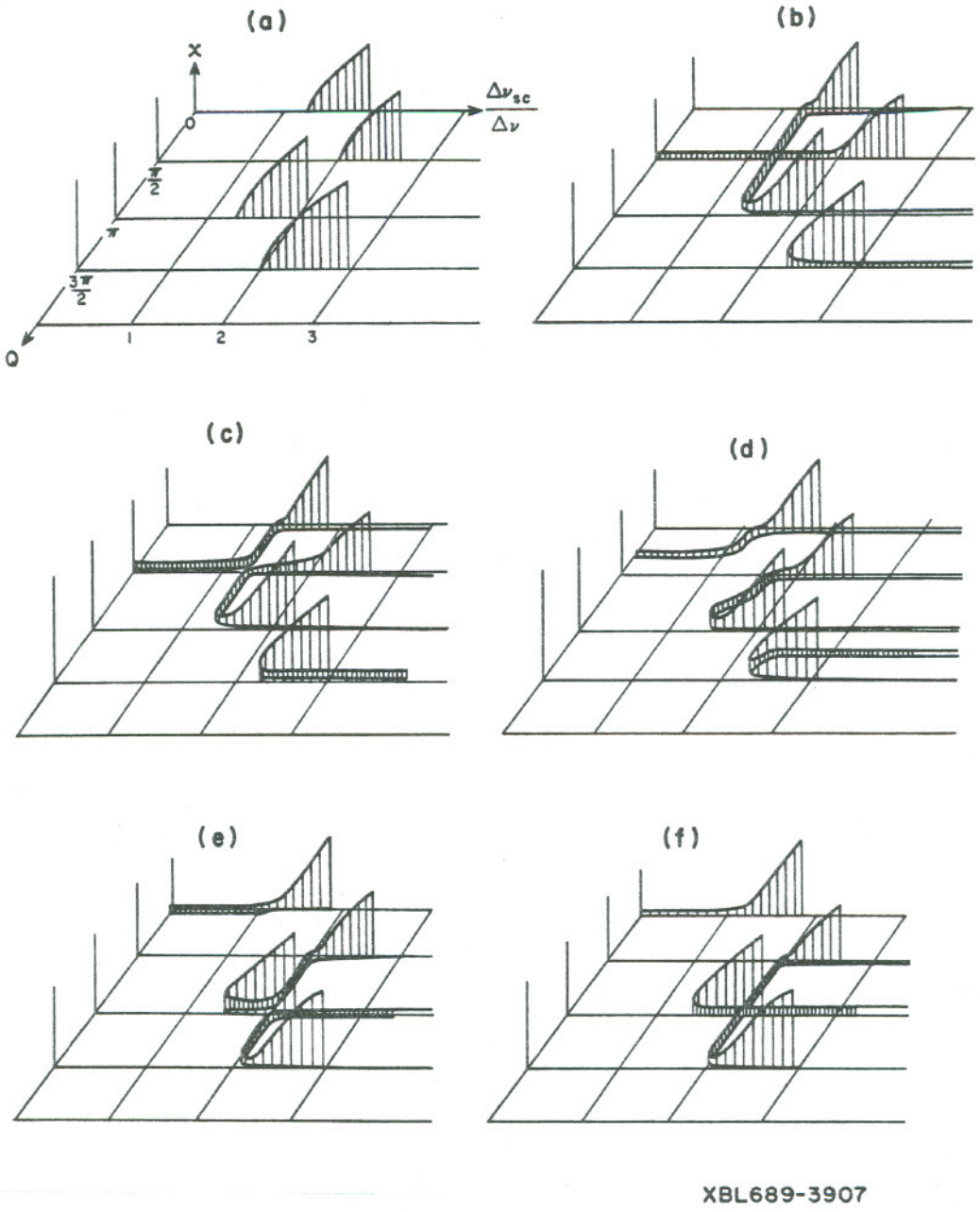

Fig. 11. The fixed points in the absence of gradient errors is shown in (a); the transition from a purely antisymmetric gradient error to a purely symmetric gradient error is shown in (b), (c), (d), (e), and (f).

Fig. 11b. The analogous situation occurs for the symmetric gradient error (Fig. 11f). This coupling between fixed points of one symmetry and gradient errors of opposite symmetry insures that the transition from a purely symmetric gradient error to a purely antisymmetric gradient error occurs in a continuous fashion, as indicated in Figs. 11 (c), (d), and (e). However, only the small-amplitude fixed points are affected, and in the following we neglect this weak nonlinear effect and assume that a mode of a given symmetry is affected only by driving terms of the same symmetry.

Resonance Crossing

If only one type of gradient error is present, the resonance crossing is similar to that for the one-dimensional beam. A nearly matched beam with $x \approx 1$, $z \approx 1$ and whose intensity is larger than the resonant value oscillates with small amplitude about a stable fixed point. If $\frac{\Delta\nu_{sc}}{\Delta\nu}$ decreases, the stable phase area around the fixed point shrinks and eventually the configuration point is forced onto the separatrix. The beam then oscillates with a larger amplitude that can be read directly from Fig. 12, which shows the maximum beam size for a point on the separatrix at the critical value of $\frac{\Delta\nu_{sc}}{\Delta\nu}$.

Note from Fig. 12 that the resonant growth for either mode of the two-dimensional beam is less than the resonant growth of the one-dimensional beam for the same value of $\frac{\Delta\nu_{s}}{\Delta\nu}$. This was to be expected, since the nonlinearity of the space-charge force is greater for the two-dimensional beam than for the one-dimensional beam.

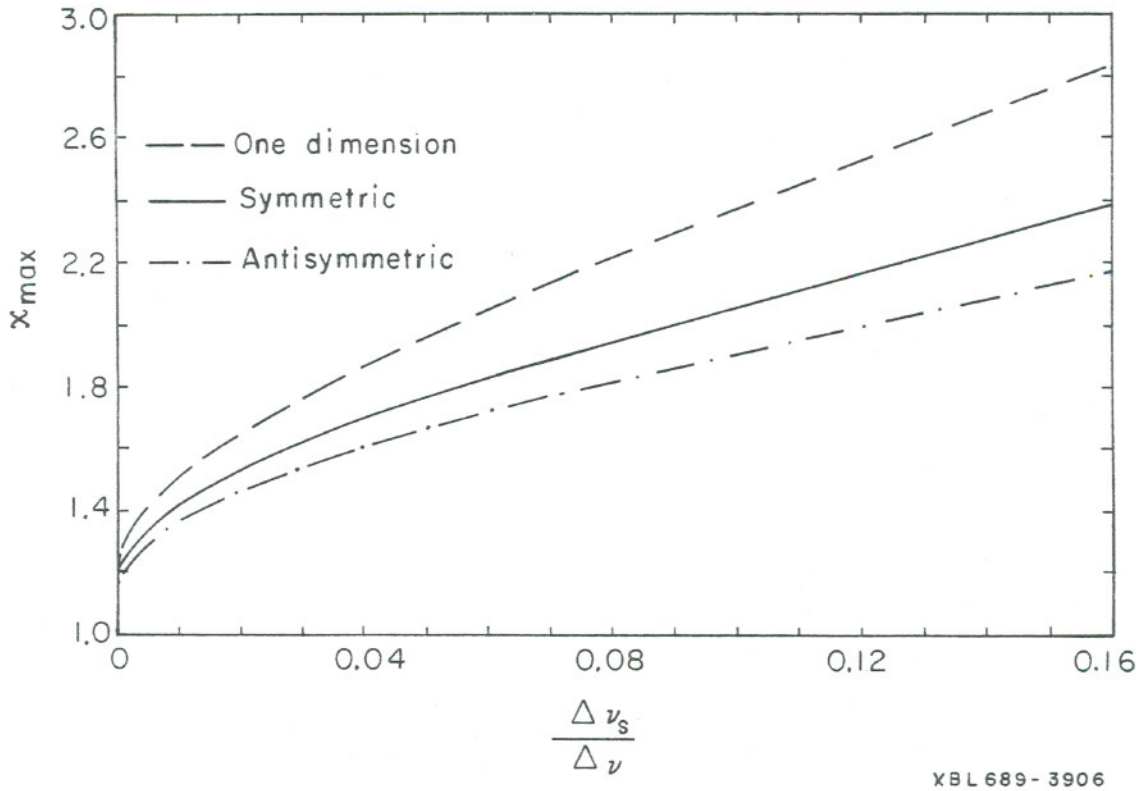

Fig. 12. The maximum beam size for a point on the separatrix at the critical value of $\frac{\Delta\nu_{sc}}{\Delta\nu}$ is shown for either mode of envelope oscillation for the cylindrical beam with a = b and $\nu_x = \nu_z$. For comparison, the maximum beam size for the one-dimensional beam is also shown (from Fig. 9).

If both types of gradient error are present, as is true in practice, both resonances may be crossed. One might estimate the total growth by adding the two separate growths from Fig. 12. However, an initially matched beam that crosses the first resonance ($\Delta\nu_{sc} = 2\Delta\nu$) will no longer be matched when it crosses the second resonance. If this mismatch is large, the total growth may be considerably larger than the sum of the two growths. On the other hand, we have so far neglected the adiabatic damping of the beam size due to the increase in $\sqrt{\beta\gamma}$, which may be large, depending on the acceleration program employed.

B. General Beam Configurations

In the remainder of this section, the envelope motion for other values of $\frac{a}{b}$ and $\frac{\nu_x}{\nu_z}$ is briefly examined. Fortunately, the effect of the nonlinearity can be largely separated from the linear effects, i.e., the normal mode solutions determined by the linearized envelope equations remain approximately valid in the nonlinear regime, the main effect of the nonlinearity being to cause the frequency of each normal mode to depend on its amplitude. Accordingly, we first examine the normal-mode solutions of the linearized envelope equations for several cases, before including the effect of nonlinearity.

We write the linearized envelope equations, omitting gradient errors, in the form

$$\frac{d^2\delta}{d\phi^2} + M\delta = 0 \quad , \tag{3-7}$$

where M is the two-by-two matrix

$$M = \begin{bmatrix} 4\nu_x^2 - \frac{2ab + 3b^2}{(a+b)^2}\omega_p^2 & \frac{b^2}{(a+b)^2}\omega_p^2 \\ \frac{a^2}{(a+b)^2}\omega_p^2 & 4\nu_z^2 - \frac{2ab + 3a^2}{(a+b)^2}\omega_p^2 \end{bmatrix}, \qquad (3\text{-}8)$$

and where $\delta = \begin{pmatrix} \delta_x \\ \delta_z \end{pmatrix}$ is related to x and z by

$$\begin{aligned} x &= 1 + \frac{b}{4(a+b)} \cdot \frac{\omega_p^2}{\nu_x} + \delta_x \quad , \\ z &= 1 + \frac{a}{4(a+b)} \cdot \frac{\omega_p^2}{\nu_z} + \delta_z \quad . \end{aligned} \qquad (3\text{-}9)$$

The normal-mode solutions have the form $\delta = \begin{pmatrix} \delta_x \\ \delta_z \end{pmatrix} e^{i\omega\phi}$, where

$$[M - \omega^2]\begin{pmatrix} \delta_x \\ \delta_z \end{pmatrix} = 0 \quad , \qquad (3\text{-}10)$$

and where ω satisfies $\det(M - \omega^2) = 0$.[18]

We have previously distinguished two limiting types of envelope motion, tightly coupled motion for which the x and z amplitudes are equal, $\delta_x = \pm \delta_z$, and loosely coupled motion for which one amplitude approaches zero while the other remains finite. We find from Eq. (3-7) that tightly coupled motion results if $\nu_z - \nu_x = \frac{a - b}{a + b} \cdot \frac{\omega_p^2}{4\nu}$ or if $\nu_z - \nu_x = 2\,\frac{a - b}{a + b} \cdot \frac{\omega_p^2}{4\nu}$, where $\nu = \frac{1}{2}(\nu_x + \nu_z)$. The former condition

produces a symmetric mode with $\delta_x = \delta_z$; the latter condition produces an antisymmetric mode with $\delta_x = -\delta_z$, and is identical to the condition that the individual particle frequencies $\nu_x - \Delta\nu_{scx}$ and $\nu_z - \Delta\nu_{scz}$ be equal. Both conditions are plotted in Fig. 13. As the parameters ν_x, ν_z, $\frac{b}{a}$, ω_p^2 depart from the curves in Fig. 13, the envelope motion approaches the one-dimensional case.

It is informative to examine a few special cases in detail. For a circular beam with $a = b$, the eigenfrequencies for either mode of envelope oscillation are

$$\omega_\pm^2 = 2\nu_x^2 + 2\nu_z^2 - \frac{5}{4}\omega_p^2 \pm \sqrt{(2\nu_x^2 - 2\nu_z^2)^2 + \frac{1}{16}\omega_p^4} \quad , \qquad (3\text{-}11)$$

and there are two limiting cases to consider. If $|2\nu_x^2 - 2\nu_z^2| \ll \frac{1}{4}\omega_p^2$, the eigenfrequencies and normal modes reduce to the tightly coupled case examined in (A),

$$\omega_+^2 = 4\nu^2 - \omega_p^2 \quad , \qquad \delta_+ = \begin{pmatrix} 1 \\ 1 \end{pmatrix} \quad ,$$

$$\omega_-^2 = 4\nu^2 - \frac{3}{2}\omega_p^2 \quad , \qquad \delta_- = \begin{pmatrix} 1 \\ -1 \end{pmatrix} \quad , \qquad (3\text{-}12)$$

where $\omega_p^2 = 4\nu\Delta\nu_{sc}$. This case requires that $|\nu_x - \nu_z| \ll \frac{1}{4}\Delta\nu_{sc}$. On the other hand if $|\nu_x - \nu_z| \gg \frac{1}{4}\Delta\nu_{sc}$, the eigenfrequencies and normal modes are

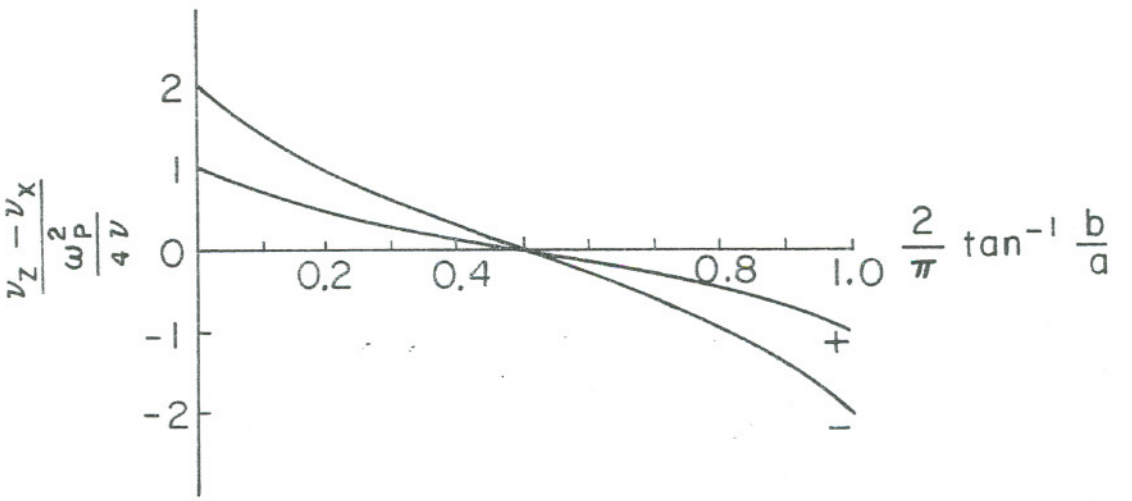

XBL689-3910

Fig. 13. The beam parameters are shown for which the x and z amplitudes of envelope oscillation are equal. The plus curve is the condition for the symmetric mode, the minus curve for the antisymmetric mode.

$$\omega_x^2 = 4\nu_x^2 - \frac{5}{4}\omega_p^2 , \qquad \delta_x = \begin{pmatrix} 1 \\ \epsilon \end{pmatrix} ,$$

$$\omega_z^2 = 4\nu_z^2 - \frac{5}{4}\omega_p^2 , \qquad \delta_z = \begin{pmatrix} \epsilon \\ 1 \end{pmatrix} , \tag{3-13}$$

where $\epsilon = \dfrac{\Delta\nu_{sc}}{4|\nu_x - \nu_z|} \ll 1$. For this case the frequency difference $|\nu_x - \nu_z|$ is sufficient to overcome the coupling due to the space-charge force, and the normal modes are one-dimensional. In practice $\Delta\nu_{sc} \approx \frac{1}{4}$, so that the dividing line between tightly coupled motion and loosely coupled motion occurs for a frequency difference of $|\nu_x - \nu_z| \approx \frac{1}{16}$. Thus, due to the weakness of the space-charge coupling, a relatively small departure from the curves of Fig. 13 suffices to produce one-dimensional motion.

Now consider the limit $\frac{b}{a} \to 0$, but keeping ab constant so that the charge density remains constant. The beam approaches a planar configuration, and

$$\omega_x^2 = 4\nu_x^2 - \frac{2b}{a}\omega_p^2 , \qquad \delta_x = \begin{pmatrix} 4\nu_x^2 - 4\nu_z^2 + 3\omega_p^2 \\ \omega_p^2 \end{pmatrix} ,$$

$$\omega_z^2 = 4\nu_z^2 - 3\omega_p^2 , \qquad \delta_z = \begin{pmatrix} 0 \\ 1 \end{pmatrix} . \tag{3-14}$$

In this case the δ_x mode can have either of the tightly coupled forms $\begin{pmatrix} 1 \\ 1 \end{pmatrix}$ or $\begin{pmatrix} 1 \\ -1 \end{pmatrix}$ for suitable values of $|\nu_x - \nu_z|$ and ω_p^2, in agreement

with Fig. 13. However, as $\frac{b}{a}$ approaches zero, larger and larger intensities are required to excite this mode. i.e., to shift ω_x to the integral frequency n of the gradient error. In the limit $\frac{b}{a} = 0$, only the δ_z mode can be excited, and this mode is identical to the one-dimensional mode examined in Section 2. In fact, the complete nonlinear envelope equations reduce to the one-dimensional form

$$\frac{d^2x}{d\phi^2} + K_x(\phi)x - \frac{\nu_x^2}{x^3} = 0 \quad , \tag{3-15}$$

$$\frac{d^2z}{d\phi^2} + K_z(\phi)z - \frac{\nu_z^2}{z^3} - \frac{\omega_p^2}{x} = 0 \quad , \tag{3-16}$$

in this limit. The space-charge forces affect only the z motion, and if ν_x is sufficiently far from a stopband that $x = 1$, Eq. (3-16) reduces to the one-dimensional envelope equation (2-6).

We conclude from these examples that the envelope motion will be one-dimensional for a wide range of beam parameters; in fact, due to the weakness of the space-charge coupling and because of the changing environment within the beam, the envelope motion is more likely to be one-dimensional than two-dimensional.

We now briefly examine the effect of the nonlinearity. We consider cases for which a is larger than or equal to b, and for which ν_z is closer to a half-integer than ν_x, so that $\lambda = \frac{\nu_z - \frac{n}{2}}{\nu_x - \frac{n}{2}} \leqslant 1$. Then the resonant amplitudes are larger in the

z direction than in the x direction, and this is usually the more serious case.

We construct simplified response diagrams for several values of $\frac{b}{a}$ and λ. The usual linearized response diagrams have a vertical asymptote (the $\Delta\nu_{sx} = \Delta\nu_{sz} = 0$ curve) at each of the two resonant intensities, and the $\Delta\nu_{sx} \neq 0$, $\Delta\nu_{sz} \neq 0$ response curves approach these asymptotes as the beam intensity approaches the resonant values. The main effect of the nonlinearity is to cause the frequency of each mode of envelope oscillation to depend on its amplitude, which distorts these linear response curves so that only bounded solutions are possible. For simplicity we consider only the distortion of the $\Delta\nu_{sx} = \Delta\nu_{sz} = 0$ asymptotes. We show in Appendix B that these curves are specified by

$$x^2 = \sqrt{1 + A^2} + A \sin(n\phi + Q) \quad ,$$
$$z^2 = \sqrt{1 + B^2} \pm B \sin(n\phi + Q) \quad , \tag{B20}$$

where A and B are determined by the integral equations

$$A = \frac{\omega_p^2}{2\nu_x \Delta\nu_x} \cdot \frac{b}{2\pi} \int_0^{2\pi} \frac{A + \sqrt{1 + A^2} \sin u}{x(ax + bz)} \, du \quad ,$$
$$B = \frac{\omega_p^2}{2\nu_z \Delta\nu_z} \cdot \frac{a}{2\pi} \int_0^{2\pi} \frac{B \pm \sqrt{1 + B^2} \sin u}{z(ax + bz)} \, du \quad , \tag{B21}$$

where $u = n\phi + Q$, $\Delta\nu_x = \nu_x - \frac{n}{2}$, and $\Delta\nu_z = \nu_z - \frac{n}{2}$. These equations were solved numerically, and the solutions are shown in Fig. 14.

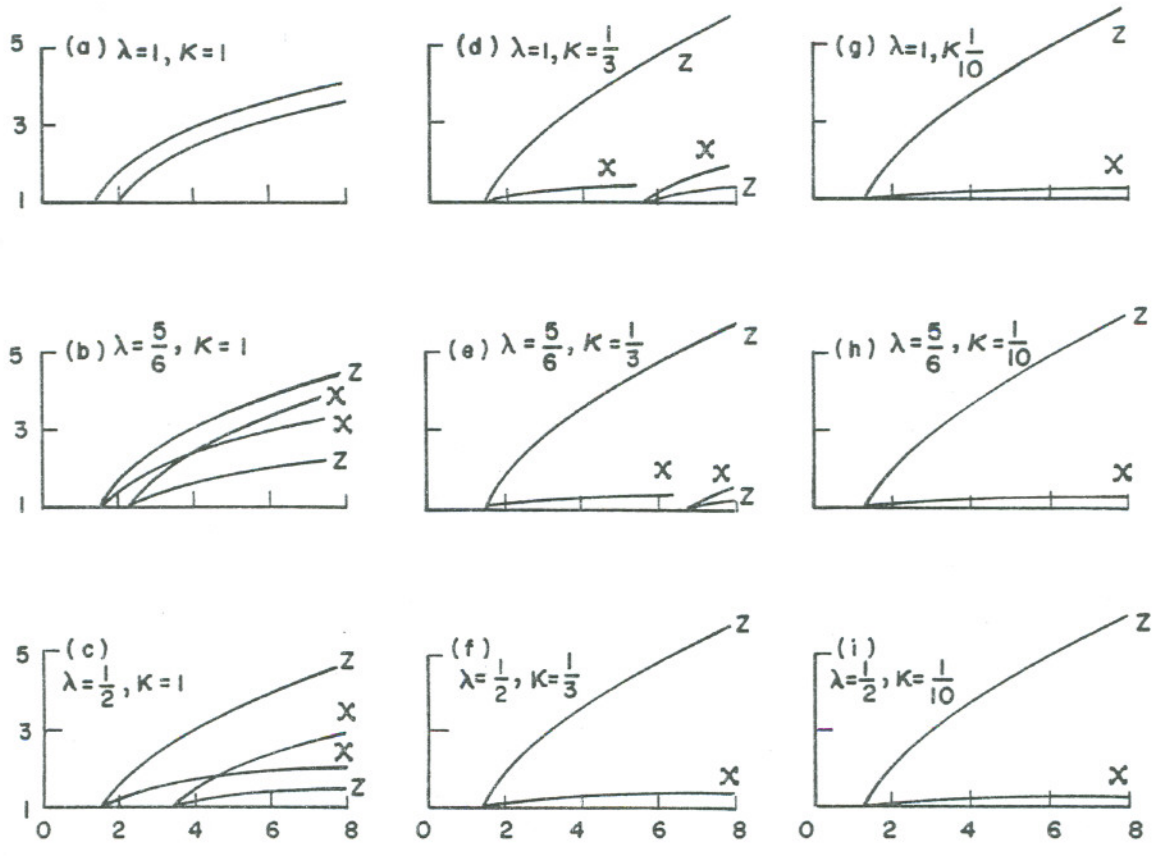

XBL689 - 3905

Fig. 14. The $\Delta\nu_{sx} = \Delta\nu_{sz} = 0$ asymptotes are shown for various values of the parameters $\lambda = \dfrac{\nu_z - \frac{n}{2}}{\nu_x - \frac{n}{2}}$ and $\kappa = \dfrac{b}{a}$. The ordinate is x_{max} or z_{max}; the abscissa is $\dfrac{\Delta\nu_{scz}}{\Delta\nu_z}\left(= \dfrac{1}{\kappa\lambda}\dfrac{\Delta\nu_{scx}}{\Delta\nu_x}\right)$.

Figure 14a shows the familiar case of equal frequencies and equal emittances (the $\frac{\Delta\nu_s}{\Delta\nu} = 0$ curves of Fig. 10). There are two resonances, corresponding to the two modes of envelope oscillation, and for each mode, the amplitude of the x motion is equal to the amplitude of the z motion. For the other cases, the two resonant intensities are further apart, and the amplitudes of the x and z motions are no longer equal. Because of the choice of parameters $\frac{\Delta\nu_z}{\Delta\nu_x} \leqslant 1$, $\frac{b}{a} \leqslant 1$, the largest amplitude occurs for the z direction and for the lower-intensity mode. As the frequencies become different, but a is kept equal to b, Fig. 14 (b) and (c) result, and the solutions approach the limiting one-dimensional modes $\delta_x = \begin{pmatrix} 1 \\ \epsilon \end{pmatrix}$ and $\delta_z = \begin{pmatrix} \epsilon \\ 1 \end{pmatrix}$ that were found before. In the other limit, $\frac{b}{a}$ approaches zero and the solutions also approach the one-dimensional case. In particular, the curves of Fig. 14 (g), (h), and (i) are indistinguishable from the $\frac{\Delta\nu_s}{\Delta\nu} = 0$ asymptote of the one-dimensional beam (Fig. 8). The intermediate case of an aspect ratio $\frac{b}{a} = \frac{1}{3}$ is shown in Fig. 14 (d), (e), and (f). In this case the lower-intensity mode is also very similar to that of the one-dimensional beam.

Summary

We have investigated the envelope motion for a uniformly charged cylindrical beam. Because of its two degrees of freedom, the envelope has two modes of oscillation that can be excited by gradient errors. The solutions for a beam with $\nu_x = \nu_z$ and $E_x = E_z$ were presented in detail; it has a symmetric mode of oscillation that is excited near the

intensity $\Delta\nu_{sc} = 2\Delta\nu$, and an antisymmetric mode that is excited near $\Delta\nu_{sc} = \frac{4}{3}\Delta\nu$. For any type of beam, the process of resonance crossing is similar to that for the one-dimensional beam. If the resonances are crossed in the direction of decreasing $\frac{\Delta\nu_{sc}}{\Delta\nu}$, the beam grows a finite amount, whereas if the resonance is crossed in the opposite direction, the beam continues to grow as $\frac{\Delta\nu_{sc}}{\Delta\nu}$ increases. As $\frac{b}{a}$ or $\frac{\Delta\nu_z}{\Delta\nu_x}$ approaches zero, the resonances become further separated and the envelope motion becomes one-dimensional. In fact for an aspect ratio of $\frac{b}{a} = \frac{1}{3}$, or for $\frac{\Delta\nu_z}{\Delta\nu_x} < \frac{1}{2}$, the resonance in the z direction dominates and the beam motion is essentially one-dimensional.

4. Conclusion and Applications

We have considered the effect of gradient errors on a beam of charged particles in an alternating gradient synchrotron. Usually, gradient errors are assumed to limit the number of particles that can be accelerated. This limit (the tranverse incoherent space charge limit) is calculated by assuming that the beam size remains constant; then the number of particles that can be accelerated is limited to that number which just lowers the effective betatron frequency to an integer or half-integer. Actually, the diameter of the beam depends on the oscillation amplitudes of the individual particles, and if a gradient error causes these amplitudes to grow, the beam size also grows. Thus the usual calculation is not self-consistent.

In Section 1 self-consistent equations of motion for the beam envelope are derived for beams with one and two degrees of freedom. We assume that all the particles within the beam have the same azimuthal velocity and execute betatron oscillations about the same equilibrium orbit, and that only linear forces act on the individual particles. The last assumption requires that the charge density within the beam be uniform and that the nonlinear components of the image force be neglected. The resulting envelope equations are nonlinear because of the nonlinear dependence of the space charge force on the shape and size of the beam.

These envelope equations were solved in Sections 2 and 3. For small amplitude oscillations of the one dimensional (planar) beam, the beam oscillates with the frequency $2(\nu - \frac{3}{4}\Delta\nu_{sc})$, and resonance occurs

for $n = 2(\nu - \frac{3}{4}\Delta\nu_{sc})$, i.e., for the beam intensity corresponding to $\Delta\nu_{sc} = \frac{4}{3}\Delta\nu$. However, for larger amplitudes of oscillation, the frequency of oscillation depends on amplitude as well as on intensity; for fixed intensity, the frequency increases with amplitude. In consequence, a slow traversal of the resonance in the direction of increasing $\frac{\Delta\nu_{sc}}{\Delta\nu}$ will cause the beam to grow arbitrarily large: near the resonant condition n = oscillation frequency, the amplitude increases, which causes the oscillation frequency to increase until the resonant condition is no longer satisfied; a further increase in $\Delta\nu_{sc}$, or decrease in $\Delta\nu$, lowers the oscillation frequency and restores the resonance condition, which causes the beam amplitude to again increase, and so on. On the other hand, a slow traversal of the resonance in the direction of decreasing $\frac{\Delta\nu_{sc}}{\Delta\nu}$ causes only a finite increase in beam size. The amount of beam growth depends only on the ratio $\frac{\Delta\nu_s}{\Delta\nu}$ and is less than 50% for $\frac{\Delta\nu_s}{\Delta\nu} \leqslant 0.01$.

The resonant behavior of the two dimensional (cylindrical) beam is very similar. In this case two resonances are possible, although for a wide range of beam parameters, including most practical configurations, only one resonance occurs. An adiabatic resonance crossing in the direction of increasing $\frac{\Delta\nu_{sc}}{\Delta\nu}$ causes an arbitrarily large increase in beam size, whereas a crossing in the direction of decreasing $\frac{\Delta\nu_{sc}}{\Delta\nu}$ causes only a finite beam growth, which is less than the one-dimensional beam growth for the same value of $\frac{\Delta\nu_s}{\Delta\nu}$.

We conclude that gradient errors will not limit beam intensity or cause particle loss, provided slow resonance crossings in the

direction of increasing $\frac{\Delta\nu_{sc}}{\Delta\nu}$ are avoided, and provided the ratio $\frac{\Delta\nu_s}{\Delta\nu}$ is sufficiently small at the resonant intensity.

Application to AGS

As an application of these results, we examine the two modes of envelope oscillation for the Brookhaven AGS. The relevant parameters are obtained from van Steenbergen,[19] who has measured the vertical phase space emittance and density distribution in the energy range 50-400 MeV.

First consider the situation immediately after the injection, when 7.7×10^{12} particles occupy most of the machine circumference ($B \approx 1$). At this time, the betatron frequencies in the absence of space charge are $\nu_x = 8.35$ and $\nu_z = 8.92$ (as extrapolated from Fig. 6 of van Steenbergen), and the vertical emittance is $\pi E_z = 11.6$ cm-mrad. Thus $b = \sqrt{\frac{E_z R}{\nu_z}} = 2.3$ cm ($R = 128$ m), and assuming an aspect ratio $\frac{a}{b} = 2$, we find $\Delta\nu_{scx} = 0.14$ and $\Delta\nu_{scz} = 0.28$ (from the equations following 3-2). These are the space-charge-induced frequency shifts for the individual particles within the matched beam, with the constant size $a = 4.6$ cm and $b = 2.3$ cm. Gradient errors cause the beam to oscillate, and for small amplitudes, the two modes of envelope oscillation are determined by Eqs. (3-8) and (3-10). In this case, the modes are nearly one-dimensional, and we find

$$\omega_x = 2\nu_x - \frac{7}{6}\Delta\nu_{scx}, \qquad \delta_x = \begin{pmatrix} 1 \\ \epsilon \end{pmatrix}, \tag{4-1}$$

$$\omega_z = 2\nu_z - \frac{4}{3}\Delta\nu_{scz} , \qquad \delta_z = \begin{pmatrix} \epsilon \\ 1 \end{pmatrix} , \qquad (4\text{-}2)$$

where $\epsilon \approx 0.1$. For the above parameters, $\frac{1}{2}\omega_x = 8.26$ and $\frac{1}{2}\omega_z = 8.73$, and these frequencies are well removed from the

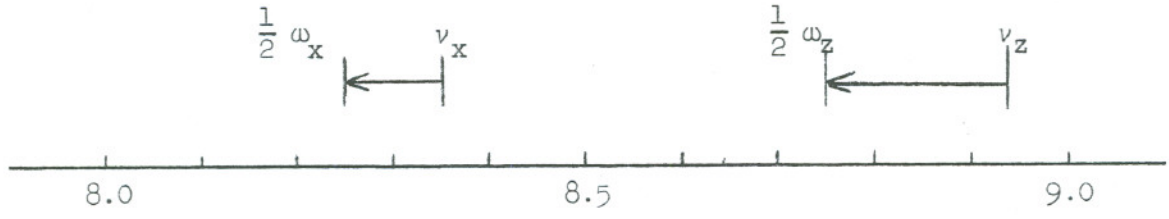

half-integral resonant values; an intensity of 17×10^{12} particles is required to shift $\frac{1}{2}\omega_z$ to the nearest value, $8\frac{1}{2}$. Therefore gradient errors are not expected to cause particle loss in this region. (These results are strictly valid only for uniformly charged beams, whereas the AGS beam has a Gaussian charge distribution. We find in Part II that the frequency shifts for the Gaussian beam are approximately 1/3 larger than those for the uniform beam, and thus the lowest resonant intensity is more nearly 13×10^{12} particles.[20])

During the first few synchrotron oscillations after injection (during the capture process), about 60% of the injected beam is lost, and smaller losses continue until 15 msec ($\beta\gamma = 0.5$). At this time, 1.9×10^{12} particles remain, and these are assumed to occupy 1/4 of the machine circumference. After this time, small particle loss occurs in two regions: the first near 20 msec ($\beta\gamma = 0.6$) is associated with a 20% increase in the normalized vertical emittance, while the second near

30 msec ($\beta\gamma = 0.8$) is associated with a 10% increase in the normalized vertical emittance. The frequencies ω_x and ω_z have been calculated for these times, using $N = 1.9 \times 10^{12}$, $B = 0.25$, and the measured values of πE_z, and they are included in Table I.

Because the zero intensity betatron frequencies ν_x and ν_z change during acceleration, the $\omega_x = 17$ resonance is crossed near $\beta\gamma = 0.8$, in agreement with the observed particle loss at 30 msec. The resonance crossing is approximately adiabatic since $\Delta\nu_{scx}/\Delta\nu_x$ changes by 0.1 during 600 revolutions, and is in the direction of decreasing $\Delta\nu_{scx}/\Delta\nu_x$. The observed 10% increase in the normalized vertical emittance is consistent with a stopband width of $\Delta\nu_s = 0.002$; in this case, $\frac{\Delta\nu_s}{\Delta\nu_x} = 0.04$, and the beam grows 100% in the x direction and about 10% in the z direction (using Fig. 3-3 and assuming that the δ_x mode retains its one-dimensional form in the nonlinear regime).

Further experiments are necessary to confirm this connection between the particle loss at 30 msec and the $\omega_x = 17$ resonance crossing. For example, if the stopband is enlarged by deliberately exciting a 17th harmonic gradient error in the machine lattice, the beam growth should exceed the available horizontal aperture and large losses should occur about 30 msec after injection.

Table I. AGS parameters near injection

$\beta\gamma$	a(cm)	$\Delta\nu_{scz}$	ν_z	ν_x	$\frac{1}{2}\omega_x$	$\frac{1}{2}\omega_z$
0.50	3.8	0.18	8.88	8.46	8.76	8.41
0.60	3.2	0.16	8.86	8.50	8.75	8.45
0.70	2.8	0.15	8.84	8.53	8.74	8.49
0.80	2.6	0.13	8.83	8.55	8.75	8.51
0.90	2.4	0.10	8.83	8.57	8.76	8.54
1.00	2.3	0.09	8.82	8.58	8.77	8.55

PART II. COLLECTIVE OSCILLATIONS OF ONE-DIMENSIONAL BEAMS CONFINED BY HARMONIC POTENTIALS

In Part I we considered only one mode of collective oscillation that occurs in only one type of beam, namely the quadrupole mode that is excited in uniformly charged beams by gradient errors. These restrictions enabled us to examine the large-amplitude nonlinear effects of space charge. In this Part we examine the other modes of collective oscillation that occur in both uniform and nonuniform beams. We restrict our attention, however, to small-amplitude oscillations and for simplicity to one-dimensional beams.

In Section 1, we use the linearized Vlasov equation to find all the normal modes and eigenfrequencies for the uniformly charged beam; in Section 2, the resulting mode structure is compared with that found by Ehrman[6] for an approximately uniform beam, and with that found by Weibel[21] for a neutralized beam (plasma) with a Gaussian charge distribution.

Before proceeding to these cases, it is informative to consider the seemingly trivial case in which the Coulomb interaction is turned off. In the absence of space charge, the equation of motion for the individual particles is

$$\frac{d^2x}{d\phi^2} + \nu_0^2 x = 0 \quad ,$$

where the symbol ν_0 will be used in the remainder of this paper to designate the unperturbed betatron frequency. Any particle distribution

rotates rigidly in the $x - \frac{1}{\nu_0}\frac{dx}{d\phi}$ space with the frequency ν_0, and has the form $f = f(r, \nu_0\phi + \theta)$, where r and θ are defined in Fig. 15. The normal modes are found by a double decomposition of f:

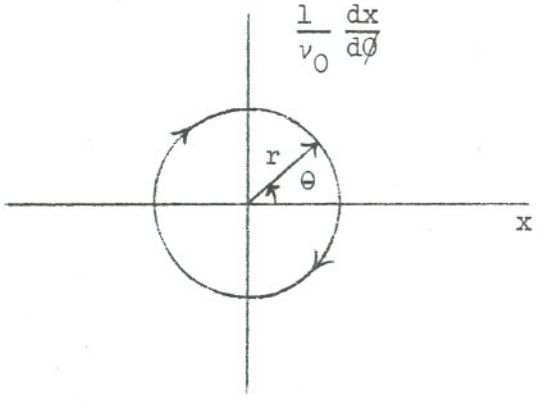

Fig. 15.

the second argument of f is expanded in a Fourier series $\sum_n g_n(r)e^{-in(\nu_0\phi+\theta)}$ where for each n, $g_n(r)$ is an arbitrary function of r and may in turn be expanded in a complete set of functions, $g_n(r) = \sum_m g_{mn}(r)$. Thus there are a two-fold infinity of normal modes of the form

$$f_{mn}(r,\theta,\phi) = g_{mn}(r)\, e^{-in\theta}\, e^{-i\omega_{mn}\phi}$$

where the eigenfrequencies $\omega_{mn} = n\nu_0$ are harmonics of the unperturbed betatron frequency. Each eigenfrequency is infinitely degenerate.

In the presence of space charge, but on the assumption that the space-charge forces are small in comparison with the external focusing forces, each eigenvalue is split into infinitely many different eigenvalues that are clustered near the value $n\nu_0$, and the new eigenfunctions are mixtures of the unperturbed eigenfunctions. Since the unperturbed eigenfunctions and the form of the space-charge interaction (Maxwell's equations) are known, the perturbed eigenvalues and eigenfunctions can be found by stationary perturbation methods.[22] However, the unperturbed eigenfunctions are infinitely degenerate, so that an infinite-order matrix must first be diagonalized. In any event the form of the eigenvalue spectrum is clear: the eigenvalues are discrete and occur in clusters near the value $n\nu_0$.

1. Normal Modes for the Uniformly Charged Beam

Formulation of the Problem

The Vlasov and Poisson equations can be written in the form

$$\frac{\partial f}{\partial \phi} + v \frac{\partial f}{\partial x} + [-\nu_0^2 x + \omega_p^2 \mathcal{E}(x, \phi)] \frac{\partial f}{\partial v} = 0 \quad , \tag{1-1}$$

$$\frac{\partial \mathcal{E}}{\partial x} = 2 \int f(x, v, \phi)\, dv \quad , \tag{1-2}$$

where $v = \frac{dx}{d\phi}$, and x measures distance from the median plane in units of the half-width of the stationary beam, a. The distribution function $f(x, v, \phi)$ is normalized to unity, and the quantity $\omega_p^2 = \frac{4\pi e^2 R^2}{\gamma^3 m v_p^2} \cdot \frac{N_l}{2a}$ (the plasma frequency) has previously been defined as $2\nu_0 \Delta\nu_{sc}$ [Eq. (2-8), Part I].

The stationary solution of (1-1) and (1-2) that has a uniform charge density is

$$f_0(x,v) = \frac{1}{2\pi\nu\sqrt{1 - x^2 - \frac{v^2}{\nu^2}}} , \qquad \mathcal{E}_0(x) = x , \tag{1-3}$$

where $\nu = \sqrt{\nu_0^2 - \omega_p^2} \approx \nu_0 - \Delta\nu_{sc}$, will be used in the remainder of this paper to designate the effective betatron frequency for the individual particles within the stationary distribution. In the $x - \frac{v}{\nu}$ space, the particles move in circular orbits, and the stationary distribution rotates rigidly with the frequency ν.

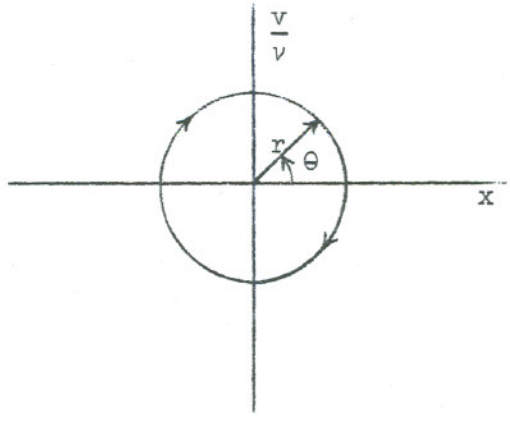

Fig. 16.

Oscillations of this distribution are described by the perturbed distribution $f(x, v, \phi) = f_0(x, v) + f_1(x, v, \phi)$, which gives rise to a perturbed electric field, $\mathcal{E}(x, \phi) = \mathcal{E}_0(x) + \mathcal{E}_1(x, \phi)$. As in Part I, we neglect the magnetic field components that arise from the transverse particle velocities. The evolution of $f_1(x, v, \phi)$ is governed by the Vlasov equation (1-1), which we linearize about $f_0(x, v)$:

$$\frac{\partial f_1}{\partial \phi} + v \frac{\partial f_1}{\partial x} - \nu^2 x \frac{\partial f_1}{\partial v} = - \omega_p^2 \mathcal{E}_1(x, \phi) \frac{\partial f_0}{\partial v} \quad . \tag{1-4}$$

The left-hand side of (1-4) is the total derivative of f_1 along an unperturbed orbit, and consequently we can invert (1-4) and write f_1 in terms of an integral of the right-hand side over an unperturbed orbit.[21] We do this explictly by writing (1-4) in terms of the polar coordinates defined in Fig. 16:

$$\frac{\partial f_1}{\partial \phi} - \nu \frac{\partial f_1}{\partial \theta} = - \frac{\omega_p^2}{\nu} \mathcal{E}_1(r \cos \theta, \phi) \sin \theta \frac{df_0}{dr} \quad . \tag{1-5}$$

For the normal mode solutions $f_1 = f(r, \theta)e^{-i\omega\phi}$, $\mathcal{E}_1 = \mathcal{E}(r \cos \theta)e^{-i\omega\phi}$, (1-5) becomes

$$e^{-i\frac{\omega}{\nu}\theta} \frac{d}{d\theta}[e^{i\frac{\omega}{\nu}\theta} f(r, \theta)] = \frac{\omega_p^2}{\nu^2} \mathcal{E}(r \cos \theta) \sin \theta \frac{df_0}{dr} \quad . \tag{1-6}$$

Since the function $f(r, \theta)$ must be periodic in θ, $f(r, \theta) = f(r, \theta + 2\pi)$, the unique solution of (1-6) is

$$f(r, \theta) = \frac{\omega_p^2}{\nu^2} \cdot \frac{df_0}{dr} \cdot \frac{e^{-i\frac{\omega}{\nu}\theta}}{1 - e^{-2\pi i\frac{\omega}{\nu}}} \int_{\theta-2\pi}^{\theta} e^{i\frac{\omega}{\nu}\theta'} \mathcal{E}(r \cos \theta') \sin \theta' \, d\theta', \tag{1-7}$$

provided $\frac{\omega}{\nu}$ is not an integer. The case of integer values of $\frac{\omega}{\nu}$ is considered later. Equation (1-7) can be written in terms of the Cartesian variables x and v as

$$f(x, v) = \frac{1}{v} \cdot \frac{\partial f_0}{\partial v} \cdot \frac{\omega_p^2}{e^{2\pi i \frac{\omega}{\nu}} - 1} \int_0^{2\pi} e^{i\frac{\omega}{\nu}u} \mathcal{E}(x') \frac{v'}{\nu} du \quad , \tag{1-8}$$

where $u = \theta' - \theta$ and

$$\begin{aligned} x' &= x \cos u - \frac{v}{\nu} \sin u \quad , \\ v' &= \nu x \sin u + v \cos u \quad . \end{aligned} \tag{1-9}$$

Equation (1-8) specifies $f(x, v)$ as an integral over the unperturbed orbit.

The perturbed electric field $\mathcal{E}_1(x, \phi)$ is related to $f_1(x, v, \phi)$ by Poisson's Equation (1-2), or alternatively by Maxwell's second equation,

$$\frac{\partial \mathcal{E}_1}{\partial \phi} = -2 \int_{-\infty}^{\infty} v f(x, v, \phi) \, dv \quad , \tag{1-10}$$

which follows immediately from Poisson's equation and the continuity equation for charge and current density. Using (1-8) and (1-10), we obtain a single integral equation for $\mathcal{E}(x)$:

$$i\omega \mathcal{E}(x) = \frac{2\omega_p^2}{e^{2\pi i \frac{\omega}{\nu}} - 1} \int_{-\infty}^{\infty} dv \frac{\partial f_0}{\partial v} \int_0^{2\pi} e^{i\frac{\omega}{\nu}u} \mathcal{E}(x') \frac{v'}{\nu} du \quad , \tag{1-11}$$

where x' and v' are given by (1-9).

General Solution

We solve (1-11) by performing two integrations by parts.[23] First integrate over v so that

$$i\omega \mathcal{E}(x) = \frac{2\omega_p^2}{e^{2\pi i\frac{\omega}{\nu}} - 1} \int_{-\infty}^{\infty} dv\, f_0 \int_0^{2\pi} e^{i\frac{\omega}{\nu}u}$$

OR

$$\times \left[-\frac{\cos u}{\nu} \mathcal{E}(x') \mp \frac{\sin u}{\nu} \frac{d\mathcal{E}(x')}{du} \right] du \quad , \quad (1\text{-}12)$$

where the integrated terms are zero at the limits $v = \pm \infty$. Then integrate by parts over u to eliminate $\frac{d\mathcal{E}}{du}$:

$$\mathcal{E}(x) = \frac{2\omega_p^2/\nu^2}{e^{2\pi i\frac{\omega}{\nu}} - 1} \int_{-\infty}^{\infty} dv\, f_0 \int_0^{2\pi} e^{i\frac{\omega}{\nu}u} \mathcal{E}(x') \sin u\, du \quad . \quad (1\text{-}13)$$

We eliminate the function $f_0 = \frac{1}{2\pi}[\nu^2(1 - x^2) - v^2]^{-\frac{1}{2}}$ from (1-13) by replacing v by $\mp \nu\sqrt{1 - x^2}\cos\eta$, so that

$$\mathcal{E}(x) = \frac{1}{2\pi} \cdot \frac{\omega_p^2/\nu^2}{e^{2\pi i\frac{\omega}{\nu}} - 1} \int_0^{2\pi} d\eta \int_0^{2\pi} e^{i\frac{\omega}{\nu}u}$$

$$\times \mathcal{E}(x\cos u + \sqrt{1 - x^2}\sin u\cos\eta)\sin u\, du. \quad (1\text{-}14)$$

Finally replace x with $\cos \xi$, so that

$$\mathcal{E}(\cos \xi) = \frac{\omega_p^2}{2\pi\nu^2} \cdot \frac{1}{e^{2\pi i \frac{\omega}{\nu}} - 1} \int_0^{2\pi} d\eta \int_0^{2\pi} e^{i\frac{\omega}{\nu}u} \mathcal{E}(\cos \psi)\, du \quad , \tag{1-15}$$

where $\cos \psi = \cos \xi \cos u + \sin \xi \sin u \cos \eta$. The angle ψ will be recognized as the angle between two vectors with polar coordinates η, ξ and 0, u respectively, as shown in Fig. 17.[24]

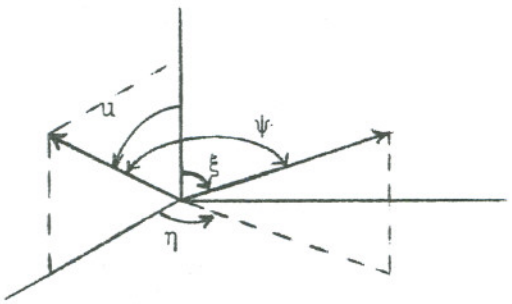

Fig. 17.

It is now easy to show that the solutions to (1-15) are just Legendre polynomials. We use the addition theorem for spherical harmonices to write

$$P_n(\cos \psi) = \frac{4\pi}{2n+1} \sum_m Y^*_{mn}(\xi, \eta)\, Y_{mn}(u, 0) \quad , \tag{1-16}$$

where the integration over η in (1-15) insures that only the $m = 0$ term $P_n(\cos \xi)\, P_n(\cos u)$ contributes to the sum. Thus, if $\mathcal{E}_{n+1}(x) = P_n(x)$, Eq. (1-15) is satisfied identically provided

$$K_{n+1}(\omega) \equiv \frac{\omega_p^2/\nu^2}{e^{2\pi i\frac{\omega}{\nu}} - 1} \int_0^{2\pi} e^{i\frac{\omega}{\nu}u} P_n(\cos u) \sin u \, du = 1, \tag{1-17}$$

which specifies the eigenfrequencies ω. A few of the functions $K_n(\omega)$ are included in Table II; the rest may be found by using the recursion relation

$$K_n(\omega) = \frac{\omega^2 - (n-3)^2\nu^2}{\omega^2 - n^2\nu^2} K_{n-2}(\omega) \quad . \tag{1-18}$$

The eigenfunctions for the perturbed electric field are therefore the Legendre polynomials

$$\mathcal{E}_m(x) = P_{m-1}(x) , \quad \text{for } m = 1,2,3,\cdots, \tag{1-19}$$

and for each value of m, the corresponding eigenfrequencies are determined by

$$K_m(\omega_{mn}) = 1, \quad \text{for } n = m,m-2,m-4,\cdots. \tag{1-20}$$

In general, each eigenfunction $\mathcal{E}_m(x)$ has more than one eigenfrequency: as can be seen from Table II, there is one eigenfrequency each for $m = 1$ and $m = 2$, but two for $m = 3,4$ and three for $m = 5,6$, and so on. We label the various eigenfrequencies of (1-20) so that in the limit of zero intensity, ω_{mn} approaches $n\nu$.

The eigenfunctions $f_{mn}(r, \theta)$ corresponding to the eigenfrequencies ω_{mn} are determined by Eq. (1-7) to be

Table II. The functions $K_n(\omega)$ are listed for $n < 7$.

n	$K_n(\omega)$
1	$\frac{\omega_p^2}{\omega^2 - \nu^2}$
2	$\frac{\omega_p^2}{\omega^2 - 2^2\nu^2}$
3	$\frac{\omega_p^2}{\omega^2 - 3^2\nu^2} \cdot \frac{\omega^2}{\omega^2 - \nu^2}$
4	$\frac{\omega_p^2}{\omega^2 - 4^2\nu^2} \cdot \frac{\omega^2 - \nu^2}{\omega^2 - 2^2\nu^2}$
5	$\frac{\omega_p^2}{\omega^2 - 5^2\nu^2} \cdot \frac{\omega^2 - 2^2\nu^2}{\omega^2 - 3^2\nu^2} \cdot \frac{\omega^2}{\omega^2 - \nu^2}$
6	$\frac{\omega_p^2}{\omega^2 - 6^2\nu^2} \cdot \frac{\omega^2 - 3^2\nu^2}{\omega^2 - 4^2\nu^2} \cdot \frac{\omega^2 - \nu^2}{\omega^2 - 2^2\nu^2}$

$$f_{mn}(r, \theta) = \frac{\omega_p^2}{\nu^2} \cdot \frac{1}{r} \cdot \frac{df_0}{dr} \sum_{k=1}^{k} \frac{R_{mk}(r)}{k^2 - \frac{\omega_{mn}^2}{\nu^2}} \left(i \frac{\omega_{mn}}{\nu} \sin k\theta - k \cos k\theta\right) , \qquad (1\text{-}21)$$

where the sum over k is finite and involves only even or only odd numbers. The radial functions $R_{mn}(r)$ are polynomials in r, and a few are listed in Table III. For $m > 2$, the sum in (1-21) has more than one term, and the simple n-fold rotational symmetry of the unperturbed eigenfunctions is absent.

Low Intensities

For $\omega_p^2 \ll \nu_0^2$, these eigenfunctions and eigenvalues reduce to the form predicted by perturbation theory. The eigenfrequencies have the form

$$\omega_{mn} = n\nu + \frac{\lambda_{mn}}{n} \Delta\nu_{sc} , \qquad (1\text{-}22)$$

where $\nu = \sqrt{\nu_0^2 - \omega_p^2} \approx \nu_0 - \Delta\nu_{sc}$ and where a few of the constants λ_{mn} are listed in Table IV. These eigenfrequencies are shown in Fig. 18a for the intensity corresponding to $\Delta\nu_{sc} = \frac{1}{4}$, but the eigenfrequencies with $m > n + 2$ are clustered too near the values $n\nu$ to be resolved. Figure 18b shows an enlarged region of the spectrum near $n\nu$: all the eigenfrequencies (except $\omega_{11} = \nu_0$) are shifted down from the unperturbed values $n\nu_0$, and as the radial mode number m increases, the eigenfrequencies approach $n\nu$. It is also evident from Eq. (1-22) or Fig. 18a that as the mode number n increases, the eigenfrequencies become more tightly clustered around the frequencies $n\nu$.

Table III. The radial functions $R_{mn}(r)$ with $m < 7$ are listed.

m \ n	1	3	5
1	r		
3	$\frac{1}{2}\left(\frac{3}{4} r^3 - r\right)$	$\frac{3}{8} r^3$	
5	$\frac{1}{8}\left(\frac{5\cdot 7}{8} r^5 - \frac{3\cdot 5}{2} r^3 + 3r\right)$	$\frac{3\cdot 5}{16}\left(\frac{7}{8} r^5 - r^3\right)$	$\frac{5\cdot 7}{8\cdot 16} r^5$

m \ n	2	4	6
2	$\frac{1}{2} r^2$		
4	$\frac{1}{4}\left(\frac{5}{2} r^4 - 3r^2\right)$	$\frac{5}{16} r^4$	
6	$\frac{5}{16}\left(\frac{7\cdot 9}{16} r^6 - 7r^4 + 3r^2\right)$	$\frac{7}{32}\left(\frac{9}{2} r^6 - 5r^4\right)$	$\frac{7\cdot 9}{16\cdot 16} r^6$

Table IV. The coefficients λ_{mn} in Eq. (1-22) are listed for $m < 7$.

m \ n	1	3	5
1	1		
3	$-\frac{1}{2^3} = -0.125$	$\frac{3^2}{2^3} = 1.125$	
5	$-\frac{1}{2^6} \approx -0.0156$	$-\frac{3^2 \cdot 5}{2^7} \approx -0.350$	$\frac{5^2 \cdot 7}{2^7} \approx 1.365$
m \ n	**2**	**4**	**6**
2	1		
4	$-\frac{1}{2^2} = -0.250$	$\frac{5}{2^2} = 1.25$	
6	$-\frac{5}{2^7} \approx -0.039$	$-\frac{7}{2^4} \approx -0.438$	$\frac{3^2 \cdot 7}{2^7} \approx 1.475$

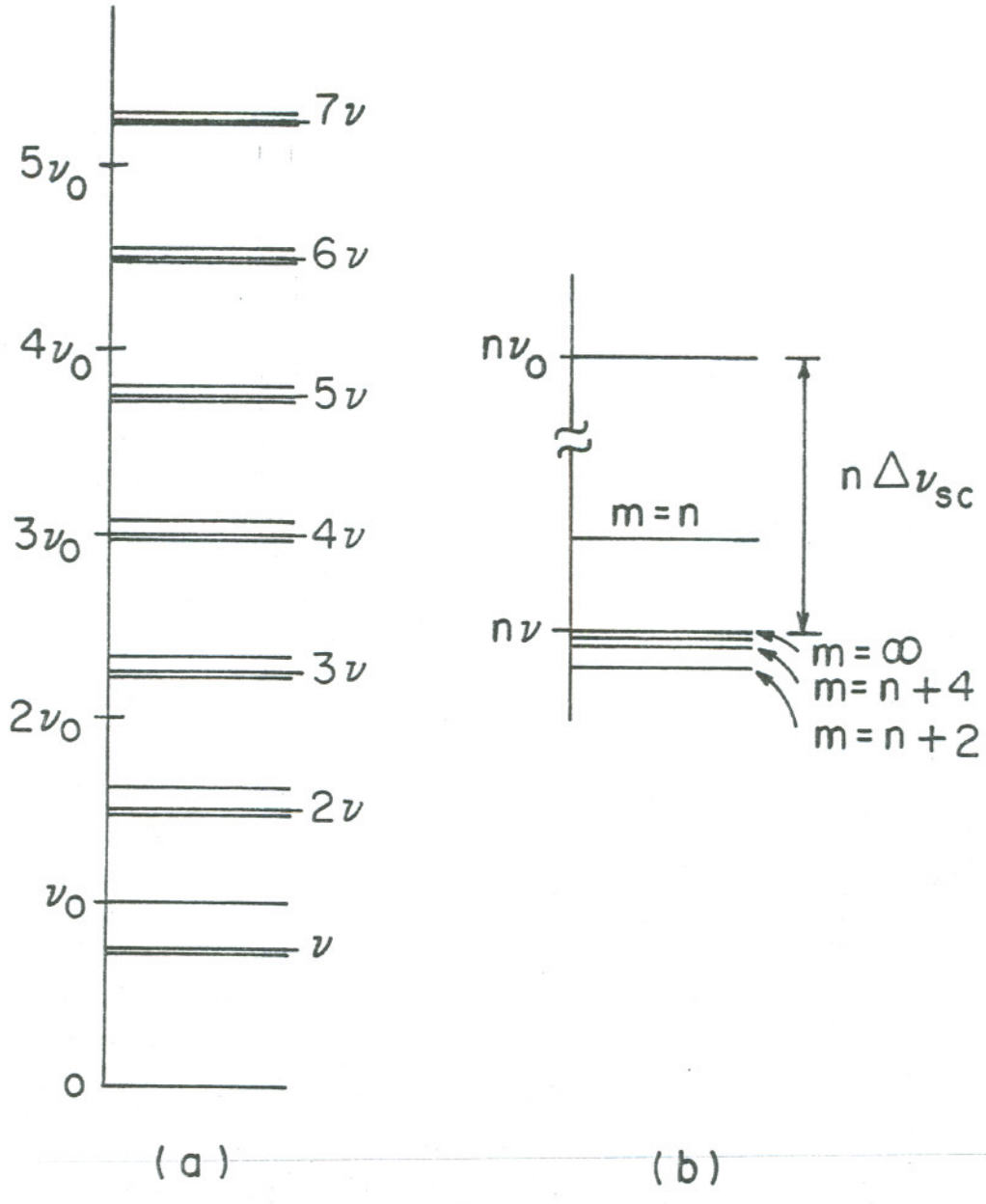

XBL689-3904

Fig. 18. Eigenvalue spectrum for $\Delta\nu_{sc} = \frac{1}{4}$; (b) is an enlarged region near $n\nu$. The eigenvalues occur in clusters near $n\nu$ and, as n increases, the clusters become more tightly grouped around $n\nu$.

The low-intensity eigenfunctions have the form

$$f_{mn}(r, \theta) = \frac{n}{\lambda_{mn}} R_{mn}(r) \frac{1}{r} \frac{df_0}{dr} e^{-in\theta} + O(\omega_p^2) , \qquad (1\text{-}23)$$

and therefore the complete distribution $f = f_0 + f_{mn}$ becomes

$$f = \frac{1}{2\pi\nu \sqrt{1 - r^2 + \epsilon R_{mn}(r) \cos n(\nu\phi + \theta)}} + O(\omega_p^2) , \qquad (1\text{-}24)$$

where the term proportional to ω_p^2 involves mixtures of other zero-order eigenfunctions. A few of the radial functions $R_{mn}(r)$ are shown in Fig. 19; note that the perturbation for the modes with $m = n$ is the largest near the surface $r = 1$, whereas the other modes are close to zero there. For this reason, the $m = n$ modes are referred to as surface modes. They produce relatively large displacements of the beam surface, as opposed to the $m \neq n$ modes for which the perturbed motion is largely confined to the interior of the distribution.

The distribution (1-24) rotates in an approximately rigid fashion in the $x - \frac{v}{\nu}$ space with the frequency $n\nu$, and has an approximate n-fold symmetry of rotation and radial variation with $\frac{m - n}{2}$ nodes; in real space, the perturbed charge density is proportional to $\frac{dP_{m-1}(x)}{dx}$. As m increases, the overall perturbed charge density tends to cancel with itself, and thus it is not surprising that the eigenfrequencies for the modes with large m approach $n\nu$; perturbations

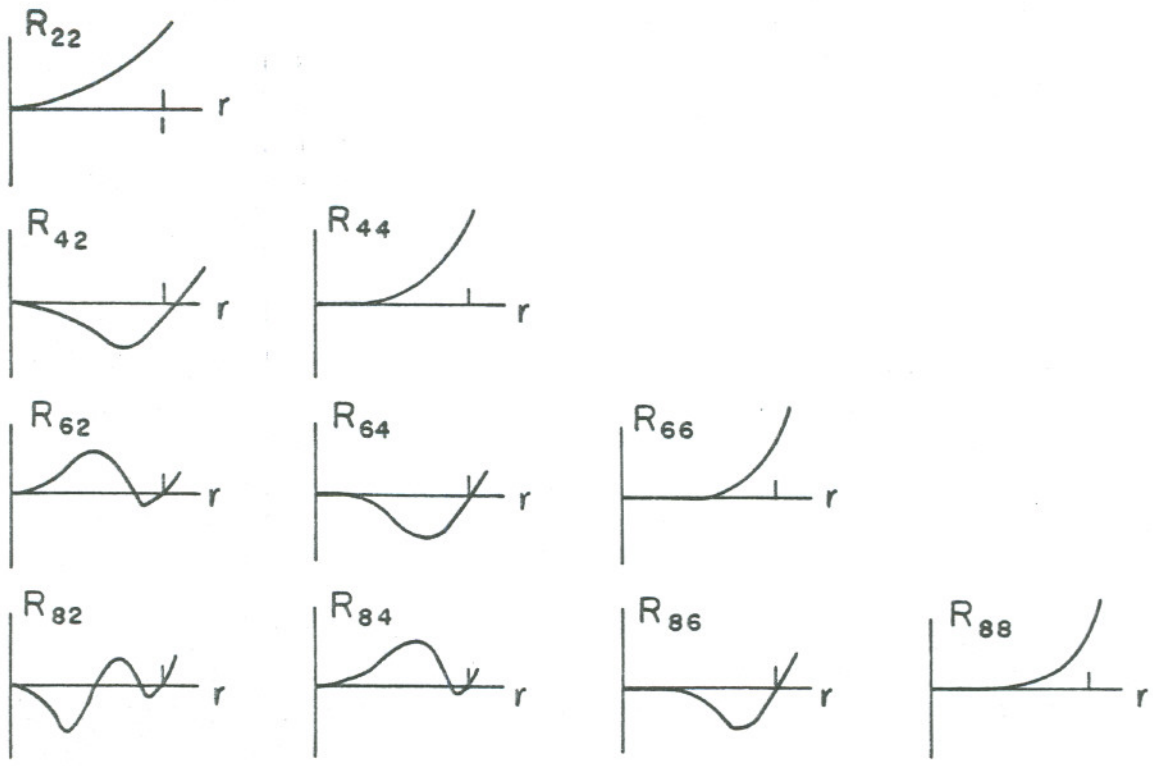

XBL689-3903

Fig. 19. The radial functions $R_{mn}(r)$ are shown for even values of m and n. The vertical scale is not indicated, and differs from figure to figure for clarity.

that produce little net charge density will only slightly perturb the stationary circular orbits, and consequently will be carried along nearly intact with the frequency ν of the stationary distribution.

The eigenfunctions $f_{mn}(f, \theta)$ found so far do not form a complete set.[25] For example, among the zero-intensity eigenfunctions (1-23), there are none with the form $g_{mn}(r)\, e^{-in\theta}$ where $n = 0$ or, in general, where $n > m$. For completeness, additional eigenfunctions are required to fill in the blanks of Table III, as well as an additional column at $n = 0$. It is shown in Appendix C that these additional eigenfunctions exist and have the eigenvalues $n\nu$ that were excluded by the form of Eq. (1-7) and following. The new eigenfrequencies do not change the form of the spectrum, but now the value $n\nu$ is degenerate.

High Intensities

In the opposite limit of very high intensities, the eigenfunctions and eigenvalues also reduce to a characteristic form. The maximum intensity occurs for $\omega_p = \nu_0$ and corresponds to that value of space-charge force for which the repulsive self-force exactly cancels the external focusing force -- no net force acts on the stationary distribution. In this case, the particles comprising the stationary distribution have no velocity (the beam emittance is zero), and f_0 is completely characterized by its charge density $en_0(x)$. Any perturbation can therefore be expanded in a single infinity of functions, rather than in the two-fold infinity required before. Furthermore, any perturbation of such a zero-temperature plasma (the external force is equivalent to a neutralizing background of immobile ions) must oscillate with the

plasma frequency ω_p. Thus, in this limit, the eigenfunctions must reduce to a single infinity of functions, and their eigenfrequencies must all have the same value $\omega_n = \omega_p$.

This is indeed the case. A few of the eigenfrequencies ω_{mn} are plotted as a function of intensity in Fig. 20; as the intensity increases to its maximum value, the eigenfrequencies ω_{mm} for the surface modes all approach the plasma frequency whereas the eigenfrequencies for the other modes approach zero. The eigenfunctions for the electric field $\mathcal{E}(x)$ [or equivalently the charge density $en(x)$] remain Legendre polynomials, and since each eigenfunction $\mathcal{E}_m(x)$ now has only one eigenfrequency, any perturbation is completely specified by the single infinity of eigenfunctions $\mathcal{E}_m(x)$.

The Dipole and Quadrupole Modes

The dipole mode with $m = 1$ and $n = 1$ is particularly simple. The eigenfrequency ω_{11} specified by $K_{11}(\omega) = 1$ is found from Table II to be

$$\omega_{11} = \sqrt{\nu^2 + \omega_p^2} \equiv \nu_0 \quad , \tag{1-25}$$

so that this mode oscillates with the unperturbed betatron frequency ν_0, independent of intensity. The perturbed electric field has the form $\mathcal{E}_1(x, \phi) = \epsilon\, e^{-i\nu_0\phi}$, and the complete particle distribution $f = f_0 + f_{11}$ is given to first order in ϵ by

$$f(r, \theta, \phi) = \frac{1}{2\pi\nu\sqrt{1 - r^2 + 2\epsilon r \cos(\nu_0\phi + \theta)}} \equiv \frac{1}{2\pi\nu\sqrt{1 - r'^2}} \quad , \tag{1-26}$$

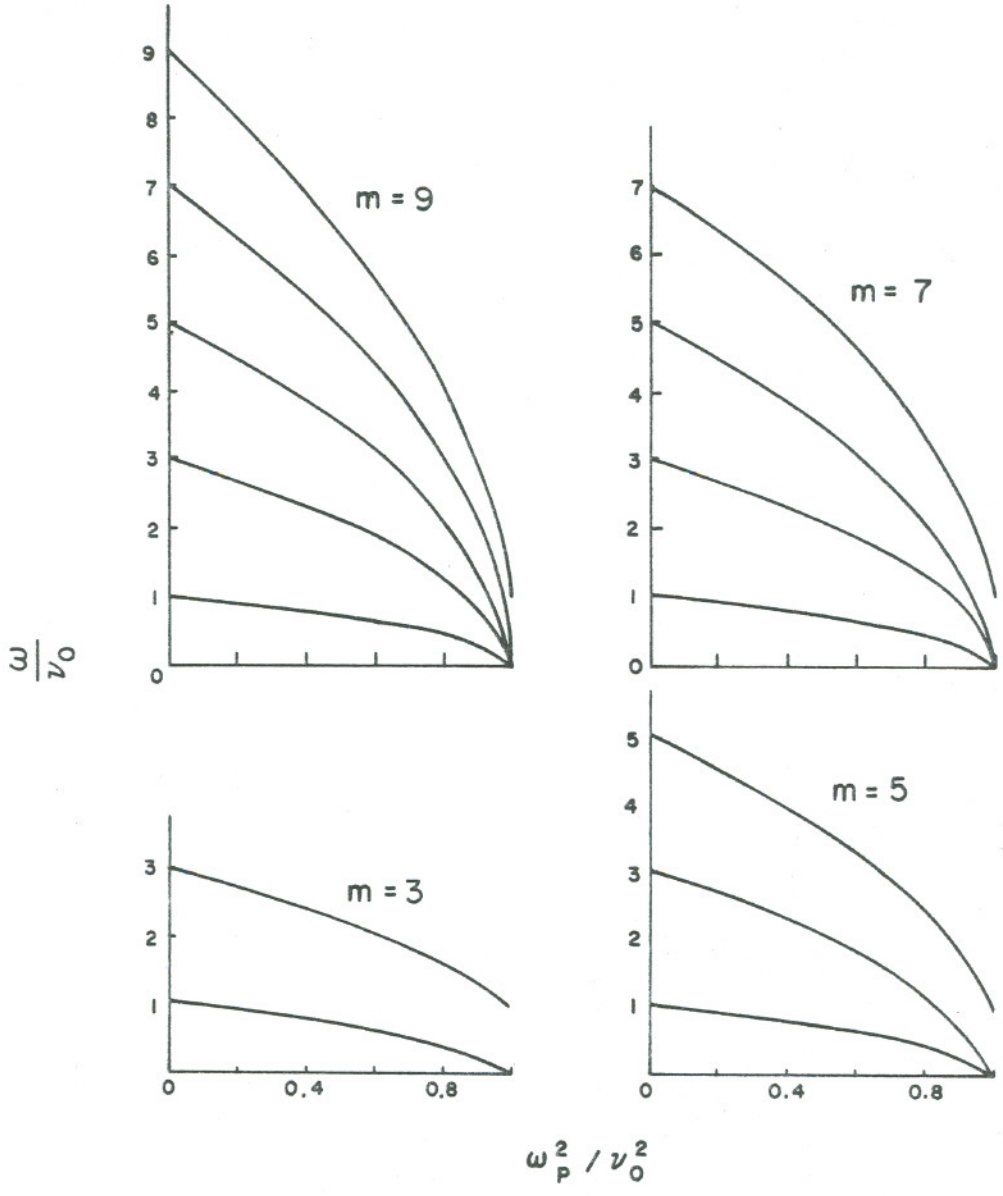

XBL689 - 3902

Fig. 20. The eigenvalues specified by $K_m(\omega_{mn}) = 1$ are shown for $m = 9,7,5$, and 3. As the intensity increases to the maximum value corresponding to $\omega_p = \nu_0$, the eigenvalues for the $m \neq n$ modes approach zero; those for the $m = n$ modes approach ω_p.

where the variable r' is measured with respect to the moving coordinates $x = \epsilon \cos(\nu_0 \phi + \theta)$ and $\frac{v}{\nu} = \epsilon \sin(\nu_0 \phi + \theta)$, as shown in Fig. 21. Therefore the entire distribution is displaced in the circular

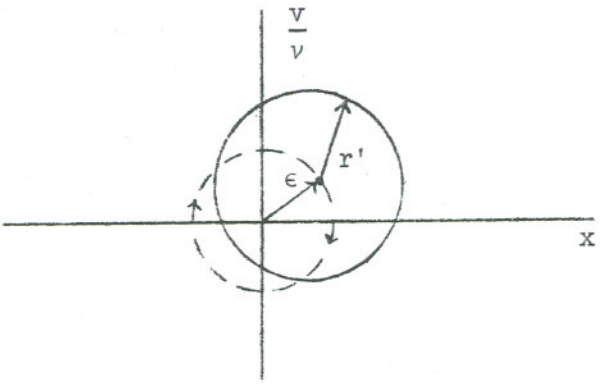

Fig. 21.

path indicated, and in real space, the beam oscillates rigidly back and forth at the frequency ν_0.

In addition to this rigid dipole mode, there is an infinite number of nonrigid dipole modes with $n = 1$ and $m = 3,5,7,\cdots$ and with a charge density proportional to $\frac{dP_{m-1}(x)}{dx}$. The charge density for these modes oscillates in a nonrigid fashion, and the eigenfrequency ω_{m1} approaches $(\nu_0 - \Delta\nu_{sc})$ as m increases.

The quadrupole mode with $m = 2$ and $n = 2$ has the eigenfrequency

$$\omega_{22} = \sqrt{\nu^2 + \omega_p^2} \approx 2(\nu_0 - \tfrac{3}{4}\Delta\nu_{sc}) \quad , \qquad (1\text{-}27)$$

which is the same frequency as was found for the small-amplitude oscillations of the one-dimensional beam examined in Part I. In fact,

it is straightforward to show that the complete distribution $f = f_0 + f_{22}$ is just the small-amplitude limit of the uniform one-dimensional distribution, Eq. (1-17) in Part I.[26] Thus, this is the "breathing mode" in which the beam expands and contracts, yet maintains a uniform charge density.

The quadrupole modes with $n = 2$ and $m = 4,6,8,\cdots$ have a nonuniform charge density proportional to $\frac{dP_{m-1}(x)}{dx}$, and their eigenfrequencies ω_{m2} approach $2(\nu_0 - \Delta\nu_{sc})$ as m increases.

Excitation by External Forces

Machine imperfections excite the various normal modes. In this case, the linearized Vlasov equation has the form

$$\frac{\partial f}{\partial \phi} + v\frac{\partial f}{\partial x} - \nu^2 x\frac{\partial f}{\partial v} = -\omega_p{}^2[\mathcal{E}(x, \phi) + E(x)\, e^{-ip\phi}]\frac{\partial f_0}{\partial v} \quad , \qquad (1\text{-}28)$$

where $E(x)\, e^{-ip\phi}$ is the known external driving term and p is an integer. The forced solutions of (1-28) oscillate with the frequency p, and can be found by the same methods that were used to find the normal mode solutions. In particular, the defining equation for $\mathcal{E}(x)$ is just Eq. (1-15), but $\mathcal{E}(\cos\psi)$ on the right-hand side is replaced by $\mathcal{E}(\cos\psi) + E(\cos\psi)$. The solution for the forced electric field is

$$\mathcal{E}(x) = \sum_n \frac{2n+1}{2} a_n P_n(x) \quad , \qquad (1\text{-}29)$$

where the coefficients a_n are determined by

$$a_{n-1} = \frac{K_n(p)}{1 - K_n(p)} \int_{-1}^{1} P_{n-1}(x)\, E(x)\, dx \quad . \qquad (1\text{-}30)$$

Thus an external driving term of the form $E(x) = P_{m-1}(x)$ excites only the $\mathcal{E}_m(x)$ modes, and resonances occur for p near any eigenfrequencies ω_{mn} where $n = m, m-2, m-4, \cdots$.

A magnetic field error has the form $E(x) = \epsilon$, and excites only the rigid dipole mode ($m = 1$ and $n = 1$) with

$$\mathcal{E}_1(x) = \frac{\epsilon\omega_p^2}{p^2 - \nu_0^2} \quad . \qquad (1\text{-}31)$$

A gradient error has the form $E(x) = \epsilon x$, and excites only the uniform quadrupole mode ($m = 2$ and $n = 2$) with

$$\mathcal{E}_2(x) = \frac{\epsilon\omega_p^2 x}{p^2 - 4\nu_0^2 + 3\omega_p^2} \quad , \qquad (1\text{-}32)$$

in agreement with Part I. Nonlinear driving terms excite the higher-order modes and cause resonances for integral values of ω_{mn}. In the next section, we examine these resonances in more detail and compare them with the resonant frequencies found by Ehrman for a nonuniform beam.

We conclude this section with a few general observations. For intensities of interest in AG synchrotrons ($\Delta\nu_{sc} \ll \nu_0$), the normal modes f_{mn} for the particle density in $x - \frac{v}{\nu}$ space have an approximate

n-fold symmetry of rotation and radial variation with $\frac{m - n}{2}$ nodes; in real space, the charge density is proportional to $\frac{dP_{m-1}(x)}{dx}$.

The distribution oscillates with the frequency $\omega_{mn} = n(\nu_0 - \Delta\nu_{sc}) + \frac{\lambda_{mn}}{n}\Delta\nu_{sc}$, which differs from the zero-intensity value $n\nu_0$ by the two frequency shifts $n\Delta\nu_{sc}$ and $\frac{\lambda_{mn}}{n}\Delta\nu_{sc}$. The first frequency shift is a purely geometric effect: a perturbation that produced no electric field would rotate rigidly with the frequency ν of the stationary distribution, giving rise to the eigenfrequency $n\nu$. However, because the perturbation is charged, the circular orbits of the stationary distribution are distorted, and this distortion gives rise to the second frequency shift. This frequency shift is largest for the lower-order, more coherent modes, and becomes progressively smaller (Table IV) for the higher-order modes, since the perturbed charge density tends to cancel with itself: the most coherent mode is the rigid dipole mode for which $\omega_{11} = (\nu_0 - \Delta\nu_{sc}) + \Delta\nu_{sc}$, whereas for the uniform quadrupole mode $\omega_{22} = 2(\nu_0 - \Delta\nu_{sc}) + \frac{1}{2}\Delta\nu_{sc}$, and for the (3,3) sextupole mode $\omega_{33} = 3(\nu_0 - \Delta\nu_{sc}) + \frac{3}{8}\Delta\nu_{sc}$. For the higher-order modes, especially the nonsurface modes, the eigenfrequencies are shifted very little from the value $n(\nu_0 - \Delta\nu_{sc})$.

Finally, because the eigenfrequencies are real and discrete, there can be no Landau damping.[27] This type of damping requires a continuous spectrum and discontinuous eigenfunctions, so that any initial perturbation that is analytic consists of an infinite number of eigenfunctions, each infinitesimally excited; in the course of time

the phase relationships between the various modes is destroyed and the perturbation damps exponentially to zero.[28] For any system of charged particles that are confined by a harmonic potential, the eigenvalue spectrum is discrete and the eigenfunctions are continuous;[29] however, a very localized perturbation contains many modes and exhibits an approximate exponential damping until the phases of the various modes become randomized.

2. Extension to Nonuniform Beams

Resonant Frequencies for the Uniform Beam

We have seen in the preceding section that an external driving term of the form $P_{m-1}(x)\, e^{-ip\phi}$ excites resonances if the integer p is near any of the eigenfrequencies ω_{mn} where $n = m, m-2, m-4, \cdots$. For low intensities, $\omega_{mn} = n\nu + \frac{\lambda_{mn}}{n} \Delta\nu_{sc}$, and therefore resonances occur for p near $m\nu$, $(m-2)\nu$, $(m-4)\nu$, $\cdots$, as indicated below:

The external field	causes resonances for p near
P_0	ν
P_1	2ν
P_2	ν 3ν
P_3	2ν 4ν
P_4	ν 3ν 5ν
P_5	2ν 4ν 6ν .

(2-1)

Dipole modes are excited by $P_0, P_2, P_4, \cdots$, quadrupole modes by $P_1, P_3, P_5, \cdots$, sextupole modes by $P_2, P_4, \cdots$, octupole modes by $P_3, P_5, \cdots$, etc. In the limit of zero intensity, these resonances reduce to those obtained from the single-particle approach; the equation of motion for the individual particles is

$$\frac{d^2x}{d\phi^2} + \nu_0^2 x = \epsilon P_{m-1}(x) \cos p\phi \quad , \tag{2-2}$$

and if we consider only small departures δx from the stationary orbits $x = A\cos(\nu_0\phi + \alpha)$, where A and α are constants, resonance occurs for $p = m\nu_0$, $(m-2)\nu_0$, $(m-4)\nu_0$, $\cdots$, as indicated in (2-1).

However, if nonlinear terms in δx are allowed in (2-2), the resonant growth caused by the driving term $x^m \cos p\phi$ is usually serious only for $m \leqslant 2$; for larger values of m the amplitude dependence of ν_0, which results from the nonlinearity of the driving term, generally causes the resonant growth to be negligible.[30] Presumably this is also true in the presence of space charge. Then, since x^m can be expressed in terms of Legendre polynomials of order less than or equal to m, only the driving terms $P_{m-1}(x)$ and resonant frequencies ω_{mn} with $m \leqslant 3$ need be considered, namely ω_{11}, ω_{22}, ω_{31}, ω_{33}.

Resonance occurs for integral values of these eigenfrequencies, and from Table IV we find:

Driving term	Resonant condition	Mode (m,n)
P_0	$\nu_0 = n$	rigid dipole (1,1)
P_1	$\nu_0 = \frac{n}{2} + \frac{3}{4}\Delta\nu_{sc}$	uniform quadrupole (2,2)
P_2	$\nu_0 = n + \frac{9}{8}\Delta\nu_{sc}$	nonrigid dipole (3,1)
	$\nu_0 = \frac{n}{3} + \frac{7}{8}\Delta\nu_{sc}$	sextupole (3,3)

(2-3)

where n is any integer. These resonant values of ν_0 are shown in Fig. 22 for the beam intensity corresponding to $\Delta\nu_{sc} = \frac{1}{4}$; additional resonances are also included, and the dipole, quadrupole, and sextupole modes are drawn separately for clarity. The rigid dipole mode is excited by P_0 at integral values of ν_0, whereas the nonrigid dipole modes are excited by $P_2, P_4, \cdots$ for ν_0 near $n + \Delta\nu_{sc}$. The uniform quadrupole mode that was examined in Part I is excited by P_1 at $\nu_0 = \frac{n}{2} + \frac{3}{4}\Delta\nu_{sc}$, whereas the quadrupole modes that do not maintain a uniform charge density are excited by $P_3, P_5, \cdots$ for ν_0 near $\frac{n}{2} + \Delta\nu_{sc}$. The sextupole, octupole, and higher-order modes are excited for ν_0 near $\frac{n}{k} + \Delta\nu_{sc}$, where $\frac{n}{k}$ are the zero-intensity subharmonic frequencies.

Comparison with the Water-Bag Distribution

Ehrman and dePackh[6] have examined the oscillations of the stationary distribution that has a uniform particle density in phase space; the particles are confined by an external harmonic potential and oscillate with the frequency ν_0 in the absence of space charge. Since the volume occupied by any group of particles in phase space is incompressible (neglecting collisions), this uniform particle distribution acts as an incompressible homogeneous fluid, and hence the name water-bag distribution.

a. The stationary distribution

We will examine the stationary distribution in more detail before describing its small-amplitude oscillations. For low intensities, the distribution has an approximately circular boundary in the

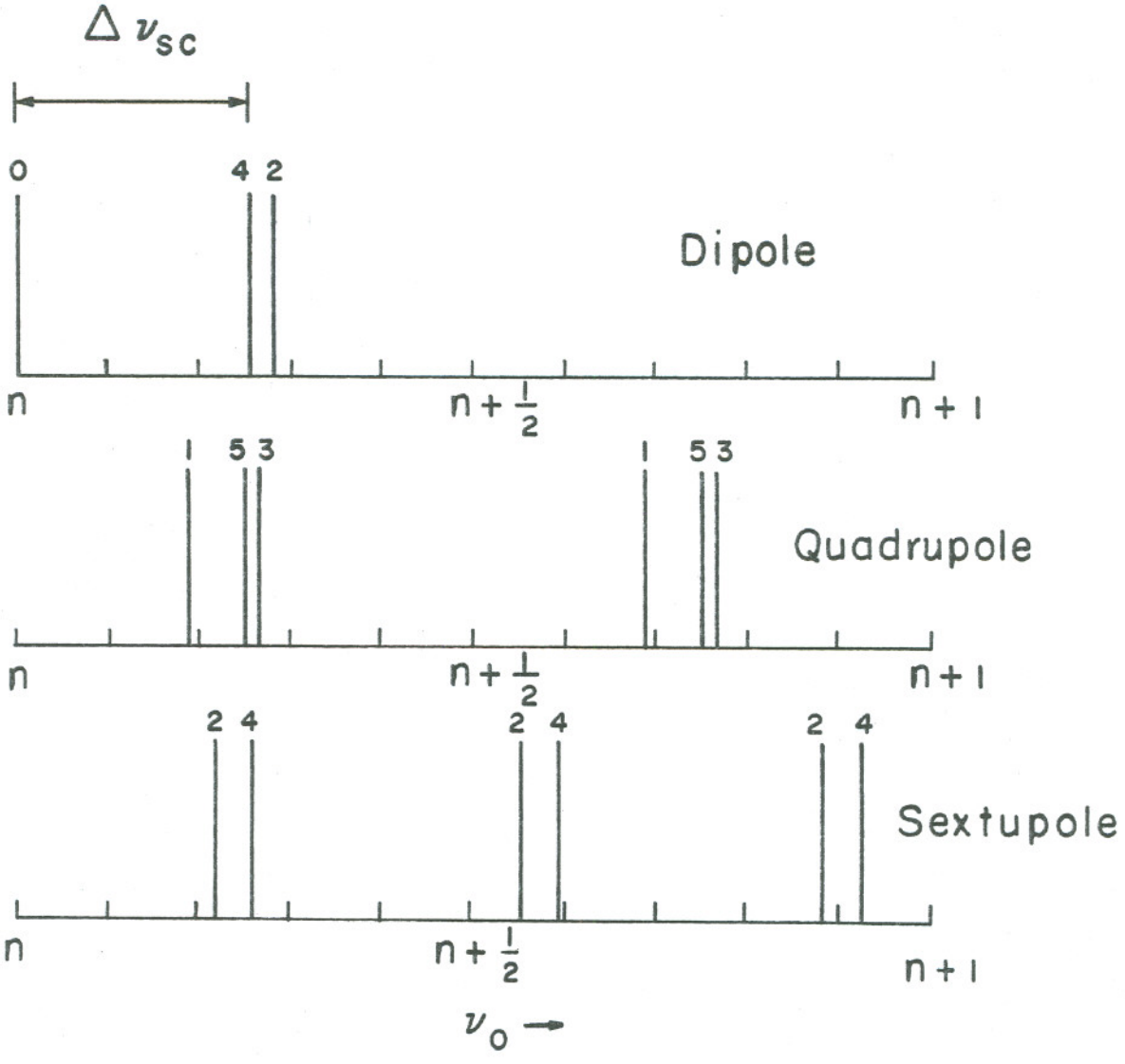

XBL689-3901

Fig. 22. The resonant values of ν_0 for the beam intensity corresponding to $\Delta\nu_{sc} = \frac{1}{4}$ are shown for the dipole, quadrupole, and sextupole modes excited by $P_m(x)$ with $m \leqslant 5$.

$x - \frac{1}{\nu_0}\frac{dx}{d\phi}$ space, and a nonuniform charge density in real space. As the intensity increases, the charge density becomes more and more uniform, until at the limiting intensity for which the space-charge force exactly balances the focusing force (the plasma frequency equals ν_0), the charge density is exactly uniform and the particles within the stationary distribution are motionless (the beam emittance is zero).

The zero-order distribution $f_0(r) = \frac{1}{\nu_0 \pi}$, $0 \leq r \leq 1$, is shown in Fig. 23b, where r is the radius of the individual particle orbits in the $x - \frac{1}{\nu_0}\frac{dx}{d\phi}$ space in the absence of space charge, and f_0 is normalized so that $\int f_0 dx dv = 1$ $(v = \frac{dx}{d\phi})$. For AG synchrotrons the space-charge forces are small in comparison with the external focusing force, $\Delta\nu_{sc} \ll \nu_0$, so that the stationary distribution in the presence of space charge differs from the zero-order distribution $f_0(r)$ by terms of order $\frac{\Delta\nu_{sc}}{\nu_0}$. For $\Delta\nu_{sc}$ typically $\frac{1}{4}$ and $\nu_0 \approx 10$, this difference is approximately 2%, which is negligible. The normalized charge density $\rho_0(x) = \int f_0(r) dv = \frac{2}{\pi}\sqrt{1 - x^2}$ for the zero-order distribution is also shown. Since the charge density is not uniform, the self-forces are not linear, and the particles within the stationary distribution oscillate with different frequencies. It is shown in Appendix D that the revolution frequencies for the individual particles within the stationary distribution are given to first order in $\frac{\Delta\nu_{sc}}{\nu_0}$ by

$$\nu(r) = \nu_0 - \Delta\nu_{sc}\, g(r) \quad , \qquad (2\text{-}4)$$

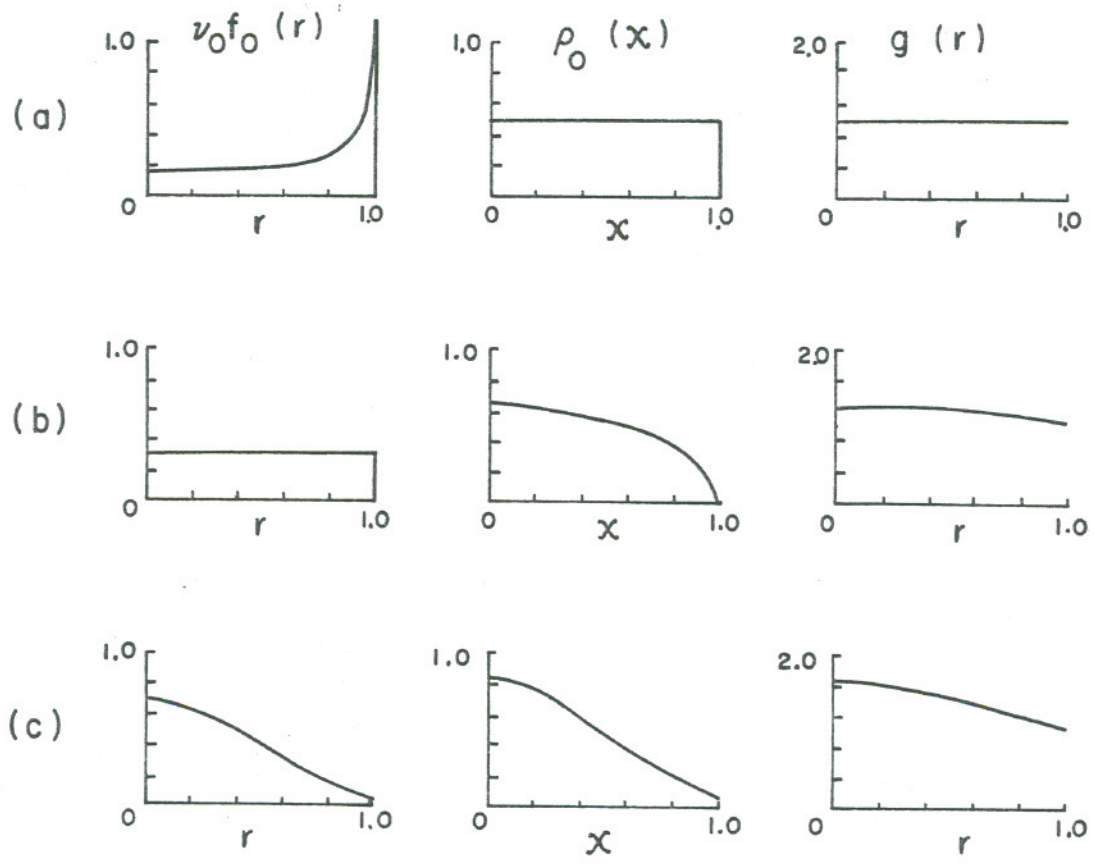

XBL689-3900

Fig. 23. The uniformly charged beam (a), water-bag beam (b), and Gaussian beam (c) are shown: $f_0(r)$ is the zero-order stationary distribution, $\rho_0(x)$ is the normalized charge density for $f_0(r)$, and $\nu(r) = \nu_0 - \Delta\nu_{sc}\, g(r)$ is the frequency of the individual particles within the stationary distribution to first order in $\frac{\Delta\nu_{sc}}{\nu_0}$.

where

$$g(r) = \frac{2}{\pi} \int_0^{2\pi} \rho_0(r \sin w) \cos^2 w \, dw \quad , \qquad (2\text{-}5)$$

involves an integration over the unperturbed orbits. The quantity $\Delta\nu_{sc}$ has been defined before [Eq. (2-8), Part I]. It is proportional to the average charge density within the beam, and is identical to the space-charge-induced frequency shift for a beam with uniform charge density, i.e., for the normalized charge density $\rho_0(x) = \text{constant} = \frac{1}{2}$, Eqs. (2-4) and (2-5) give $\nu(r) = \text{constant} = \nu_0 - \Delta\nu_{sc}$. For comparison, the zero-order distribution for the uniformly charged beam $\left(f_0 = \frac{1}{2\pi\nu_0\sqrt{1 - r^2}}\right)$ is also shown (Fig. 23a), as well as the Gaussian distribution observed in the Brookhaven AGS[19] (Fig. 23c), namely $f_0 = \frac{2.2}{\nu_0\pi} e^{-2.2r^2}$, with the normalized charge density $\rho_0(x) = \sqrt{\frac{2.2}{\pi}}\, e^{-2.2x^2}$. Note that the charge distribution for the water-bag beam is intermediate between that of the uniform beam and the Gaussian beam.

For the same total charge N_1, and the same beam size a, the water-bag and Gaussian beams have a higher central charge density than the uniform beam. As a result, the space-charge-induced frequency shifts $\Delta\nu_{sc} g(r)$ are larger for the nonuniform beams, since the $\cos^2 w$ term in Eq. (2-5) weights the integration over $\rho_0(r \sin w)$ in the favor of small values of the argument $r \sin w$. For the water-bag beam $\nu(r)$ varies between $\nu(0) = \nu_0 - \frac{4}{\pi}\Delta\nu_{sc}$ and

$\nu(1) = \nu_0 - \frac{32}{3\pi^2}\Delta\nu_{sc} \approx \nu_0 - 1.08\,\Delta\nu_{sc}$; for the Gaussian beam it varies between $\nu(0) \approx \nu_0 - 1.67\,\Delta\nu_{sc}$ and $\nu(1) \approx \nu_0 - 1.09\,\Delta\nu_{sc}$.

b. Small-amplitude oscillations

Ehrman has found the small-amplitude oscillations that perturb the boundary of the stationary water-bag distribution while maintaining the uniform particle density in phase space, namely the surface modes. These modes, for which the perturbation is large only near the beam boundary, are very similar to the $m = n$ surface modes of the uniformly charged beam. The additional nonsurface modes that perturb the uniform particle density within the boundary were not found.

For low intensities, the surface modes have an approximate n-fold rotational symmetry in the $x - \frac{1}{\nu_0}\frac{dx}{d\phi}$ space, and oscillate with the frequencies[31]

$$\omega_n = n\nu(1) + \frac{8}{3\pi}\frac{n}{n^2 - \frac{1}{4}}\Delta\nu_{sc} \quad , \tag{2-6}$$

where $n = 1,2,3,\cdots$. For $n = 1$, $\omega_1 = \nu_0$, and this is the rigid dipole mode for which the beam oscillates rigidly back and forth at the zero-intensity betatron frequency. For the first three surface modes we find

Water-bag	Uniform beam
$\omega_1 = \nu_0$	$\omega_{11} = \nu_0$
$\omega_2 = 2\nu(1) + 0.454\ \Delta\nu_{sc}$	$\omega_{22} = 2\nu + \frac{1}{2}\Delta\nu_{sc}$
$\omega_3 = 3\nu(1) + 0.291\ \Delta\nu_{sc}$	$\omega_{33} = 3\nu + \frac{3}{8}\Delta\nu_{sc}$. (2-7)

For larger values of n, the frequency shift from $n\nu(1)$ is very nearly $\frac{8}{3\pi n}\Delta\nu_{sc}$, which has the same form as the frequency shift $\frac{\lambda_{nn}}{n}\Delta\nu_{sc}$ for the uniform beam, where λ_{nn} is a number of order one that increases slowly with n (Table IV). As n approaches infinity, the eigenfrequencies ω_n approach $n\nu(1)$; the perturbed charge density tends to cancel with itself, and the perturbation is carried along nearly intact at the frequency of the boundary particles, $\nu(1) \approx \nu_0 - 1.08\ \Delta\nu_{sc}$.

As the intensity increases to its limiting value, corresponding to $\omega_p = \nu_0$, the eigenfrequencies ω_n approach the plasma frequency ω_p in the same manner (Fig. 3 of Ehrman[6]) as do the eigenfrequencies for the surface modes of the uniform beam (Fig. 20). We conclude that the eigenfrequencies for the surface modes of both distributions are very similar.

The low-intensity resonant conditions for the first three surface modes of the two distributions are

Water-bag	Uniform beam
$\nu_0 = n$	$\nu_0 = n$
$\nu_0 = \frac{n}{2} + 0.853\ \Delta\nu_{sc}$	$\nu_0 = \frac{n}{2} + \frac{3}{4}\ \Delta\nu_{sc}$
$\nu_0 = \frac{n}{3} + 0.983\ \Delta\nu_{sc}$	$\nu_0 = \frac{n}{3} + \frac{7}{8}\ \Delta\nu_{sc}$. (2-8)

The driving terms that excite these water-bag modes have not been determined, but it is reasonable to assume that they are similar to those for the uniform beam. For example, we expect a gradient error to excite primarily the $n = 2$ quadrupole mode, but also to excite weakly the additional nonsurface quadrupole modes. In the same spirit, we expect only the low-order water-bag resonances listed in (2-8), plus perhaps one or two nonsurface modes, to be detected in accelerators; the nonlinearity of the driving terms required to excite the higher-order modes should prevent additional modes from being observed.

Gaussian Beam

The eigenfrequencies for the Gaussian beam have not been found, but Weibel[21] has solved a very similar problem. He considers a one-dimensional system of electrons in an external harmonic potential, and finds the eigenfrequencies for the small-amplitude oscillations about a stationary Gaussian distribution. However, he considers only the case for which the charge density of the stationary distribution is completely neutralized by a background of immobile positive ions so that all the particles within the stationary distribution oscillate with the same frequency ν_0. In contrast, the charge within an accelerator is not

neutralized and the individual particle frequencies for the Gaussian distribution vary between $\nu(0) \approx \nu_0 - 1.67\,\Delta\nu_{sc}$ and $\nu(1) \approx \nu_0 - 1.09\,\Delta\nu_{sc}$. In any event, the eigenfrequencies found by Weibel have a form very similar to those of the uniform beam and the water-bag beam.

For the neutralized Gaussian distribution $f_0(r) = \frac{2.2}{\pi\nu_0} e^{-2.2r^2}$, Weibel finds[32]

$$\omega_{11} = \nu_0 + 1.22\,\Delta\nu_{sc}\,, \qquad \omega_{31} = \nu_0 + 0.131\,\Delta\nu_{sc}\,,$$

$$\omega_{22} = 2\nu_0 + 0.356\,\Delta\nu_{sc}\,, \qquad \omega_{42} = 2\nu_0 + 0.089\,\Delta\nu_{sc}\,,$$

$$\omega_{33} = 3\nu_0 + 0.222\,\Delta\nu_{sc}\,, \tag{2-9}$$

and it can be seen that the frequency shifts from $n\nu_0$ are very similar to the frequency shifts from $n\nu(1)$ for the water-bag beam (Eq. 2-7) and from $n(\nu_0 - \Delta\nu_{sc})$ for the uniform beam. In particular, the frequency shifts for the surface modes are:

m = n	Gaussian	Water bag	Uniform
1	$1.22\,\Delta\nu_{sc}$	$1.08\,\Delta\nu_{sc}$	$\Delta\nu_{sc}$
2	$0.356\,\Delta\nu_{sc}$	$0.454\,\Delta\nu_{sc}$	$\frac{1}{2}\,\Delta\nu_{sc}$
3	$0.222\,\Delta\nu_{sc}$	$0.291\,\Delta\nu_{sc}$	$\frac{3}{8}\,\Delta\nu_{sc}$.

(2-10)

For the two nonsurface modes of (2-9),

(m,n)	Gaussian	Uniform
(3,1)	$0.131\ \Delta\nu_{sc}$	$0.125\ \Delta\nu_{sc}$
(4,2)	$0.089\ \Delta\nu_{sc}$	$0.125\ \Delta\nu_{sc}$.

(2-11)

These results for the neutralized beam can be extended to the charged beam provided the effect of the frequency spread $\nu(0) - \nu(1)$ within the charged beam can be neglected: we assume that all the particles within the stationary distribution oscillate with the same frequency $\bar{\nu}$ and replace ν_0 in (2-9) by the effective frequency $\bar{\nu}$. The value of $\bar{\nu}$ is determined by the requirement that the rigid dipole mode, which in this case is obviously the $m = 1$, $n = 1$ mode, oscillate with the frequency ν_0. Then $\bar{\nu} \approx \nu_0 - 1.22\ \Delta\nu_{sc}$; this is near the mean frequency $\int \nu(r)\ f_0(r)\ dxdv \approx \nu_0 - 1.28\ \Delta\nu_{sc}$ within the stationary distribution and is a reasonable extrapolation from the effective frequencies $\nu_0 - \Delta\nu_{sc}$ and $\nu_0 - 1.08\ \Delta\nu_{sc}$ for the uniform and water-bag beams. With this replacement in Eqs. (2-9), the resonant conditions for the Gaussian beam become

$$\nu_0 = n\ , \qquad \nu_0 = n + 1.09\ \Delta\nu_{sc}\ ,$$

$$\nu_0 = \frac{n}{2} + 1.04\ \Delta\nu_{sc}\ , \qquad \nu_0 = \frac{n}{2} + 1.07\ \Delta\nu_{sc}\ ,$$

$$\nu_0 = \frac{n}{3} + 1.15\ \Delta\nu_{sc}\ , \tag{2-12}$$

which are reasonable extrapolations from the known resonant conditions for the uniform and water-bag beams (Eq. 2-8).

3. Conclusion

We have investigated the small-amplitude oscillations of a one-dimensional system of charged particles that interact with one another by Coulomb forces and are held together by an external harmonic potential. Because the large number of discrete particles (approximately 10^{12}), each with two degrees of freedom, has been replaced by a continuous distribution, the system has a twofold infinity of degrees of freedom and therefore a twofold infinity of normal modes and eigenfrequencies.

In the limit of zero intensity, the eigenfrequencies for any stationary distribution are just harmonics of the zero-intensity betatron frequency ν_0, and each eigenfrequency is infinitely degenerate. Resonances occur for integral values of $n\nu_0$, and these are just the integral, half-integral, and subharmonic resonances that are familar from single-particle theory. For intensities of interest in AG synchrotrons ($\Delta\nu_{sc} \ll \nu_0$), the degeneracy is at least partially removed, and the eigenfrequencies occur in clusters near the unperturbed eigenvalues $n\nu_0$. For larger intensities, the charge density of the stationary distributions becomes more and more uniform until at the limiting intensity, for which $\omega_p = \nu_0$, the charge density is exactly uniform. Consequently, the eigenfrequencies for the surface modes approach the plasma frequency, while the eigenfrequencies for the nonsurface modes approach zero.

The eigenfrequencies and normal modes for the stationary distribution that has a uniform charge density in real space have been investigated in detail. The eigenfunctions for the perturbed electric

field are particularly simple, being just Legendre polynomials. For low intensities, the eigenfrequencies are $\omega_{mn} = n\nu + \frac{\lambda_{mn}}{n}\Delta\nu_{sc}$, where $\nu = \nu_0 - \Delta\nu_{sc}$ is the revolution frequency of the particles within the stationary distribution and $\frac{\lambda_{mn}}{n}\Delta\nu_{sc}$ is the frequency shift induced by the collective oscillation. In the $x - \frac{1}{\nu_0}\frac{dx}{d\phi}$ space, the eigenfunctions have an approximate n-fold rotational symmetry and a radial variation with $\frac{m - n}{2}$ nodes; in real space the perturbed charge density is proportional to $\frac{dP_{m-1}}{dx}$. The frequency shift from $n\nu$ is relatively large for the low-order, coherent modes, while it is very small for the higher-order modes, for which the perturbed charge density tends to cancel with itself.

External driving terms of the form $P_k(x) \cos p\phi$ excite the $m = k + 1,\ n = k + 1,\ k - 1,\ k - 3, \cdots$ modes and cause resonances for ω_{mn} near the integer p. However, the resonances with $m \geqslant 4$ will generally be suppressed by the nonlinearity of the driving term required to excite them. Therefore, from the twofold infinity of possible modes, only four are likely to be serious for the uniformly charged beam: the rigid dipole mode $(m = 1,\ n = 1)$, which is excited by magnetic field errors for integral values of ν_0; the quadrupole mode $(m = 2,\ n = 2)$, which is excited by gradient errors for $\nu_0 = \frac{n}{2} + \frac{3}{4}\Delta\nu_{sc}$; the sextupole mode $(m = 3,\ n = 3)$, which is excited by $P_2(x)$ for $\nu_0 = \frac{n}{3} + \frac{7}{8}\Delta\nu_{sc}$; and the nonrigid dipole mode $(m = 3,\ n = 1)$, which is excited by $P_2(x)$ for $\nu_0 = n + \frac{9}{8}\Delta\nu_{sc}$.

Two beams with nonuniform charge density were also examined, a Gaussian beam similar to that observed in the Brookhaven AGS and the

water-bag beam, which has a charge distribution intermediate between that of the uniform beam and the Gaussian beam. Despite the relatively different charge distributions, the eigenfrequencies for the surface modes of the water-bag and uniform beams have the same form and very similar numerical values. The eigenfrequencies for the Gaussian beam were extrapolated from the known eigenfrequencies for a neutralized Gaussian distribution, and are also very similar in form and numerical content to those for the uniform and water-bag beams. Because of this similarity, it is reasonable to assume that corresponding modes in the three distributions are excited by the same driving terms; for example, a gradient error is expected to excite primarily the $n = 2$ surface modes, causing a resonance for $\nu_0 = \frac{n}{2} + \frac{3}{4} \Delta\nu_{sc}$ in the uniform beam, for $\nu_0 = \frac{n}{2} + 0.853\ \Delta\nu_{sc}$ in the water-bag beam, and for $\nu_0 = \frac{n}{2} + 1.04\ \Delta\nu_{sc}$ in the Gaussian beam. In the same spirit, only the first three surface modes and one or two nonsurface modes are expected to be observable in accelerators, in analogy with the uniform beam.

For the future, it is possible that the exact eigenfrequencies and normal modes for any distribution, at least to first order in $\frac{\Delta\nu_{sc}}{\nu_0}$, can be found by stationary perturbation methods, i.e., the methods that are used in quantum mechanics to compute perturbed eigenfunctions and energy levels. Since only five or six modes need be examined, the perturbation approach should converge without excessive calculation. Perturbation methods might also be applied to two-dimensional beams to examine the effects of space charge on sum and

difference resonances, and to three-dimensional beams to examine the space-charge coupling between longitudinal and transverse motions. Since relatively few modes are involved, it might also be feasible to determine the large-amplitude behavior of these modes by analytical methods.

ACKNOWLEDGMENTS

I am very grateful to Lloyd Smith for his guidance and cooperation in this work, and also to Alper A. Garren, Philip L. Morton, L. Jackson Laslett, and David L. Judd for many helpful discussions.

This work was done under auspices of the U.S. Atomic Energy Commission.

APPENDICES

A. The Nonexistence of Uniformly Charged Three-Dimensional Beams

We are given an ensemble of three-dimensional harmonic oscillators with the Hamiltonian

$$H(\vec{p}, \vec{q}) = p^2 + q^2 , \qquad 0 \leqslant H \leqslant 1 \quad . \tag{A1}$$

Because of the inequality, the accessible region in phase space is a six-dimensional unit sphere; in configuration space it is a 3-sphere. Does there exist a spherically symmetric distribution $f(p^2 + q^2)$ that has a uniform projection onto the 3-sphere? The following necessary condition for the existence of such a distribution has been found by Maurice Neuman.

Theorem: The spherically symmetric distribution $f(p^2 + q^2)$ does not exist if its projection $\rho(q^2) = \int f(p^2 + q^2) d^3p$ violates any of the following inequalities:

$$\rho(\tau) \begin{cases} \leqslant \frac{4}{\pi^2} \left(\frac{3}{4\tau}\right)^{3/2} , & 0 \leqslant \tau \leqslant \frac{3}{4} , \\ \leqslant \frac{8}{\pi^2} \sqrt{1 - \tau} , & \frac{3}{4} \leqslant \tau \leqslant 1 \quad . \end{cases} \tag{A2}$$

The maximum permissible value of $\rho(\tau)$, which corresponds to the equal sign, is shown in Fig. (A1). An immediate consequence of this theorem is the nonexistence of a spherically symmetric distribution $f(p^2 + q^2)$ with a uniform projection, $\rho(q^2) = \text{constant}$.

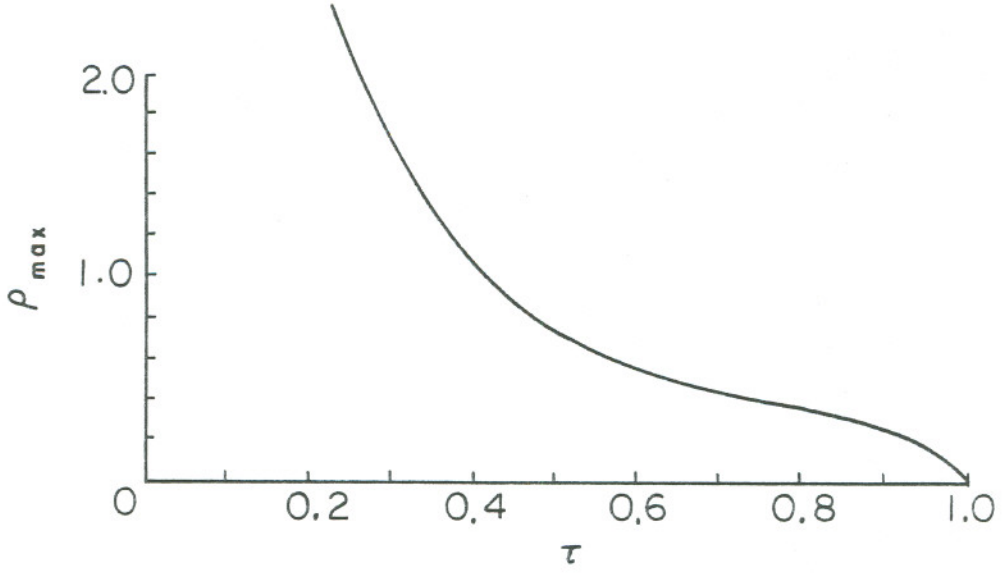

Fig. A1. The maximum value of $\rho(\tau)$ from Eq. A2 is shown as a function of τ.

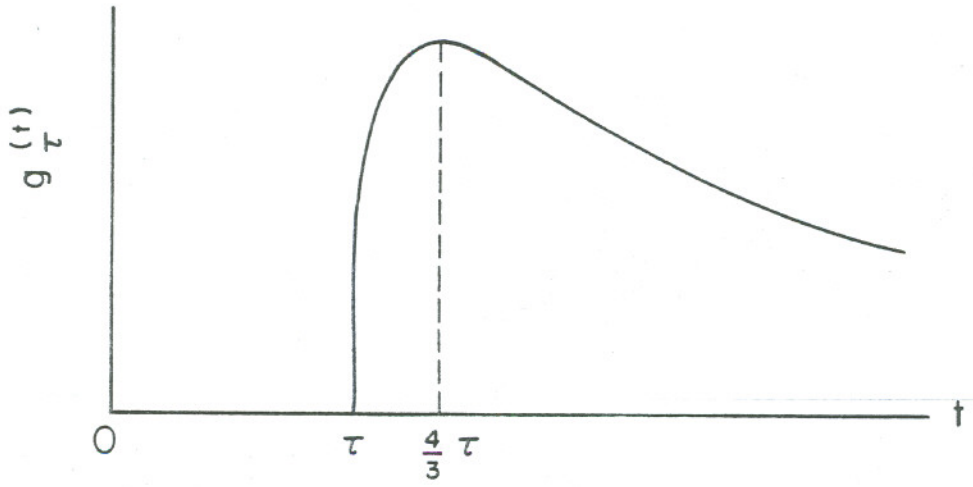

XBL689-3915

Fig. A2. The function $g_\tau(t)$ specified by Eq. (A8) is shown as a function of t.

Proof of Theorem: f is normalized by

$$\int f(p^2 + q^2)d^3pd^3q = \frac{\pi^3}{4} \int_0^1 f(t)t^2\, dt = 1 \quad . \tag{A3}$$

The mean of any function $g(t)$ is

$$\text{mean } g = \frac{\pi^3}{4} \int_0^1 g(t)\, f(t)\, t^2\, dt \quad , \tag{A4}$$

and the resulting number can neither exceed the largest nor fall beneath the smallest value of $g(t)$ $(0 \leqslant t \leqslant 1)$:

$$\inf g \leqslant \text{mean } g \leqslant \sup g \quad . \tag{A5}$$

The projection of f is

$$\rho(q^2) = \int f(p^2 + q^2)d^3p = 2\pi \int_0^\infty f(t + q^2)t^{\frac{1}{2}}\, dt \tag{A6}$$

or

$$\rho(\tau) = 2\pi \int_\tau^1 f(t)\, (t - \tau)^{\frac{1}{2}}\, dt \quad . \tag{A7}$$

Consider the function

$$g_\tau(t) = \frac{(t - \tau)^{\frac{1}{2}}}{t^2} \qquad \text{for } 0 \leqslant \tau \leqslant t \leqslant 1$$

$$= 0 \qquad \text{for } t < \tau \quad , \tag{A8}$$

which is shown in Fig. A2. Its mean value is proportional to $\rho(\tau)$,

$$\frac{\pi^2}{8}\,\rho(\tau) \;=\; \text{mean}\;\; g_\tau \;\leqslant\; \sup\, g_\tau \quad . \tag{A9}$$

But for $\frac{4}{3}\,\tau < 1$, $\sup\, g_\tau = \max\, g_\tau = g_\tau\left(\frac{4\tau}{3}\right) = \frac{1}{16}\left(\frac{3}{\tau}\right)^{\frac{3}{2}}$, and

for $\frac{4}{3}\,\tau > 1$, $\sup\, g_\tau = g_\tau(1) = \sqrt{1-\tau}$. Q.E.D.

B. The Amplitude-Phase Equations for Two-Dimensional Beams

In the absence of space charge and gradient errors, the solutions of the two-dimensional envelope Eqs. (3-1) and (3-2) can be written in the form

$$x^2 = \sqrt{1 + A^2} + A \sin(2\nu_x \phi + \alpha) \quad ,$$

$$x \frac{dx}{d\phi} = \nu_x A \cos(2\nu_x \phi + \alpha) \quad ,$$

$$z^2 = \sqrt{1 + B^2} + B \sin(2\nu_z \phi + \beta) \quad ,$$

$$z \frac{dz}{d\phi} = \nu_z B \cos(2\nu_z \phi + \beta) \quad , \qquad \text{(B1)}$$

where A, B, α, and β are constant. When Eqs. (B1) are inserted into the complete envelope equations with space charge and gradient errors, we obtain the following first-order equations for A, B, Q_x, Q_z:

$$\frac{dA}{d\phi} = \frac{\omega_p^2}{\nu_x} \sqrt{1 + A^2}\, I_x - \Delta\nu_{sx} \sqrt{1 + A^2} \cos Q_x \quad , \qquad \text{(B2)}$$

$$\frac{dB}{d\phi} = \frac{\omega_p^2}{\nu_z} \sqrt{1 + B^2}\, I_z - \Delta\nu_{sz} \sqrt{1 + B^2} \cos Q_z \quad , \qquad \text{(B3)}$$

$$A \frac{dQ_x}{d\phi} = -\frac{\omega_p^2}{\nu_x} M_x + \Delta\nu_{sx} \sqrt{1 + A^2} \sin Q_x + 2A\Delta\nu_x \quad . \qquad \text{(B4)}$$

$$B \frac{dQ_z}{d\phi} = -\frac{\omega_p^2}{\nu_z} M_z + \Delta\nu_{sz} \sqrt{1 + B^2} \sin Q_z + 2B\Delta\nu_z \quad , \qquad \text{(B5)}$$

plus additional terms that vary with the frequencies $2\nu_x$, $2\nu_z$, $4\nu_x$, $4\nu_z$, etc. We have defined $Q_x = (2\nu_x - n)\phi + \alpha$, $Q_z = (2\nu_z - n)\phi + \beta$, $\Delta\nu_x = \nu_x - \frac{n}{2}$, $\Delta\nu_z = \nu_z - \frac{n}{2}$, and

$$I_x = \frac{b}{2\pi} \int_0^{2\pi} \frac{\cos u}{x(ax + bz)}\, du \quad \text{with} \quad u = n\phi + Q_x \quad , \tag{B6}$$

$$M_x = \frac{b}{2\pi} \int_0^{2\pi} \frac{A + \sqrt{1 + A^2}\, \sin u}{x(ax + bz)}\, du \quad , \tag{B7}$$

with similar definitions for I_z and M_z. The quantities I_x and I_z are related by

$$aAI_x + bBI_z = 0 \quad . \tag{B8}$$

A. Equal Frequencies and Emittances

In general, Eqs. (B2) - (B5) are very difficult to solve; however, for the special case of equal frequencies $(\nu_x = \nu_z)$ and equal emittances $(a = b)$, analytic solutions exist with the forms

$$x^2 = \sqrt{1 + A^2} + A \cos(n\phi + Q) \quad ,$$

$$z^2 = \sqrt{1 + A^2} \pm A \cos(n\phi + Q) \quad , \tag{B9}$$

where the plus sign occurs for a symmetric gradient error $(\Delta\nu_{sx} = \Delta\nu_{sz})$ and the minus sign for an antisymmetric gradient error $(\Delta\nu_{sx} = -\Delta\nu_{sz})$. For either gradient error, $I_x = I_z = 0$ and $M_x = M_z$, so that Eqs. (B2) - (B5) reduce to

$$\frac{dA}{d\phi} = \Delta\nu_s \sqrt{1 + A^2} \sin Q \quad , \tag{B10}$$

$$A \frac{dQ}{d\phi} = -4\Delta\nu_{sc} M_{\pm} + \Delta\nu_s \sqrt{1 + A^2} \cos Q + 2A\,\Delta\nu \quad , \tag{B11}$$

where

$$M_+ = \frac{\sqrt{1 + A^2} - 1}{2A} \quad , \qquad \text{for } + \text{ in B9} \tag{B12a}$$

and

$$M_- = \frac{1}{2k}\left[1 - \frac{2}{\pi} \cdot \frac{k^2}{A^2} K(k)\right] \quad , \quad \text{for } - \text{ in B9} \tag{B12b}$$

and $K(k)$ is the complete elliptic integral of the first kind with modulus $k = \dfrac{A}{\sqrt{1 + A^2}}$.

The phase trajectories in A, Q space are found by dividing (B10) by (B11) and integrating the result:

$$\text{constant} = A \cos Q + \frac{2\Delta\nu}{\Delta\nu_s} \sqrt{1 + A^2} - 4 \frac{\Delta\nu_{sc}}{\Delta\nu_s} \int \frac{M_{\pm}}{\sqrt{1 + A^2}}\, dA \quad , \tag{B13}$$

where

$$\int \frac{M_+ dA}{\sqrt{1 + A^2}} = \frac{1}{2} \ell n\left(1 + \sqrt{1 + A^2}\right) \tag{B14}$$

and

$$\int \frac{M_- dA}{\sqrt{1 + A^2}} = \frac{1}{2}\left[\ell n\ A - \frac{2}{\pi}\int \frac{K(k)}{k}\, dk\right] \quad . \tag{B15}$$

The fixed points $\frac{dA}{d\phi} = 0$, $\frac{dQ}{d\phi} = 0$ satisfy

$$Q = 0, \qquad A = -\frac{1}{2}\frac{\Delta\nu_s}{\Delta\nu}\sqrt{1 + A^2} + 2\frac{\Delta\nu_{sc}}{\Delta\nu} M_{\pm}$$

or (B16)

$$Q = \pi, \qquad A = \frac{1}{2}\frac{\Delta\nu_s}{\Delta\nu}\sqrt{1 + A^2} + 2\frac{\Delta\nu_{sc}}{\Delta\nu} M_{\pm} \quad ,$$

and are shown in Fig. 10. For $\Delta\nu_s = 0$, these equations specify the amplitude of the free envelope oscillations that are periodic.

Because of the nonlinearity in the envelope equations, a gradient error of one symmetry also affects the normal mode solutions of opposite symmetry. Thus the symmetric fixed points of (B16) are modified by an antisymmetric gradient error, and vice versa. For example, in the absence of all gradient errors, the symmetric envelope oscillation has the form

$$x^2 = z^2 = \sqrt{1 + A^2} + A \cos n\phi \quad , \tag{B17}$$

where

$$A = 2\frac{\Delta\nu_{sc}}{\Delta\nu} M_{+} \quad .$$

An antisymmetric gradient error transforms these fixed points into

$$x^2 = \sqrt{1 + A^2} + A \cos(n\phi + Q) \quad ,$$

$$z^2 = \sqrt{1 + A^2} - A \cos(n\phi - Q) \quad , \tag{B18}$$

where for $\frac{\Delta\nu_s}{\Delta\nu} \ll 1$, Eqs. (B2) - (B5) become

$$A \cos \phi = \frac{\Delta\nu_s}{\Delta\nu} \quad ,$$

$$\frac{A^2}{\sqrt{1 + A^2} - 1} = \frac{\Delta\nu_{sc}}{\Delta\nu} \quad . \tag{B19}$$

For small values of $\frac{\Delta\nu_s}{\Delta\nu}$ they approach very closely the form (B17), as shown in Fig. 11. The symmetric gradient error modifies the antisymmetric fixed points in an analogous manner.

B. General Beam Configurations

The response curves for $\nu_x \neq \nu_z$ and $a \neq b$ can be obtained from Eqs. (B2) - (B5) by numerical methods. However, for simplicity, we consider only the $\Delta\nu_{sx} = 0$, $\Delta\nu_{sz} = 0$ asymptotes, in other words, the free envelope oscillations that are periodic. Equations (B2) and (B3) then require that $I_x = I_z = 0$, and this condition is satisfied if $Q_x - Q_z = 0, \pi$, so that

$$x^2 = \sqrt{1 + A^2} + A \sin(n\phi + Q) \quad ,$$

$$z^2 = \sqrt{1 + B^2} \pm B \sin(n\phi + Q) \quad . \tag{B20}$$

The quantities A and B are then determined by (B4) and (B5):

$$A = \frac{\omega_p^2}{2\nu_x \Delta\nu_x} \cdot \frac{b}{2\pi} \int_0^{2\pi} \frac{A + \sqrt{1 + A^2}\,\sin u}{x(ax + bz)}\,du \quad ,$$

$$B = \frac{\omega_p^2}{2\nu_z \Delta\nu_z} \cdot \frac{a}{2\pi} \int_0^{2\pi} \frac{B \pm \sqrt{1 + B^2}\,\sin u}{z(ax + bz)}\,du \quad . \tag{B21}$$

These integral equations were solved numerically, and the solutions are shown in Fig. 14.

$$\sin\theta_0 = \frac{1}{\sqrt{1 - \left(\frac{\lambda}{r}\right)^2}} \geq \frac{1}{\sqrt{r^2 - \lambda^2}}$$

C. Normal Modes that Oscillate with the Frequencies $n\nu$

The uniformly charged beam (Section 1, Part II) has normal-mode solutions that oscillate with the frequencies $n\nu$, where n is an integer and $\nu = \sqrt{\nu_0^2 - \omega_p^2}$. The electric field for these modes has the form $\mathcal{E}_m(x) = P_{m-1}(x)$, and the perturbed particle density is determined by Eq. (1-6) to have the form

$$f(r, \theta) = f_{mn}(r, \theta) + e^{-in\theta} g_{mn}(r) \quad , \tag{C1}$$

where $f_{mn}(r, \theta)$ is given by Eq. (1-21) with $\omega_{mn} = n\nu$. The function $g_{mn}(r)$ is determined by the condition that $f(r, \theta)$ produce the required electric field, $P_{m-1}(x)$:

$$\frac{dP_{m-1}(x)}{dx} = 2 \int f(r, \theta)\, dv \quad . \tag{C2}$$

If (C1) is inserted into (C2), we obtain the following condition for $g_{mn}(r)$:

$$[1 - K_m(n\nu)] \frac{dP_{m-1}(x)}{dx} = \int_{|x|}^{1} \frac{\cos n\theta_0\, g_{mn}(r)}{\sqrt{r^2 - x^2}}\, r dr \quad , \tag{C3}$$

where $\cos \theta_0 = \frac{x}{r}$. For even values of n, the right-hand side of (C3) is an even function of x, and therefore m must be even; for odd values of n, m must be odd.

There is an infinite number of solutions for $n = 0$, i.e., an infinite number of stationary distributions that differ from $f_0(r)$ by

an infinitesmal perturbation. Using Abel's theorem[10] to invert (C3), we find

$$g_{20}(r) = \frac{1}{2}\left(1 + \frac{\omega_p^2}{4\nu^2}\right) f_0(r) \quad ,$$

$$g_{40}(r) = \frac{1}{2}\left(1 + \frac{\omega_p^2}{64\nu^2}\right) (15r^2 - 11) f_0(r) \quad ,$$

$$g_{60}(r) = \frac{5}{4}\left(1 + \frac{\omega_p^2}{16\cdot 16\nu^2}\right) (42r^4 + 14r^2 - 1) f_0(r) \quad ,$$

$$\vdots \qquad (C4)$$

Consequently, for $m = 2$ and $n = 0$,

$$f(r, \theta) = -\frac{\omega_p^2}{\nu^2}\frac{df_0}{dr} r \cos 2\theta + \frac{1}{2}\left(1 + \frac{\omega_p^2}{4\nu^2}\right) f_0 \quad , (C5)$$

and similarly for the higher values of m. Since these solutions all have the same eigenvalue $\omega = 0$, any combination will also be a solution.

For n greater than zero, $K_m(n\nu)$ is infinite if $m \geq n$. Therefore the functions $g_{mn}(r)$ specified by (C3) exist only for $m < n$, and these values correspond exactly to the blanks in Table III. For example, for $n = 1$ or $n = 2$ there are no solutions. For $n = 3$ there is one solution, with the form

$$f = f_{13}(r, \theta) + e^{-i3\theta} g_{13}(r) \quad .$$

{In this case the left-hand side of (C3) is zero, and it is more convenient to determine $g_{13}(r)$ by the equivalent relation

$$[1 - K_m(n\nu)] P_{m-1}(x) = -\frac{1}{n} \int_{|x|}^{1} rdr \sin n\theta_0 \, g_{mn}(r) \quad . \qquad (C6)$$

Equation (C3) is the derivative of (C6) with respect to x.} For $n = 4$ there is also one solution, whereas for $n = 5,6$ there are two solutions, and so on for the higher values of n.

D. Frequency Spread for Nonuniform Stationary Distributions

The Hamiltonian for the individual particles within a stationary distribution $f(p, q)$ is

$$H = \frac{1}{2}(p^2 + \nu_0^2 q^2) + \omega_p^2 \Phi(q) \quad , \tag{D1}$$

where

$$\frac{d^2\Phi}{dq^2} = -2 \int f(H)\, dp \quad , \tag{D2}$$

and where $\int f(p, q)\, dp\, dq = 1$. We have chosen the units of q so that the beam boundary is $q = \pm 1$, and have defined ω_p as the plasma frequency for the average charge density.

The revolution frequency of the individual particles is determined by (D1) and (D2). For AG snychrotrons, $\omega_p^2 \ll \nu_0^2$, and it suffices to find H to first order in $\left(\frac{\omega_p}{\nu}\right)^2$, namely $H \approx H_0 + H_1$, where $H_0 = \frac{1}{2}(p^2 + \nu_0^2 q^2)$ and $H_1 = \omega_p^2 \Phi_0(q)$ with

$$\frac{d^2\Phi_0}{dq^2} = -2 \int f(H_0)\, dp \equiv -2 \rho_0(q) \quad . \tag{D3}$$

In terms of the action and angle variables J, w given by

$$q = \sqrt{\frac{2J}{\nu_0}} \sin w \quad , \qquad w = \nu_0 \phi + \text{constant}, \tag{D4}$$

the zero-order Hamiltonian is $H_0 = \nu_0 J$; the transformed first order Hamiltonian $H_1(J)$ is just the average of $H_1(p, q)$ over the unperturbed orbit,[33]

$$H_1(J) = \frac{\omega_p^2}{2\pi} \int_0^{2\pi} \Phi_0 \left(\sqrt{\frac{2J}{\nu_0}} \sin w \right) dw \quad . \tag{D5}$$

The frequency of revolution of the individual particles is then

$$\nu(J) = \nu_0 + \frac{\omega_p^2}{2\pi} \frac{d}{dJ} \int_0^{2\pi} \Phi_0 \left(\sqrt{\frac{2J}{\nu_0}} \sin w \right) dw \quad . \tag{D6}$$

If the differentiation is performed, followed by an integration by parts, Eq. (D6) becomes

$$\nu(r) = \nu_0 - \Delta\nu_{sc} \frac{2}{\pi} \int_0^{2\pi} \rho_0(r \sin w) \cos^2 w \, dw \quad , \tag{D7}$$

where $r = \sqrt{\frac{2J}{\nu_0}}$ is the radius of the unperturbed orbits and

$\Delta\nu_{sc} = \frac{\omega_p^2}{2\nu_0}$.

FOOTNOTES AND REFERENCES

1. Lloyd Smith, Effect of Gradient Errors in the Presence of Space Charge Forces, in Proceedings of the International Conference on High-Energy Accelerators, Dubna, 1963, p. 897.

2 P. M. Lapostolle, Oscillations in a Synchrotron under Space Charge Conditions, in Proceedings of the International Conference on High-Energy Accelerators, Dubna, 1963, p. 900.

3. Frank Sacherer, The Behavior of Intense Charged Beams in the Presence of Gradient Errors, Lawrence Radiation Laboratory report, UCID-10189, June 1966.

4. P. M. Lapostolle and L. Thorndahl, Beam Envelope Oscillation with Space-Charge Forces: A Numerical Study for Circular Machines, CERN report, ISR/300 - LIN/66-27 Revised, April 1967.

5. Kenneth J. Harker, Longitudinal Oscillations in Unbounded One-Dimensional Nonuniform Plasmas, Phys. Fluids 8, 1846 (1965).

6. J. B. Ehrman, Analytical Determination of the Eigenfrequencies of a Bounded, One-Dimensional Electron Plasma, Plasma Physics 8, 377 (1965), also D. C. dePackh, Water-Bag Model of a Sheet Electron Beam, J. Electron. Control 13, 417 (1962).

7. L. C. Teng, Transverse Space-Charge Effects, Argonne report ANLAD-59, Feb. 1960.

8. L. J. Laslett, On Intensity Limitations Imposed by Transverse Space-Charge Effects in Circular Particle Accelerators, in Proceedings of the 1963 Summer Study on Storage Rings, Accelerators and Experimentation at Super-High Energies, Brookhaven report BNL 7534, 324 (1963).

9. The proton-proton collision time [Equation 5-26 of Spitzer, Physics of Fully Ionized Gases, 2nd Ed. (Interscience, N.Y., 1962)] for a particle whose transverse velocity is 10^{-3} c is approximately $t_c \approx \frac{10^7}{n}$, where n is the number of particles per cm^3. For n typically 10^6 particles/cm^3, $t_c \approx 10$ seconds, whereas we are concerned with times of the order of milliseconds.

10. Whittaker and Watson, Modern Analysis, 4th Ed., (Cambridge University Press, 1958), p. 229.

11. Aimar Sørenssen, The Effect of Strong Longitudinal Space-Charge Forces at Transition, CERN report MPS/Int. Mu/Ep 67-2, July 1967.

12. The constant in (1-20) is determined by the requirement

$$\text{constant} \int dv_1\, dv_2 = \int f\, d^4v = \int f\, \text{Det}\, D d^4x = N_2\, \text{Det}\, D \quad .$$

The integration over $dv_1\, dv_2$ is just the area of a circle of unit radius, and $\text{Det}\, D = \frac{1}{\sqrt{\text{Det}\, M}}$, so that

$$\text{constant} = \frac{N_2}{\pi \sqrt{\text{Det}\, M}} \quad .$$

13. I. M. Kapchinsky and V. V. Vladimirsky, Limitations of Proton Beam Current in a Strong Focusing Linear Accelerator Associated with the Beam Space Charge, in Proceedings of the Conference on High Energy Accelerators and Instrumentation, CERN, 1959, p. 274.

14. The envelope equation in the absence of space charge and gradient errors,

$$\frac{d^2X}{ds^2} + K(s)X - \frac{E^2}{X^3} = 0 \quad ,$$

is equivalent to the two "Cartesian" equations

$$\frac{d^2y}{ds^2} + K(s)y = 0 \quad ,$$

$$\frac{d^2z}{ds^2} + K(s)z = 0 \quad ,$$

where $X^2 = y^2 + z^2$ and $E = y\frac{dz}{ds} - z\frac{dy}{ds}$. Thus if ν falls within a stopband, both y and z and consequently X grow arbitrarily large while E remains constant.

15. E. D. Courant and H. S. Snyder, Theory of the Alternating-Gradient Synchrotron, Ann. Phys. 3, 1 (1958).

16. It is easy to show that the resonance cannot occur for the intensity $\Delta\nu_{sc} = \Delta\nu$. The equation of motion for the individual particle is

$$\frac{d^2x_p}{d\phi^2} + K(s)x_p - \frac{2\nu\Delta\nu_{sc}}{x}x_p = 0$$

where x_p is the x coordinate of a particle, and the envelope has the form

$$x = 1 + \frac{\Delta\nu_{sc}}{2\nu} - \frac{2\nu\Delta\nu_s \cos n\phi}{4\nu^2 - 6\nu\Delta\nu_{sc} - n^2} \quad ,$$

plus free oscillations. Combining the two equations, one obtains

$$\frac{d^2x_p}{d\phi^2} + \left[\nu^2 - 2\nu\Delta\nu_{sc} + 2\nu\Delta\nu_s \cos n\phi - 2\nu\Delta\nu_{sc} \times \frac{2\nu\Delta\nu_s \cos n\phi}{4\nu^2 - 6\nu\Delta\nu_{sc} - n^2}\right] x_p = 0 \quad ,$$

where the nonresonant, free oscillations are neglected. For the intensity $\Delta\nu_{sc} = \Delta\nu$, this equation becomes

$$\frac{d^2x_p}{d\phi^2} + \left(\frac{n}{2}\right)^2 x_p = 0 \quad .$$

Thus the envelope modulation produces an electric field that exactly cancels the gradient perturbation for this intensity, and no resonance occurs.

17. Jahnke and Emde, Tables of Functions, (Dover Publications, New York, 1943), p. 52.

18. The resonant intensities for all values of $\frac{a}{b}$ and $\frac{\nu_x}{\nu_z}$ have been calculated by W. Hardt, On the Incoherent Space Charge Limit for Elliptic Beams, CERN report ISR/Int 300 GS/66.2, Jan. 1966.

19. A. van Steenbergen, Effective Transverse Phase Space Dilution and Beam Density Distribution in the AGS, Sixth International Conference on High Energy Accelerators at Cambridge, 1967, p. 431.

20. We find in Part II (Equation 2-12) that the resonant condition for a one dimensional Gaussian beam with a charge distribution similar

to that in the AGS is $\frac{n}{2} = \nu_0 - 1.04\,\Delta\nu_{sc}$. The resonant condition for the corresponding uniform beam is $\frac{n}{2} = \nu_0 - \frac{3}{4}\Delta\nu_{sc}$, and the frequency shifts from ν_0 are in the ratio $\frac{1.04}{0.75} \approx \frac{4}{3}$. Assuming that the same ratio applies to the two-dimensional resonant conditions (4-1) and (4-2), we conclude that the resonant conditions for the corresponding Gaussian distribution are approximately

$$\frac{n}{2} = \nu_x - \frac{7}{9}\Delta\nu_{scx} \quad ,$$

$$\frac{n}{2} = \nu_z - \frac{8}{9}\Delta\nu_{scz} \quad .$$

21. Erich S. Weibel, Oscillations of a Nonuniform Plasma, Phys. Fluids 3, 399 (1960).

22. For a similar application see Leonard Schiff, Quantum Mechanics, 2nd Ed., (McGraw-Hill Book Company, Inc., New York, 1955), p. 151.

23. This derivation, which is considerably more direct than my original derivation, was contributed by R. Gluckstern (University of Massachusetts, Amherst), private communication.

24. See, for example, John David Jackson, Classical Electrodynamics, (John Wiley and Sons, Inc., New York, 1962), p. 67.

25. Discussions with Andrew Sessler were very helpful in clarifying this point.

26. The uniform one-dimension distribution is (Part I, Eq. 1-17)

$$f(x, x', s) = \frac{N_1}{2\pi\sqrt{E^2 - (Xx' - X'x)^2 - \left(\frac{Ex}{X}\right)^2}} \quad .$$

For small amplitudes, $X = \sqrt{\frac{E}{\nu}} + \delta X e^{-i\omega\phi}$ where ϕ has been used in place of s. If the distribution is expanded to first order in δX, there results

$$f(x, v, \phi) = \frac{1}{2\pi\nu}\left[1 - x^2 - \frac{v^2}{\nu^2} + 2\epsilon\left(x^2 - i\frac{\omega}{\nu}\, x\frac{v}{\nu} - \frac{v^2}{\nu^2}\right)e^{-i\omega\phi}\right]^{-\frac{1}{2}}$$

where now x is measured in units of $\sqrt{\frac{E}{\nu}}$, $v = \frac{dx}{d\phi}$, and $\epsilon = \frac{\delta X}{\sqrt{\frac{E}{\nu}}}$. This expression is identical with $f = f_0 + f_{22}$, where

$$f_{22} = -\frac{\epsilon}{2}\frac{df_0}{dr}\, r\left(i\frac{\omega}{\nu}\sin 2\theta - 2\cos 2\theta\right)e^{-i\omega\phi} .$$

27. L. Landau, on the Vibrations of the Electronic Plasma, J. Phys. (U.S.S.R.) 10, 25 (1946).

28. N. G. van Kampen, On the Theory of Stationary Waves in Plasmas, Physica 21, 949 (1955); also K. M. Case, Plasma Oscillations, Ann. Phys. 7, 349 (1959).

29. For nonharmonic external potentials, there is a spread in zero intensity betatron frequencies; the orbits for the individual particles in $x - \frac{v}{\nu_0}$ space are not circular, and the frequency of revolution $\nu_0(J)$ differs for each orbit. In terms of the action and angle variables J, w defined for the individual particle Hamiltonian, the zero-intensity eigenfunctions and eigenvalues are

$$f_{pn}(J, w) = e^{-inw}\,\delta(J - p), \qquad \omega_{pn} = n\nu_0(J) \quad ,$$

where $\delta(x)$ is the usual delta function and p is a continuous parameter that varies between zero and J_{max}. The normal modes are now discontinuous functions in analogy with the Van Kampen modes (Ref. 28) for an infinite homogeneous medium, and the eigenvalue spectrum is continuous in sections near $n\nu_0(0)$.

30. P. A. Sturrock, Nonlinear Effects in Alternating-Gradient Synchrotrons, Ann. Phys. 3, 113 (1958).

31. Ehrman writes the eigenfrequencies in the form

$$\omega_n = n\nu_0\left(1 - \frac{4}{3\pi}\,\frac{n^2 - 1}{n^2 - \frac{1}{4}}\,\frac{\omega_p^{\,2}}{\nu_0^{\,2}}\right) \quad ,$$

where his ω_p is the plasma frequency for the central charge density, which is $\frac{4}{\pi}$ times the average charge density. In our units,

$$\omega_n = n\left(\nu_0 - \frac{16}{3\pi^2}\,\frac{n^2 - 1}{n^2 - \frac{1}{4}}\,\Delta\nu_{sc}\right) \equiv n\nu(1) + \frac{8}{3\pi}\,\frac{n}{n^2 - \frac{1}{4}}\,\Delta\nu_{sc} \quad .$$

32. Weibel writes the eigenfrequencies in the form

$$\omega_{mn}^{\,2} = n^2\nu_0^{\,2} + \lambda_{mn}\,\omega_p^{\,2} \quad ,$$

where his ω_p is the plasma frequency for the central charge density, which is $2\sqrt{\frac{2}{\pi}}$ times the average charge density. In

our units,

$$\omega_{mn} = n\nu_0 + \frac{1.67}{n} \lambda_{mn} \Delta\nu_{sc} \quad .$$

The eigenfrequencies are not labeled according to Weibel's notation, but according to the notation for the uniform beam. The values of λ_{33} and λ_{42} are obtained from Fig. 2 of Weibel.

33. H. C. Corben and Philip Stehle, Classical Mechanics, 2nd Ed., (John Wiley and Sons, Inc., New York, 1960), p. 245.